Cold-water corals and anthropogenic stressors – effects of sediment load on respiration, growth and behaviour of juvenile *Caryophyllia huinayensis*

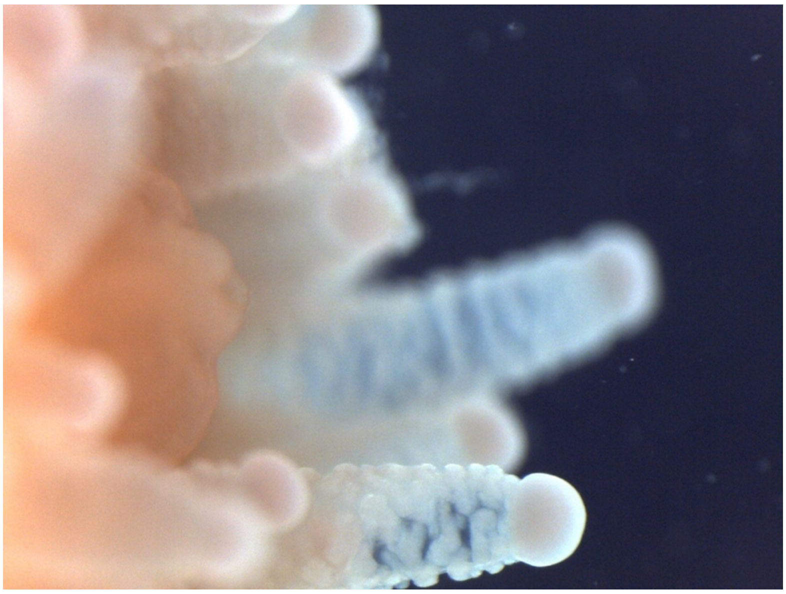

Master's thesis in the degree program Marine Environmental Sciences at the University of Oldenburg to obtain the title "Master of Science".

Submitted by Melanie Fähse
on 12. October 2021
Matriculation number: 5410777

First supervisor: Dr. Sven Rohde
Second supervisor: Dr. Jürgen Laudien

Carl von Ossietzky
Universität Oldenburg

1-Fach-Masterstudiengang, Marine Umweltwissenschaften

Masterarbeit

Cold-water corals and anthropogenic stressors – effects of sediment load on respiration, growth and behaviour of juvenile *Caryophyllia huinayensis*

vorgelegt von Melanie Fähse

Betreuender Gutachter: Dr. Sven Rohde

Zweiter Gutachter: Dr. Jürgen Laudien

Oldenburg, 12. Oktober 2021

Acknowledgement

Foremost, I would like to thank my supervisor Dr. Jürgen Laudien, who supported me in my Master thesis, examined it and assisted me with helpful suggestions. My very special thank goes to my co-supervisor Covadonga Orejas, for her scientific advice and encouraging words, for her trust and her support to present my work at my first international congress. I would like to thank Sven Rohde for his interest, and the opportunity to conduct this study.

Furthermore, my thanks goes to iAtlantic for allowing this study to be part of the Working Group 4 on the impacts of multiple stressors.

I would also like to thank Jürgen Titschak from the Marum for the precise analyses of the sediment samples and for taking the time to discuss these results with me.

I thank Esther Lüdtke and Ulrike Holtz who supported my work in the laboratory and always helped me with technical questions. Further, I would like to thank Ulrike Boettjer for the sediment processing. A big thanks goes to Kristina Beck I could turn to with any question and for her scientific support. My thanks also go to all the others in the Bentho-Pelagic Processes Section, particularly to Pradipta Das and Thomas Heran. Further I would like to thank Marie Koch, for conducting the pre-experiment to this study. Special thanks to Christoph Naab, who always made the long days in the lab seem shorter with a coffee break and good conversations, who helped me in his free time, even on weekends and became a friend.

Finally, I would like to thank my family, Jonas and my friends, who always believe in me, support, encourage and motivate me.

The research leading to the results in this master thesis received funding from the European Union's Horizon 2020 iAtlantic project (Grant Agreement No. 818123). This manuscript reflects the authors' view alone, and the European Union cannot be held responsible for any use that may be made to the information contained herein.

Contents

List of figures

List of tables

List of abbreviation

Not commonly used abbreviations are listed:

AFDM	Ash-free-dry-mass
ANOVA	Analysis of variance
AWI	Alfred-Wegener-Institute Helmholtz Centre for Polar and Marine Researche
CWC	Cold-water coral
DM	Dry mass
FNU	Formazine Nephelometric Units
H_2O_2	Hydrogen peroxide
MQ	Milli-Q-Water
NH_4	Ammonium
NO_2	Nitrogen dioxide
NO_3	Nitrate
PSU	Partical Salinity Unit
PO_4	Phosphate
SD	Standard deviation
SRH-test	Scheirer-Ray-Hare test
TA	Total alkalinity
R^2	Coefficient of determination
Ω_{arag}	Aragonite saturation state

Abstract

The steep walls of Chilean fjords are biodiversity hotspots and characterized by high precipitation rates, high river run-off and natural landslides with an inherent high sediment input. These sedimentation rates are likely to increase in the future due to expanding salmonid farming and coastal road construction. *Caryophyllia huinayensis*, is a Scleractinia, solitary cold-water coral (CWC) growing on steep slopes and overhanging portions of the fjord walls, which may indicate a sensitivity to sedimentation. However, actual data on the susceptibility to sediment of this CWC species is lacking. Furthermore, there is a deficit of information on juvenile CWC dealing with sedimentation stress, which is why this is the first study on this topic. The aim of this work was to investigate whether increased sediment concentrations affect the overall performance of juvenile specimens of *C. huinayesis,* measuring over three-months the coral growth, behaviour and respiration rates. The study consists of an *ex-situ* experiment which included three different treatments: i) the control treatment: with the current natural sediment concentration of Comau Fjord, ii) a 100-fold sediment concentration and iii) a 1000-fold sediment concentration than the control. The most remarkable result demonstrates that corals under the highest sediment concentrations display a significant decreased polyp activity (60 % lower) hence affecting pray capture thus nutrition, leading to a significant reduced growth rate (natural 0.14 ± 0.09 mg d^{-1}; 100-fold: 0.09 ± 0.07 mg d^{-1}; 1000-fold concentration: 0.003 ± 0.009 mg d^{-1}). Furthermore, polyps partly retracted their tissue with increasing sediment load. The results show that all these effects seem to be lower for corals facing vertical downwards than for individuum's growing horizontally. Another important result reveals that long-time exposed (13 weeks) juveniles significantly decrease their oxygen consumption which is directly related to increasing sediment load. Whereas newly exposed individuals (24 h) showed no significant change in their respiration rate under the influence of increased sedimentation load. The results of this experiment contribute to a better understanding of the abilities of CWC recruits to cope with anthropogenic impacts. This information is fundamental as the viability of the juveniles is indispensable for future coral populations and the so called 'Cold-Water Stony Coral Forests'. Consequently, management plans for the fjord need to consider the harmful effects of increased sedimentation on threatened CWC's.

Keywords Sedimentation stress • Juvenile *Caryophyllia huinayensis* • Cold-water Scleractinia • Physiological performance • Comau Fjord • Growth • Coral behaviour

1 Introduction

In greater depths down to 3000 m (Hoegh-Guldberg et al., 2017) cold-water corals (CWC) can be found in all the world's oceans from the intertidal zone to abyssal depths (Freiwald and Roberts, 2005; Henry and Roberts, 2016; Hoegh-Guldberg et al., 2017) in water temperatures of 4 to 12 °C (Roberts, 2006). Here they form reefs and three-dimensional, forest-like structures on the ground, that are comparable in size and complexity to warm-water coral reefs (Henry and Roberts, 2016; Roberts, 2006). These biodiversity-rich ecosystems act like forests, providing niches and nurseries for a variety of species, including commercial fish species, in an otherwise flat and featureless environment (Henry and Roberts, 2016; Roberts, 2006). As they occur in depths where light is limited or not available, CWC typically lack photoautotrophic symbionts (characteristic for the related warm-water relatives) and, as heterotrophic suspension feeders, are dependent on sufficient food nourishment from surface water or thanks to lateral transport (Freiwald and Roberts, 2005; Henry and Roberts, 2016). Therefore, CWCs occur in places with high food supply, for example from downwelling events and internal waves encountering elevated structures (e.g., seamounts or underwater canyon) where bottom current speeds are high and large reefs can develop (Wagner et al., 2011; Henry and Roberts, 2016).

Despite their importance for humans through their biological diversity and productivity, vulnerable CWC reefs are endangered by a range of anthropogenic disturbances, both locally and globally (Henry and Roberts, 2016; Sweetman et al., 2017). Increasing permanent global threats, such as man-made climate change, the associated temperature and sea-level rise, as well as ocean acidification are challenging the marine calcifiers. Additionally, there are other local influences, such as waste pollution, excess of nutrients, increases of oxygen minimum zones, trawling and increasing sediment loads, which can have devastating effects, especially on benthic non-mobile species such as habitat-forming corals (Thrush and Dayton, 2002; Roberts, 2006; Larsson and Purser, 2011; White et al., 2012).

Sediment displacement by storms or tides (Miller et al., 2002), as well as sediment input into the oceans is a natural phenomenon, the latter particularly prevalent at river mouths (Walling, 2006). However, through anthropogenic activities, sediment input to marine habitats is increasing (Walling, 2006; Moeller et al., 2017; Jones et al., 2019). High sedimentation rates result from a variety of inland or coastal influences, such as agriculture expansion and deforesting, thus the native vegetation cannot reduce the run off anymore (Walling, 2006). Coastal developments, including the construction of hotels or roads along the coast, lead to increased sediment discharge during and after construction (Beschta, 1978; Walling, 2006; Min et al., 2012). Existing studies on general sedimentation from roads are scarce and are only approximations, as they are always depending on other environmental conditions (e.g., precipitation, climate) as well as the soil substrate and therefore vary greatly locally. However, Reid und Dunne (1984) reported an increase in sedimentation of 130 %

between a heavily used and abounded road. They also display that a gravel road shows 99 % higher sedimentation rates than a paved road. In addition, increased precipitation and glacier melt due to climate change locally enhance terrestrial material input (Häussermann and Försterra, 2007; Lu et al., 2010; Bianchi et al., 2020). Direct sediment inputs into the open ocean occurs for instance during offshore drilling, while during the construction of oil or gas platforms, sediment particles (drill cuttings) are released; these particles can still be found several years after drilling at a distance of 4 km (Lepland and Mortensen, 2008; Roberts, 2006). Another influencing factor contributing to increasing sediment supply is the fish industry; bottom trawling resuspends sediment, which may affect the survival of CWC reefs (Roberts, 2006). Further, fish farms can have several negative impacts on their immediate environment (Buschmann et al., 2006; Försterra, 2009). Through the organic waste of aquaculture, the sedimentation below and in close vicinity is increased. Under a mussel farm, sedimentation rates more than twice as high as the natural rate were detected (Grant et al., 1995). While in a radius of 250 m to a salmon farm, within a Norwegian fjord, nine times higher values occupied (Kutti et al., 2007). The increased sedimentation due to high input of organic material (e.g., waste feed, fecal matter) and dissenting phytoplankton thus may lead to hypoxic or anoxic conditions near the bottom, when aerobic microbial decomposition takes place. Oxygen consuming animals are suffering or cannot survive low oxygen events. In addition, high nutrient inputs fertilise algae, which in some cases can lead to harmful algal blooms (Buschmann et al., 2006; Hargrave, 2010; Häussermann and Försterra, 2007).

The effects of sedimentation on Scleractinia corals is well researched for warm-water corals (i.e., Loya, 1976; Rogers, 1990; Jones et al., 2015, 2019; Duckworth et al., 2017). Some studies have been conducted with the ubiquitous branching CWC *Lophelia pertusa* (Allers et al., 2013; Larsson et al., 2013; Larsson and Purser, 2011); for instance, Allers et al. (2013) reported mucus release and withdrawn tentacles for colonies of *L. pertusa*, when exposed to increased sedimentation rates.; the mucus release is a clearing behaviour also known from warm-water corals (i.e. Thompson and Bright, 1977; Rogers, 1990; Wild et al., 2004; Jones et al., 2019). Increased activity (e.g., mucus production), decreases available energy and can therefore have a negative effect on growth and reproduction (Rogers, 1990; Jones et al., 2015; Moeller et al., 2017). Furthermore, sediment can alter polyp behaviour and respiration as response to increased sediment (Thompson and Bright, 1977; Rogers, 1990; Allers et al., 2013). Another effect of resuspended fine materials is, that under high levels the suspension feeding mechanism can clog (Maynou and Cartes, 2012; Järnegren et al., 2020). If corals further are covered under sediment they can smother and die (Miller et al., 2002; Larsson and Purser, 2011; Jones et al., 2019;). Therefore, some corals even change their morphology under increased sediment and in the end variations in the coral communities can appear (Rogers, 1990; Erftemeijer et al., 2012).

The effect of sediment on the performance of CWC depends not only on the amount but also in its characteristics: grain size and type, origin, organic content, duration of the sediment inputs as well as suspension and retention in the water column play a fundamental role (Miller et al., 2002; Larsson and Purser, 2011; Liefmann et al., 2018).

However, some coral species as the CWC *L. pertusa,* seem to tolerate a natural increased sediment input (A. Larsson et al., 2013). Nevertheless, the stress caused by increasing sediment loads has different effects on individual species, including on their life cycles (Miller et al., 2002). For instance, Jones et al. (2015) indicated that the survival and settlement of warm-water coral larvae is negatively affected under sedimentation. Although, juveniles are important in ensuring the survival of the species and, in the case of habitat building species, for the ecosystem (Jones et al., 2015; Järnegren et al., 2020), studies on juvenile corals are rudimentary (Wittenberg and Hunte, 1992; Moeller et al., 2017) and absent for CWC's. To bridge this knowledge gap and improve predictions of environmental impact studies, it is important to consider the early life stages of corals.

1.1 Study area: Comau Fjord

The Comau Fjord (approx. 42°11' – 42°29'S and 72°35' – 72°22'E) is part of the Chilean fjord system off the Gulf of Ancud (Fig. 1). The fjord stretches from north to south over a length of 45 km and a width of 8.5 km with a maximum water depth of nearly 500 m. It is part of a longitudinal structural fault of the Liquiñe-Ofqui fault zone, which underwent major alteration during the Quaternary. The fjord is characterised by steep slopes and mountains up to 2000 m above sea level. This continues in the underwater seascape with steep basaltic-walls dropping rapidly into the depths (Bustamante, 2009; Häussermann et al., 2012; Hervé et al., 2009; Pantoja et al., 2011; Vásquez, 2017). Along the coast rocky beaches with slopes predominate (Hervé et al., 2009; Hromic, 2009). The steep walls along the fjord are repeatedly interrupted by valleys and bays which feed the fjord with watercourses (e.g Loncochaigua and Vodudahue river) (Bustamante, 2009). This results in an annual inflow of more than 6000 ml of rainwater (Försterra, 2009; Hromic, 2009). Thus, the fjord shows a low-salinity-layer (2-20, Partical Salinity Unit (PSU)) that varies seasonally and locally in depth (0-10 m depth). With greater depth, the salinity slowly increases from 20-30 (5-20 m depth) to more than 32 in a depth of 20 m and more. The water temperature also varies seasonally and between the water layers from around 10 °C to 20 °C at the surface, to 10 °C to 12 °C at depths of more than 20 m (Bustamante, 2009; Fillinger and Richter, 2013; Sanchez et al., 2011). The pH value in the fjord fluctuates between ~ 8.3 to 7.9 in the upper water layer, decreasing to ca. 7.4 in depths of over 200 m (Fillinger and Richter, 2013; Jantzen et al., 2013a). Oxygen saturation drops below 60 % within the first 50 m depth and remains around that value in greater depths (Jantzen et al., 2013a). The tidal current is rather weak due to the wide mouth and the great depth, but can account for a tidal range of more than 7 m during spring tides (Försterra, 2009).

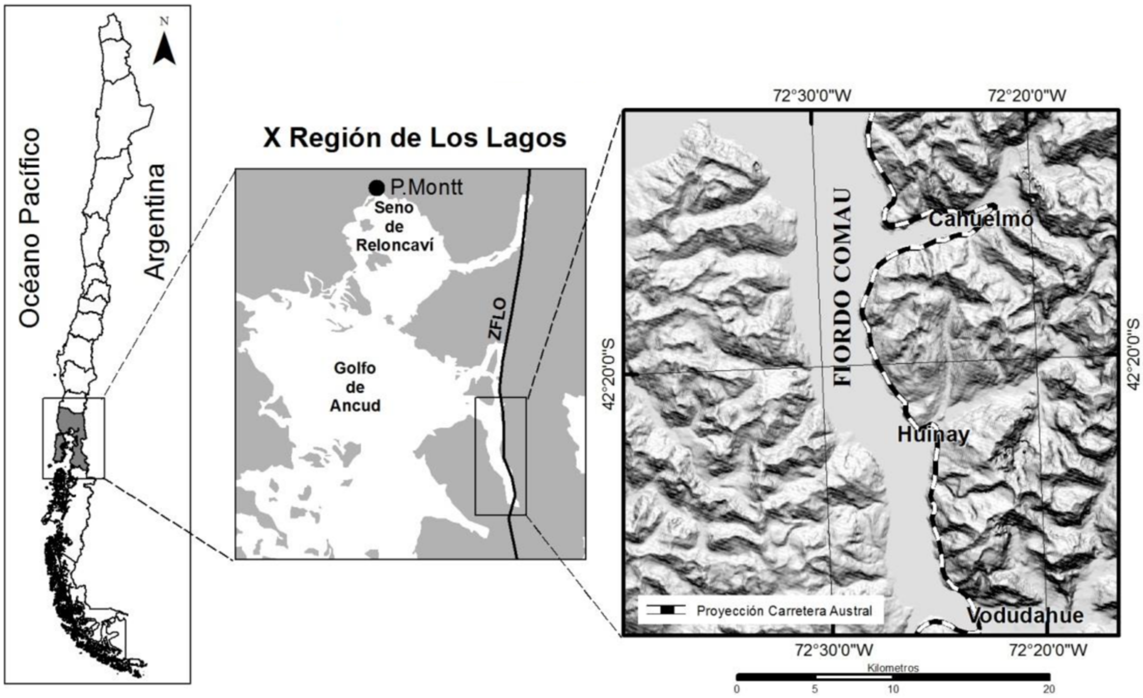

Figure 1: Location of Comau Fjord with planned route of the Carretera Austral for the section Cahuelmo - Vodudahue. Image from Vásquez (2017)

Through the high levels of precipitation around the year with a minimum of more than 100 mm in a month (Soto, 2009), heavy rainfalls lead to small ephemeral streams, which are formed every few meters on the slopes. The often highly torrential water runoff and through the dense forest vegetation slowed water drainage, carry high inorganic (e. g. dissolved nutrients, glacial silt, gravel and boulders) and organic material (e.g. organic acids, leaves, trees) with them (Försterra, 2009; Pantoja et al., 2011). These also contribute to the fact, that the region is characterised by frequent landslides and avalanches, some of them even continuing under water, erasing benthic life (Försterra, 2009). Furthermore, especially streams, that carry glacial or volcanic sediments leading to high sediment input and bury benthic life. Depending on the sediment characteristics, this can have a local effect or extend far along the fjord (Försterra, 2009).

The Comau Fjord is a biodiversity hotspot, with the greatest diversity restricted to rocky slopes, on the vertical walls and overhangs, where sediment stress is relatively low (Fig. 2) (Försterra, 2009; Försterra et al., 2017). In the upper 10 m, which is under the influence of freshwater, mussels and barnacles dominate the benthic community. Below this, the community is more heterogeneous, displaying its highest diversity below the low-salinity layer (> 15 m depth); here habitat forming suspension feeders as cold-water stony corals, hydrocorals, gorgonians, sponges, ascidians among others form the so called “animal forest”, which is a complex ecosystem building unique habitats and niches for a variety of animals as (Försterra et al., 2017). Furthermore, the Comau Fjord is one of the three fjords in this region, were dense coral banks of solitary Scleractinia *Desmophyllum dianthus* thrive (Försterra, 2009). Since 2010, a 75-metre-wide strip along the entire coast of Fundo Huinay has been designated as a multi-purpose marine and coastal protected area (Försterra et al., 2017).

Figure 2: Dense aggregation of *Desmophyllum dianthus* under overhanging portion of a rock wall. Image from Försterra and Häusermann (2003)

However, in the last decade, the Chilean estuarine system, which is rather inaccessible to humans, has gained the attraction of different interest groups: Chile is the world's second largest producer of farmed salmon (FAO, 2021). In Comau Fjord there are a number of salmon farms – some of which are even located in the protected area (Häussermann et al., 2013; Försterra et al., 2017) – that lead to an increase of eutrophication and sedimentation in the fjord (Häussermann and Försterra, 2007; Hargrave, 2010; Försterra et al., 2014, 2017; Häussermann et al., 2021).

Another threat for this vulnerable ecosystem (VME = "vulnerable marine ecosystems are hotspots of biodiversity and ecosystem functioning but characterised by a high vulnerability to disturbances and low recovery potential" (Ashford et al., 2019)) is the planned road construction of the "Carretera Austral" along the eastern shore of the fjord (Fig. 1). The road will run through steep faces covered with forests, for which parts of the rock walls must be blasted. This leads to a high input of rock material and sediment into the fjord, and later also to increased sedimentation through the unpaved road. In addition, the clearing of forests and the associated fragmentation or removal of the root system reduce the stability of the soil. This increases the risk of landslides (Fig. 3) in these steep areas with a low organic cover (Försterra, 2009; Häussermann et al., 2013; Vásquez, 2017). Vásquez

(2017) pointed out, that the susceptibility to landslides is higher on the eastern side, where economic activities are concentrated and the Austral motorway is to be built.

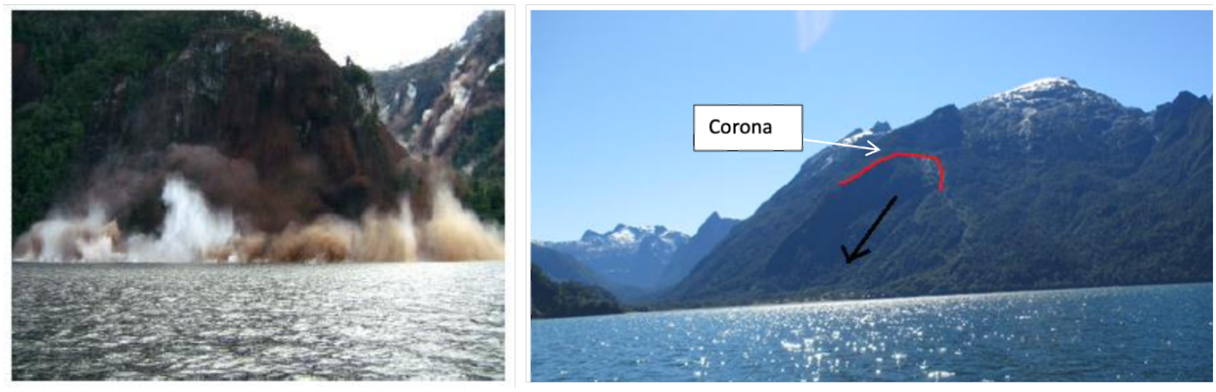

Figure 3: Pictures of landslides along the Chilean fjord region. Left: soil and forest mass movements on a 120 m high escarpment on a fjord 1 km east of Isla Mentirosa, Chile, right: Huinay landslide "Corona" 1957 at the Comau Fjord. Images from Vásquez (2017)

1.2 The targeted species: *Caryophyllia huinayensis*

A habitat forming coral species contributing to the animal forests in Comau Fjord is *Caryophyllia huinayensis* (Fig. 4), an azooxanthellate, solitary growing Scleractinia CWC (Cairns et al., 2005). The species was first described by Cairns et al. in 2005 and belongs to the family Carophylliidae and the suborder Carophylliina (Cairns et al., 2005).

The cup coral can reach a height of 18.7 mm and a calyx diameter of 8.7 mm (Cairns et al., 2005). The almost cyclic calyx of *C. huinayensis* is formed by a corallite with 48 septa. The polyp is located within the calyx and encompasses 48 tentacles that are more transparent than the oral disc (Cairns et al., 2005; Försterra and Häussermann, 2010). Corals show a pinkish, red-orange or whitish transparent tissue (Fig. 4), while some light-exposed specimens may have a pinkish or greenish appearance through corallites stained by endolithic algae (Cairns et al., 2005). The coral is heterotroph and captures zooplankton organisms (Wurz, 2014).

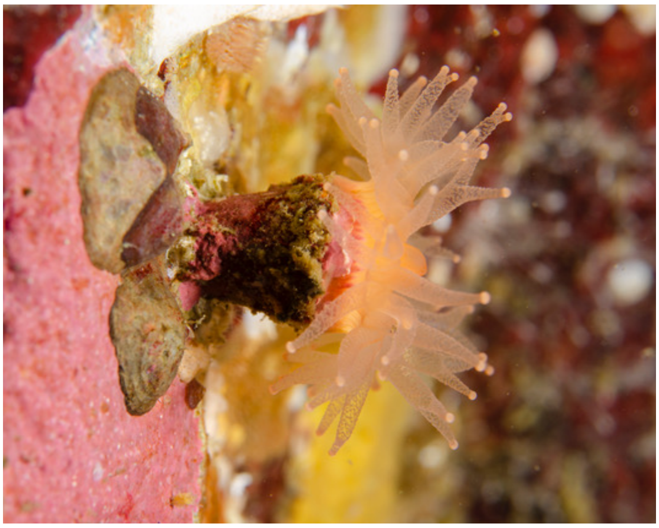

Figure 4: Adult *C. huinayensis* in Comau Fjord, © T. Heran

C. huinayensis is endemic in the Chilean waters were it occurs below the influence of the low salinity layer (salinity < 20) between 16-256 m depth in Comau Fjord and up to ~800 m along the

Chilean coast (Cairns et al., 2005; Häussermann and Försterra, 2007; Sellanes et al., 2008), tolerating temperatures ranging from 8 to 13.5°C and a salinity from 28.5 to 34.1 (Cairns et al., 2005). Within the fjord, *C. huinayensis* abounds on steep slopes and on overhangs, facing horizontally or downwards, on primary and biogenic hard substratum, as on living molluscs (Cairns et al., 2005). Here they form dense aggregations of up to 2211 ± 180 ind. m^{-2} (Wurz, 2014). The species is often found associated with the CWC *D. dianthus* and *Tethocyathus endesa* (Cairns et al., 2005; Försterra et al., 2017). While *T. endesa* dominates the uppermost part of the overhang, *C. huinayensis* is mostly found on the almost vertical walls and *D. dianthus* below that. Furthermore, Cairns et al. (2005) found large schools of scorpaenid fish (*Sebastes capensis*) around *C. huinayensis* banks, which may clean the corals of sediment through their movements due to a sweeping effect. This natural occurrence of *C. huinayensis* in habitats protected from sedimentation may indicates a high sensibility to sediment stress.

Figure 5: Accumulation of sediment on two individuals of *C. huinayensis* in Comau Fjord, © T. Heran

1.3 Objectives of this work

The main aim of this study is to understand and predict how increased sedimentation might affect the physiological performance of CWC *Caryophyllia huinayensis*. To achieve this aim, growth, polyp behaviour and respiration rates will be measured over a three-month period in juvenile specimens, which is one of the most sensitive life phases.

The following hypotheses will be investigated:

Hypothesis 1: With increased sedimentation load, the growth rate of juvenile individuals of the CWCs *C. huinayensis* decreases.

Null-hypothesis 1: The growth rate of juvenile *C. huinayensis* is not affected with increasing sediment load.

Hypothesis 2: Higher sedimentation rates lead to decreased activity of *C. huinayensis* polyps.

Null-hypothesis 2: The activity of *C. huinayensis* polyps is not affected by increasing sedimentation rates

Hypothesis 3: When exposed to increased sedimentation, more corals retract their tissue.

Null-hypothesis 3: Retraction of tissue is not affected by increasing sedimentation

Hypothesis 4: The respiration rate of *C. huinayensis* increases with increased sediment load.

Null-hypothesis 4: With an increasing sediment load the respiration rate of *C. huinayensis* does not increase.

For this purpose, a three-month *ex*-situ experiment was conducted in which the corals were exposed to the natural sediment concentration from their region of origin, a 100-fold higher and a 1000-fold higher sediment concentration.

2 Material and methods

2.1 Sediment sampling and preparation

Since it was not possible to obtain sediment from Comau Fjord, substitute sediment from the Wadden Sea was used, which is also a marine sediment and is also mainly influenced by terrestrial runoff. The sediment needed to conduct the experiments was collected at low tide from the Wadden Sea next to the pier of Spieker-Neufeld, Germany (53° 47′ 25.3′′ N 8° 32′ 49.0′′ E) on 12th and 27th of October 2020, and 16th of February 2021. The upper first 1 cm of sediment was collected with a garden shovel and temporarily stored in a bucket. Gottschlich et al. (2014) showed that sediment of Comau Fjord (sampled for 4 weeks, 20.01 – 16.02.14, at Jetty station in front of the research station Fundación Huinay, near the coast in the central Comau Fjord) mainly consists of grain size fractions from fine sand (63 – 125 µm) to middle silt (< 63 – 6 µm). In order to simulate the sediment from Comau Fjord, the Wadden Sea sediment was separated into grain size fractions and thereafter only the fractions occurring in the sediment obtained by Gottschlich et al. (2014) from Comau Fjord were used in the respective proportions.

The collected sediment was wet sieved through standardized sieves (ATECHNIK GmbH, Leinburg, Germany) on a series of meshes (250 µm, 125 µm, 63 µm; ISO3310-1). Fractions of < 125 µm – > 63 µm and ≤ 63 µm were stored in wide-neck containers and excess water was pipetted off after two days when the sediment had settled. The two fractions were mixed analogous to the grain size analyses by Gottschlich (2014), with 70 % of the finer fraction (≤ 63 µm, 3.5 l) and 30 % of the coarser material (< 125 µm – > 63 µm, 1.5 l).

The organic components of the sediment were removed, as the sediment would be organically enriched in different ways due to the causes, which may lead to increased sedimentation, mentioned in chapter 1.1. In order to remove the organic matter from the sediment, the latter was first freeze dried. Therefore, sediment was placed in Whirl-Pak bags (Nasco, Madison, Wisconsion), frozen in a freezer and subsequently freeze dried for six to seven days in a freeze dryer (Beta 1-8 LDplus, Christ, Osterode am Harz, Germany). Afterwards the freeze-dried sediment was heated on a boiler plate (to speed up the reaction) with hydrogen peroxide (H_2O_2, 35 % stabilized, VWR International GmbH, Darmstadt, Germany), until it stopped reacting. Thereafter, the sediment was washed by adding Milli-Q-Water (MQ, conductivity: 18.0 MΩcm; Sartorius arium pro, Sartorius Corporate Administration GmbH, Göttingen, German) to the sediment in a beaker. The sediment was allowed to settle for five days, which ensured that the fine fraction could settle out of the water column and excess water was pipetted. Any H_2O_2 left in the sediment was removed by repeating the washing and settling two to three times before use. Although there are several potential treatments to remove the organic matter from the sediment, the treatment with H_2O_2 was chosen, as it showed the closest match in terms of grain size to the fjord sediment after processing, compared to other methods which were priori tested (i.e. sediment that was muffled by 500 °C for 12 h, sediment treated with H_2O_2 without prior freeze drying; see appendix supplementary material 1). The grain size of the Wadden Sea sediment before and after the removal of the organics were analysed and compared to the grain size range of sediment from Comau Fjord. Grain size analyses were conducted at the centrum for marine environmental science (MARUM, Bremen, Germany) by Dr. Jürgen Titschack with a Beckman Coulter Laser Diffraction Particle Size Analyzer LS 13320 (Beckmann Coulter GmbH, Krefeld, Germany).

A natural concentration with a sedimentation rate of 2.25 mm a^{-1}, a 100-fold increase of the natural concentration and a 1000-fold increase of the natural concentration were used in this study (Table 1). The selection of the natural concentration was based on the work by Verse (2019), who compared sedimentation rates of the Comau Fjord from three previous studies (Kilian et al., 2007; Gottschlich, 2014; Mayr et al., 2014) and determined a mean sedimentation rate of 2.25 mm a^{-1}, which was equal to an addition of 0.0042 ml sediment per liter. Stock solutions for each of the treatments were prepared mixing MQ and organic free sediment (natural: 1:499, 100-fold: 1:4, 1000-fold concentration: undiluted). The stock solution was portioned and stored in falcon tubes in the fridge at 5 °C until used.

To allow comparison with previous studies, the dry mass (DM) of the sediment was calculated as followed: 1 ml of the 1000-fold sediment concentration was pipetted into each of three aluminium bowls, dried for 1 week in a drying cabinet at 40 °C and weight on a high-resolution scale (CPA225D-0CE, Sartorius Weighing Technology, Göttingen, Germany). The dry weight (g) per ml was than calculated to mg l^{-1} for all concentrations (Table 1).

Table 1 Sediment concentrations used for the experiment. With sedimentation rate determined according to Verse (2019), which corresponds to addition in ml l^{-1} and its dry weight in mg l^{-1}.

	Natural	100-fold	1000-fold
Sedimentation rate	2.25 mm a^{-1}	225 mm a^{-1}	2250 mm a^{-1}
Sediment concentration	0.0042 ml l^{-1}	0.42 ml l^{-1}	4.2 ml l^{-1}
Equivalent dry sediment	1.6 mg l^{-1}	160 mg l^{-1}	1600 mg l^{-1}

To check whether the test corals were exposed to the corresponding sediment concentration applied over the entire test period and whether there was any clarification of the test water or grain size shifts due to sedimentation in the test beaker, sediment suspension water of the treatments were analysed for grain size distribution. Therefore, overflowing water was collected during the water change (see chapter 2.2) and allowed to settle for one week. Multiple samples from the same treatments were pooled to ensure sufficient material. After excess water was removed from the samples with a pipette tip attached to a tube, they were treated with H_2O_2 to remove any organic material (e.g., excrements, food leftovers). Thus, the analyses from the outflowing sediment-suspension can be compared with the first added. Due to the low amount of sediment in the natural concentration, this treatment was excluded from the analyses.

2.2 Long-time exposure stress experiment

2.2.1 Preparation of coral recruits

For the three-month *ex-situ* experiment, coral recruits were taken from the aquarium facilities of the Alfred-Wegener-Institute (Bremerhaven, Germany). These were offspring of adults of *C. huinayensis* collected by scientific SCUBA divers in 2015 from Comau Fjord, which have successfully acclimatized and reproduced in the laboratory aquaria (see Laudien et al., 2021).

Juveniles of a similar size and age (~123 to ~780 days, calix diameter: 1.5 to 3.2 mm) were carefully separated from the aquarium glass with a razor blade and collected with a tweezer. Subsequently they were glued (Super Glue Gel, GLUETEC, Industrieklebstoffe GmbH & Co. KG, Greußenheim, Germany) under water on polyamide screws (6kt 933 poly screws, M4 x 30mm, TOOLCRAFT, Conrad, Germany) in two natural growth directions, horizontal and vertical facing downwards (Fig. 6,7). For later identification of the individuals the screws were labelled with bee opalite number plates (Abelo, York, United Kingdom). Corals were placed in an extra aquarium to previous glued juveniles (October 2020) and left for one week to acclimatization and solidifying the glue. Before the coral specimens were placed in the experimental beaker, corals were visually inspected for polyp activity and full tissue covering under a stereomicroscope (LEICA MZ 16, Leica Microsystems GmbH, Wetzlar, Germany).

Figure 6: *C. huinayensis* colony (yellow arrow points on some individuals) on an overhang in the Comau Fjord, below *Sebastes oculatus*; © T. Heran

2.2.2 Experimental set-up

Artificial seawater, mimicking the main physical and chemical properties (see Laudien et al., 2021) of the water at Cross-Huinay (the sampling spot of adult corals in Comau Fjord) was taken from the husbandry aquarium and filtered with a pressure filtration device (Sartorius AG, Göttingen, Germany) through a glassfibre prefilter (13400-100-K, Sartorius AG, Göttingen, Germany) and a cellulose acetate filter (pore size 0.2 µm; Sartorius AG, Göttingen, Germany) to remove any larger particles (> 0.2 µm, e.g. hydrozoan, bacteria).

Before the experiment started, used equipment was once rinsed with MQ. To prepare the sediment suspension, 650 ml of filtered artificial seawater was poured into a reservoir glass. The falcon tube of the stock solution (see chapter 2.1) was shaken briefly to loosen settled material and homogenized by holding it on a vortex (V 1 SOOO, IKA®-Werke GmbH & Co. KG, Staufen, Germany) for five seconds each before pipetting into the reservoir glasses. The three sediment stock solutions (i.e., control and treatment 1: 1.365 ml, treatment 2: 2.73 ml) were added to the corresponding reservoir glass. The 650 ml reservoir glasses were then equipped with a stirrer and placed on a multi-magnetic-stirring-plate (MIX 15, 2mag AG, München, Germany) at 350 rpm, to prevent sediment from settling, on a shelf above the experimental set-up (Fig. 8, D).

For the sediment-exposure experiment, beakers served as incubation glasses for the coral recruits. Beakers were placed in plexiglass aquaria or a laboratory tray, to collect the overflow water when the water exchange was performed and functioned as water bath to keep stable the temperature within the beakers. These were positioned on multi-magnetic-stirring-plates (treatment 1 and 2: MIX 15, 2mag AG, München, Germany; natural concentration: RO 15 power IKAMAG 115V, IKA®-Werke GmbH & Co. KG, Staufen, Germany) with 200 rpm, to keep the sediment in suspension. Further, Styrofoam plates were placed on top of the aquaria and trays to diminish the evaporation and to maintain a constant temperature and salinity within the beakers (Fig. 8).

The beakers were equipped with a stir bar and filled completely (340 ml) with the sediment solution by flushing 650 ml of the sediment solution by gravity from the reservoir glasses through infusion sets (Intrafix SafeSet, B. Braun Melsungen AG, Melsungen, Germany) into the beakers. Therefore, the water was sucked into a hose of the infusion sets with a 25 ml syringe and placed in the beaker. Once the reservoir glass was empty, the hose was taken from the beaker in order to avoid further disturbance of a possible solution of softeners of the hoses. Overflowing water was up to a marked point on the collection tanks removed to ensure a constant amount of water in the water bath.

After the beaker were filled with the suspension water coral-screws from the husbandry aquarium were carefully cleaned with a toothbrush to remove any fouling organisms e.g., hydrozoan. Then, a screw with a horizontal and a screw with a vertical glued coral were screwed in Plexiglas sticks and placed on top of a beaker (Fig. 7). For each treatment, there were 10 beakers, in each beaker were two corals, one oriented vertical downwards and one horizontally oriented.

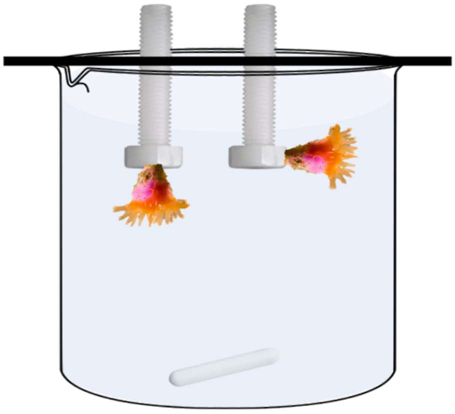

Figure 7: Example of beaker set-up. Figure shows corals glued horizontally and vertically facing downwards on a plastic screw, which is screwed in a Plexiglas stick, and placed on a glass beaker with a magnetic stir bar.

The set-up was located in a dark, air-conditioned 8 °C cool room in the aquaria facilities of the Alfred-Wegener-Institute (Bremerhaven, Germany) and the experiment was run from the 19. January to 16. April 2021. For handling, only headlamps were used to not disturb the corals.

The three experimental runs with different treatments started sequentially due to the time required for the preparation of the set-up and the previously measured growth variables, the initial masses of the coral-screws and the calix area (see chapter 2.4.1). To ensure an adequate supply of nutrients during the experiment, the corals were fed with two different types of food three times a week. For each feeding event 85.7 mg *Artemia persimilis* (Item no.: 10745, Black Label, REBIE, Bielefeld, Germany) eggs were hatched in a cultivation funnel for 48 h at 25 °C, then rinsed with filtered artificial seawater and added to a beaker with 65 ml filtered artificial seawater; from this suspension, 2 ml of the *Artemia persimilis*-nauplii-water-mix and 2.04 µl liquid coral food (MIN S, Fauna Marin GmbH, Holzgerlingen, Germany) were pipetted in each beaker. After four hours, feeding was stopped by changing the water of each beaker (see above).

After 6 weeks, in the measurement of the growth parameters, the beakers were completely cleaned and refilled. Corals, detached from screws during the experiment, were weighed, re-glued and weighed again after a few days. The corals may fall off due to the retraction of their coral tissue or insufficient adhesion to the screw or when handling during the measurements by accidentally touching it with the brush (see chapter 2.4.1.2). This concerned three animals from the control treatment at the beginning of the experiment and one coral from each of the 100-fold and 1000-fold concentration after the calix and growth measurement in the mid of the experiment.

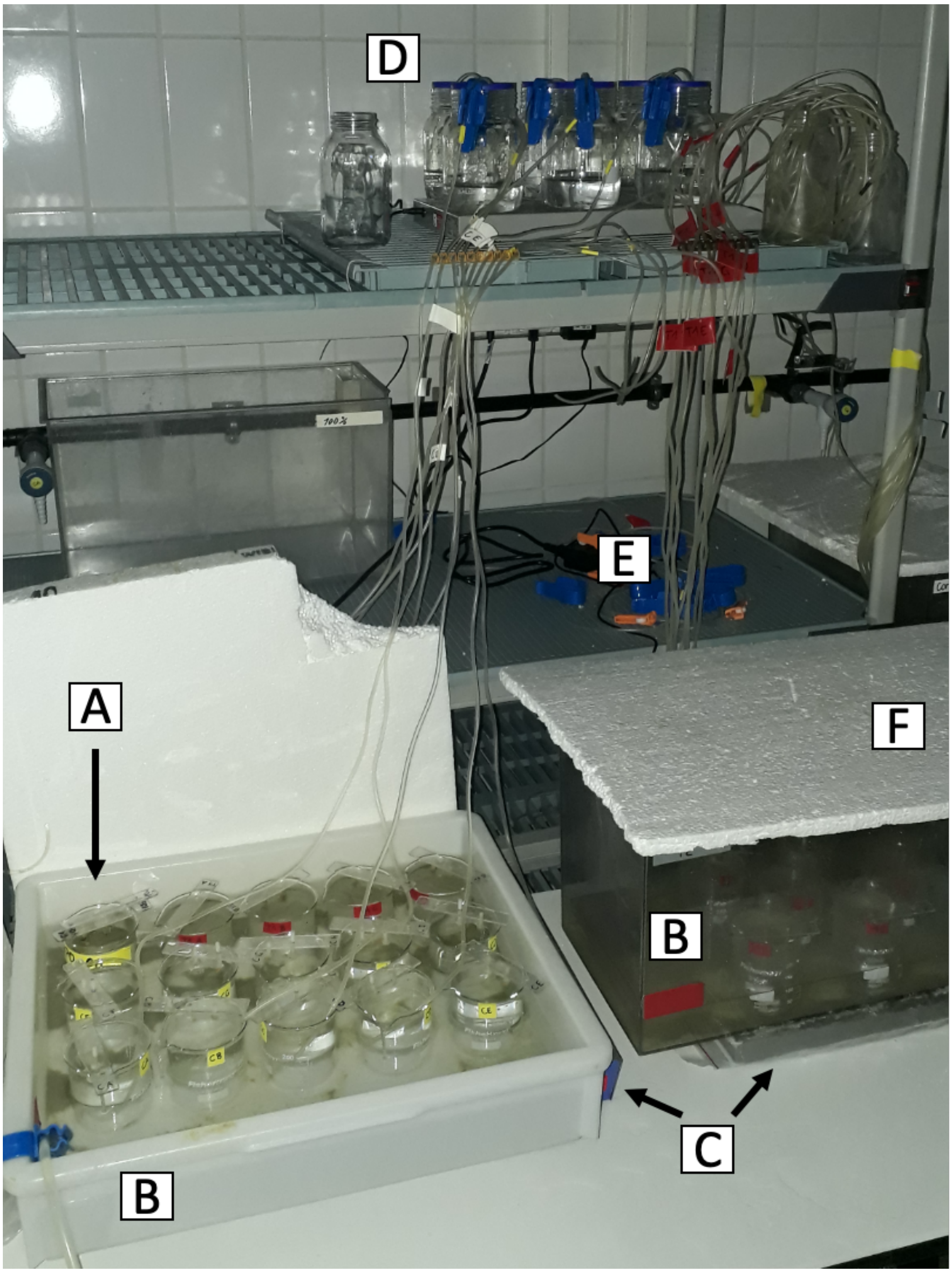

Figure 8: Experimental set-up during water change; A: beaker filled with sediment suspension and on top plexiglass stick with coral screws, B: overflow collection trays and water bath, right: laboratory tray, left: aquarium, C: multi-magnetic-stirring-plate, D: reservoir glasses with sediment suspension on top of a multi-magnetic-stirring-plate, E: hoses for flushing suspension water into the beakers, F: Styrofoam plates, to slow down evaporation and keep a stable temperature in the beaker.

2.2.3 Experimental controls

To exclude external influences control screws were used on the changes in mass (e.g., swell due to osmosis, dissolution of substances from the plastic). Four control screws were used for each treatment. One of them consisted only of a screw on which the opalite plate was glued. The other three were additionally set with a coral skeleton as follows: nine corals of similar size to those used for the experiment were taken from the aquarium and deadened by pouring boiling water over them. To remove any tissue, they were rinsed with MQ and soaked in a 6 % Sodium hypochlorite solution (NaClO, Carl Roth GmbH & Co. KG, Karlsruhe, Germany) for 24 hours. This was repeated once to ensure that all tissue was removed. Afterwards, the coral skeletons were rinsed with MQ before gluing them underwater horizontally on the screw. Additionally, the calix was coated with glue to prevent sediment from settling inside the skeleton mimicking the removed tissue. Finally, the respective screw was marked with an opalite plate.

In order to exclude that coral growth is influenced by differences in phosphate concentration resulting from a different input via the distinct sediment concentrations, a control experiment was conducted. For this, 650 ml filtered artificial seawater was mixed with 2.73 ml l^{-1} sediment, resembling the highest sediment concentration used for the long-term experiment. This suspension was stirred with a stirrer in a beaker placed on a stirring-plate for two days in the cooling room (see previous chapter). Afterwards, the water was filtered with a vacuum pump over a cellulose membrane filter (round filter 589^3, Schleicher & Schuell, Dassel, Germany) to gain water with enriched phosphate concentrations, but without the sediment. Corals facing vertically downwards (glued at the begin of the experiment) were placed in a beaker, which was filled with the filtered, phosphate enriched water and placed next to the control treatment on a multi-magnetic-stirrer (see previous chapter) and treated the same way. After 36 days the mass difference was determined.

2.3 Control of water parameters during the long-term experiments

2.3.1 Nutrient concentrations

Nitrate, Nitrite, Ammonium and Phosphate were analysed three times a week during the entire duration of the long-time experiment. Every Monday, precise measurement was carried out using test sets for a photometer (NOVA 60, Spectroquant; Spectoquant ® Ammonium Test 114752, Spectroquant ® Nitrite Test 114776; Spectroquant ® Phosphate Test 114848; Spectroquant ® Nitrate test in seawater 114942; Spectoquant ® Ammonium Test 114752, Merck KGaA, Darmstadt, Germany). Wednesdays and Fridays an aquarium test kit from JBL was used to check whether the values showed acceptable saturation (JBL PROAQUATEST NO2 Nitrit; JBL PROAQUATEST NO3 Nitrat; JBL PROAQUATEST PO4 Phosphate Sensitiv; JBL PROAQUATEST NH4 Ammonium; JBL GmbH & Co.KG, Neuhofen, Germany). Through a personal communication with a coral aquarist expert (Pedro Siles, Instituto de Ciencias del Mar, CSIC), the phosphate test from Salifert (Salifert Phopsphate PO4 Profi Test, Salifert, Duiven, Holland) was used halfway through the time, as it provided better results. This could be confirmed by comparing the PO_4-values of the mentioned three test for the same water sample.

Due to the volume of water required for the various analyses (Nutrients, TA, Turbidity), the water was pooled for these, as otherwise the corals would no longer have been completely submerged. For the nutrients a volume of 35 ml (5 ml excess water to be able to pipette accurately) was needed.

For this, approx. 7 ml was taken from five beakers of one treatment with a 60 ml syringe and filtered through a syringe prefilter with a glass fiber filter (GF/F, 25 mm, Whatman, Buckinghamshire, United Kingdom) into a 50 ml falcon tube, to remove particles before the photometric tests were conducted. For each treatment, there were two samples, each consisting of the pooled water from five beakers. The water was taken before the corals were fed and analysed immediately. Additionally, coeval filtered artificial seawater, left in a 5 l apothecary bottle from the last water change, was tested for all parameters (mentioned above) as a reference.

2.3.2 Physical water parameters and total alkalinity

Each beaker was checked for temperature (Thermometer, TTX 100 type T, ebro Electronic GmbH & Co. KG, Ingolstadt, Germany), salinity (Salinometer Cond 3110, WTW, Weilheim, Germany), pH (ph3310, WTW, Weilheim, Germany) and dissolved oxygen concentration (DO-instrument, ProODO dissolved oxygen instrument, YSI Incorporated, Yellow Springs, USA) every second day before water exchange.

Total alkalinity (TA) describes the acid binding capacity of water and depends on the amount of dissolved carbonates. One of these is aragonite, which is used by Scleractinia corals to build their skeletons (Gazeau et al., 2015; Hoegh-Guldberg et al., 2017; Jiang et al., 2015). To ensure optimal growing conditions due to an oversaturation of aragonite, TA was measured weekly and aragonite values were calculated. For this purpose, 60 ml of sediment suspension were taken with a 60 ml syringe from five beakers (~12 ml each) from one concentration (n = 2). In addition, freshly filtered seawater from to the same filtration time was sampled. The samples were filtered analogous to the nutrient samples and filled directly into a 50 ml falcon tube up to the top, that as little air as possible was trapped when closing the tube. The samples were kept in a fridge (6 °C) and analysed after one day due to time constraints and to avoid changes in seawater chemistry.

For this 25 ml samples were pipetted individually in titration glasses and placed in an automatic sample changer (TW alpha plus, Xylem Analytics Germany Sales GmbH & Co. KG, Weilheim, Germany) equipped with a stirring rod. This was controlled via the software TitriSoft (Xylem analytics, Weilheim, Germany) and connected to an automatic Titrator (TitroLine alpha plus, SCHOTT Instruments GmbH, Mainz, Germany), which uses potentiometric titration. Before every measurement the pH-electrode was two-point calibrated and the titrant pipe was cleared of air bubbles to ensure accurate additions of Hydrochloric acid (HCl, 0.05 N; Titrisol, Merck KGaA, Darmstadt, Germany). Besides, the artificial seawater and the experimental samples, a North Sea water standard was measured as a reference with each run of the titrator.

TA was calculated from linear Gran plots (Gran, 1952) with the TitriSoft software. TA-values (mol l^{-1}) were then computed in µmol kg^{-1} seawater, taking salinity and density of the water into account. In addition, the values were standardized with the difference between the measured value of the North Sea standard, which is corrected against Dickson standard seawater (Batch02), and the expected value as a blank. Aragonite values were calculated with the excel-sheet CO2sys_v2.1 (Environmental Sciences Division, 2012).

2.3.3 Turbidity

To monitor the suspended sediment in the water column, which the corals were exposed to during the periods between water changes, the turbidity was measured every day and twice a day when a water exchange took place.

Measurements were conducted just before feeding in the morning and after the water change. For this, 2 ml from each of 5 beakers from one treatment were pooled in a 20 ml-syringe (in total 10 ml) and filled in sample cells (Cat. 2434706, Hach Lange GmbH, Düsseldorf, Germany). The cells were always cleaned with a drop of silicone-oil and a lint-free cloth to remove possible small scratches and other accretions on the glasses. The cells were carefully turned upside down a few times without generation air bubbles and placed in a Turbidimeter (2100Qis, Hach Lange GmbH, Düsseldorf, Germany). Each sample was measured three times and the mean value was calculated.

A calibration curve with the coefficient of determination (R^2) was determined for better assessment of sediment input and sediment in suspension. For this purpose, a beaker was placed on a stirring plate and sediment was added, equivalent to the calculated concentrations of the treatments. The amount of sediment was slowly increased from the natural concentration to 1000-times the natural concentration. In between, the turbidity of the sediment solution in the beaker was determined as described before. The amount of sediment added was then plotted against the turbidity values and the R^2 value calculated.

2.4 Measure of the response variables

To understand and predict the sensitivity of juvenile *C. huinayensis* towards sediment stress, growth, behaviour and respiration were measured as response variables.

2.4.1 Growth

As growth is an important indicator of coral vitality, it is a good response variable to indicate possible stress situations (Smith et al., 2005). Hence, the increase in mass and calix diameter over time was determined.

2.4.1.1 Mass variations

The skeletal growth rate of the corals was determined using the buoyant weight method (Davies, 1989). This was successfully used in earlier studies for warm- (e.g., Davies, 1989; Anthony et al., 2002) and cold-water corals (e.g. Orejas et al., 2011; Naumann et al., 2013; Jantzen et al., 2013b). The polyp-glue-screw conglomerates were weight two days before the experiment started, six weeks after the start of the experiment and after twelve weeks, in the end of the experiment. To conduct the buoyant mass, an aquarium was always filled with the same amount (marked with an adhesive strip on the aquarium; see Fig. 9) of artificial sea water and placed under a high-resolution scale (readability ≤ 0.1 mg, error-free result lies with a statistical certainty of generally 95 %, CPA225D-0CE, Sartorius Weighing Technology, Goettingen, Germany) with underfloor weighing device. A weighing basket was attached underneath with help of a nylon cord, which was completely immersed in the water. To ensure a constant temperature (Mean ± standard deviation (SD): 11.3 °C ± 0.3 °C) during the measurements, cooling packs were placed around the aquarium to slow down the heating of the water (Fig. 9, D). Air bubbles, which lead to water movements during dissolution and thus trigger measurement inaccuracies, were gently removed with a brush from the basket and the aquarium walls.

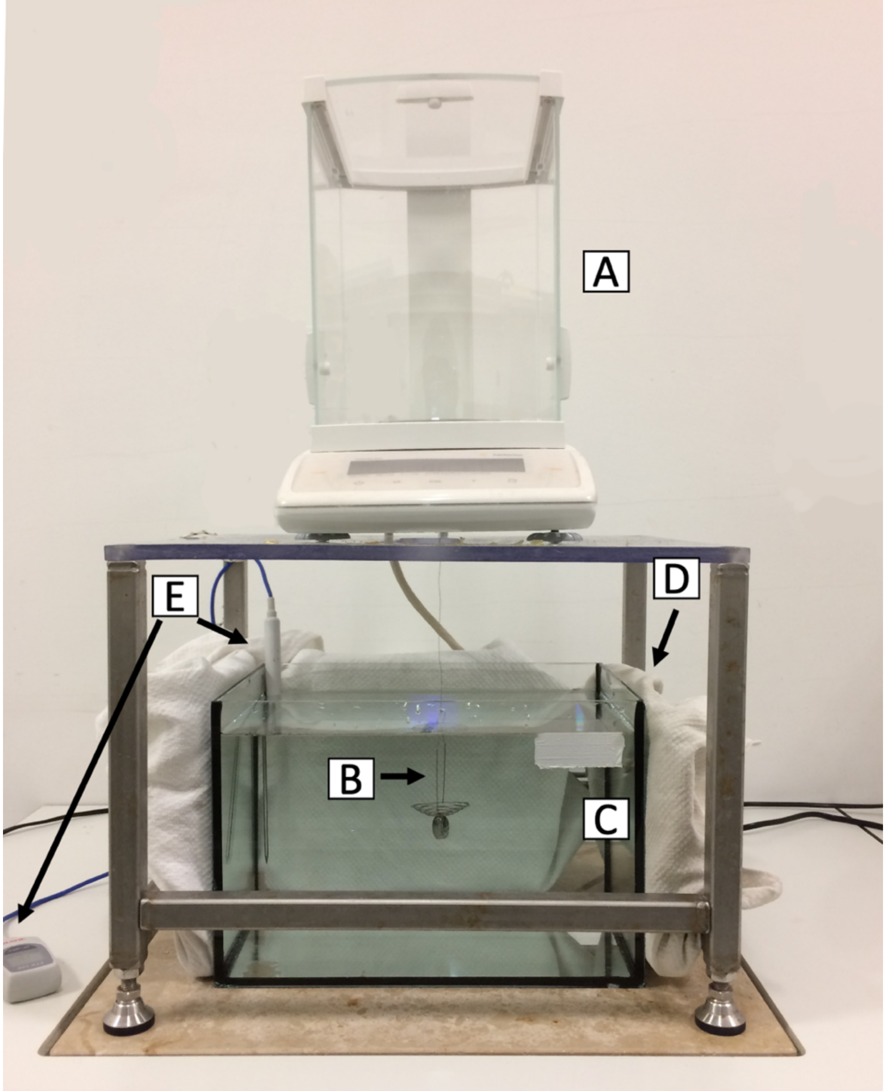

Figure 9: Fine balance set-up used for buoyant weight technique; A: high-resolution balance on a balance table, B: weighing basket with nut (for faster balancing), which is connected to the under-floor weighing device of the balance via a nylon cord, C: aquarium filled with artificial seawater and marking (top right) for constant water level D: cooling packs, to minimise heating of the water; E: thermometer, with immersed probe. Missing from the picture: Salinometer, otherwise attached next to the thermometer.

Prior to weighing the corals, they were carefully cleaned with a toothbrush and a brush to remove any fouling organisms or sediment on the polyp-glue-screw conglomerate. Furthermore, temperature and salinity were measured in the underfloor aquarium before weighing in order to be able to calculate the water density. Thereafter, each polyp-glue-screw conglomerate was weighted at least three times until the differences between the determined replicated values were ≤ 0.0005 g. Mass values were averaged and the skeletal mass in air calculated after Jokiel et al. (1978). The skeletal density of *C. huinayensis* was calculated after Davies (1989), as followed:

$$M_d = \frac{M_w}{\left(1 - \frac{\rho_s}{\rho_c}\right)} \quad \text{(Eq. 1)}$$

where M_d is the dry mass (g)
M_w = Buoyant weight (g)
ρ_s = Seawater density (g/cm^3)
ρ_c = In coral density (2.7397 g/cm^3 for *C. huinayensis* determined after Davies (1989) by Beck, K. (unpublished data))

With the skeletal mass the daily skeleton growth rate in percent (equation Eq. 2) and the mass increase in mg per day (Eq. 3) and year (Eq. 4) were computed. Since the screw does not change its weight, only the skeletal growth is measured. Furthermore, the daily increase in calcium carbonate (100.09 g mol^1) was calculated (Eq. 5). Calculated values were corrected by subtracting the mass increase of control-screws (chapter 2.2.3).

$$G(\%\ d^{-1}) = \frac{(M_{d+1} - M_d)}{(M_d \times (T_{t+1} - T_t))} \times 100 \quad \text{(Eq. 2)}$$

$$G(mg\ d^{-1}) = \frac{(M_{d+1} - M_d)}{(T_{t+1} - T_t)} \times 1000 \quad \text{(Eq. 3)}$$

$$G\ (mg\ y^{-1}) = G(mg\ d^{-1}) \times 365 \quad \text{(Eq. 4)}$$

$$G(\mu mol\ CaCO_3\ mg^{-1}\ d^{-1}) = G(mg\ d^{-1}) \times \frac{1000}{100.09} \quad \text{(Eq. 5)}$$

where
G = Growth rate
T_t = Time (T_t = Start, T_{t+1} = End)

An empirical study showed that the glue strongly influences the mass gain of the coral-screws during the first weeks (K. Beck, personal communication). Therefore, the mass increase in the first six weeks of the corals were excluded from further calculations. The same applies to corals that fell off during the experiment and were re-glued. However, the re-glued individuals were still used for the other response variables (calix diameter increase, behaviour, tissue rejection) and they also served to keep the homogeneity in the beakers the same. Negative growth rates, which occurred in treatment 2, were set to zero, as they are within the range of measurement accuracy (< 0.005).

2.4.1.2 Calix diameter

Pictures of individuals were taken from the zenithal view using a stereomicroscope (LEICA MZ 16, Leica Microsystems GmbH, Wetzlar, Germany) and the software Leica Acquire 3.4.1. Build 9072 © 2006-2013 (Leica Microsystems GmbH, Wetzlar, Germany). To get a clear picture of the calix with the skeleton nicely visible, corals were carefully distracted with air bubbles or a brush, resulting in the retraction of the tentacles. Once the picture was taken, a scale was burned in the image (same software as mentioned above). The calix area was measured using the opensource software ImageJ (Version 1.53) by drawing a line around the calix and using the burned scale to measure the calix area (Fig. 10). The diameter was calculated from the near round calix (Cairns et al., 2005) area (Eq. 6) and the increase per day (Eq. 7). Negative values were set to zero because they were within the measurement error (< 1 %) or due to an overestimation by the tissue overlying the calix in a previous measurement.

$$D_C = \sqrt{\frac{A_C}{\pi}} \times 2 \qquad \text{(Eq. 6)}$$

$$G(\%\ d^{-1}) = \frac{(D_{C+1} - D_C)}{(D_C \times (T_{t+1} - T_t))} \times 100 \qquad \text{(Eq. 7)}$$

where

A_C = Area

D_C = Calix diameter (D_I= Final, D_B = Begin)

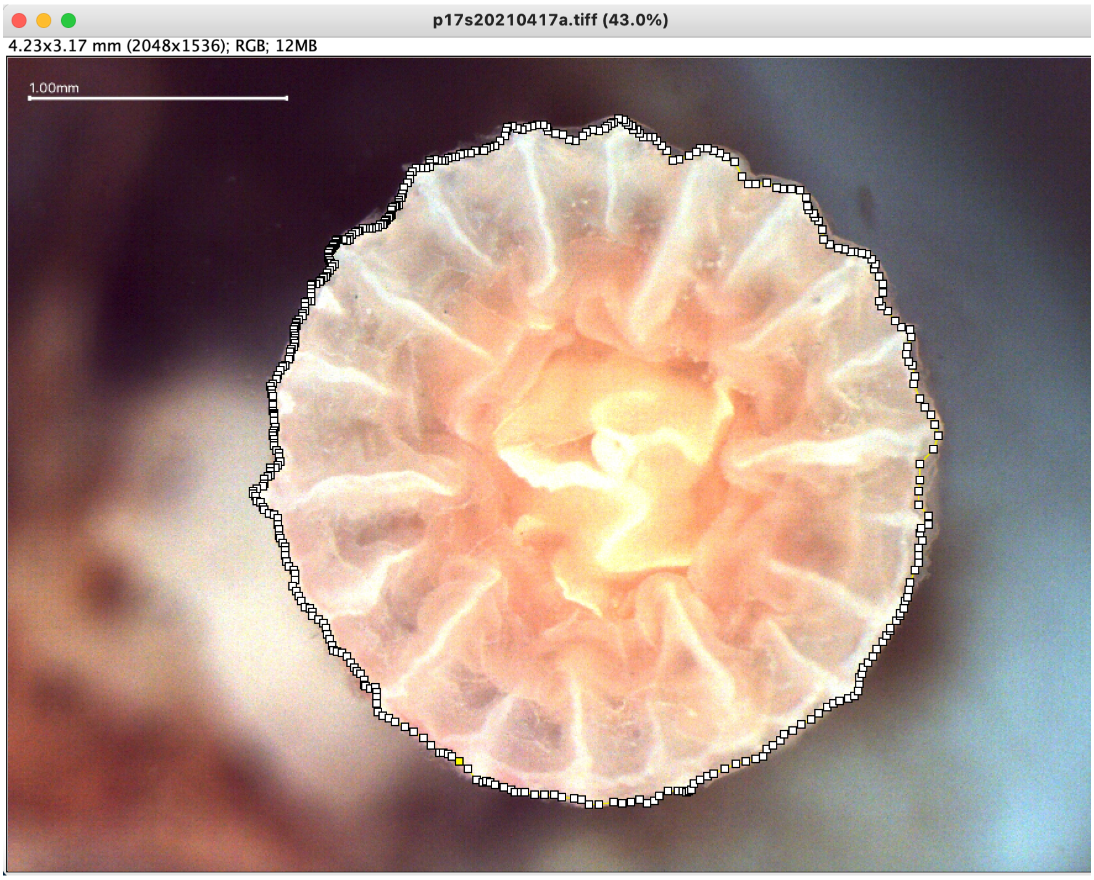

Figure 10: Example measuring the calix area of *C. huinayensis* (zenital view) in ImageJ. With the help of the burnt-in scale, the number of pixels can be specified in a unit of length. By placing a polygon (yellow line with white squares) around the calix, the area is measured. The picture was taken under a stereomicroscope.

2.4.2 Behaviour

Since the behaviour of animals can provide information about their performance, the extension of the polyps and the retraction of tissue of individuals of *C. huinayensis* under the different treatments was investigated.

2.4.2.1 Polyp extension

Observation of polyp extension began on 29 January, one week after the start of the experiment, to rule out possible effects on behaviour from moving the animals into the beaker and continued until the end of the experiment on 16 April 2021. Polyp extension was documented four times a week at 12 noon (± 1 h) for each individual. Thereby the polyp extension was documented three times a week, two hours into feeding and one day without feeding. This was done to see if there is an influence on the behaviour under food supply. The regular measurements of the water parameters (e.g., salinity measurements, chapter 2.3.2) were carried out after the observations of the polyp extension had been completed in order to avoid any disturbances. Polyp behaviour was observed by illuminating only the targeted coral briefly with a spotlight torch. The influence on other corals is excluded, since visually, no differences in the behaviour of the corals could be detected in low light. Polyp extension activity was categorized into three groups: A = polyp fully extended (polyp fully visible, 100 %), B = polyp partly extended (polyp partly visible, 50 %) and C = polyp fully retracted (polyp tentacles not visible, 0 %; Fig. 11). Results of the observations were expressed as "mean extension rate" of the replicated individuals of a treatment per observation day and over time.

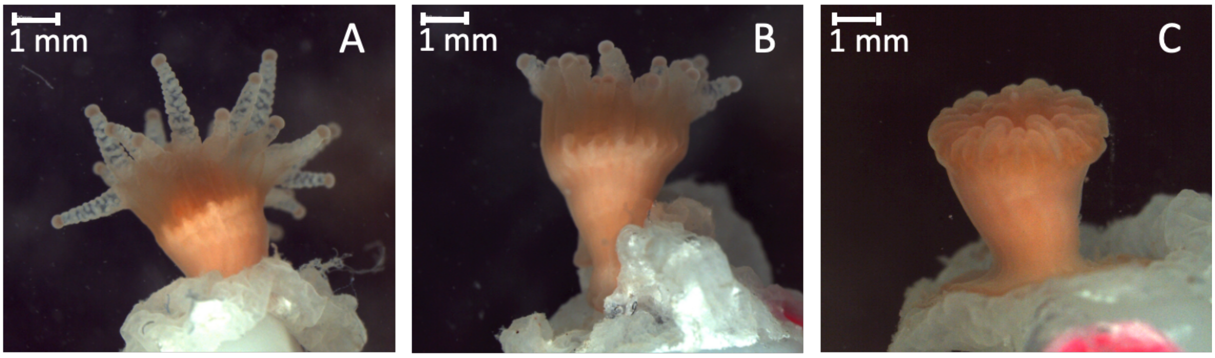

Figure 11: Polyp extension of juvenile *C. huinayensis* with A: fully expanded, B: partly expanded, C: fully retracted, lateral view. Pictures were taken under a stereomicroscope when photographing the calix and capturing the state of the tissue.

2.4.2.2 Tissue retraction

Potential changes in extension of the soft tissue (i.e. tissue retraction) were also documented. Corals were photographed from lateral view using a stereomicroscope (LEICA MZ 16, Leica Microsystems GmbH, Wetzlar, Germany) and the software Leica Acquire 3.4.1. Build 9072 © 2006-2013 (Leica Microsystems GmbH, Wetzlar, Germany) at the beginning, in the middle and at the end of the experiment. The images of the corals were then visually examined to see whether or not the animals had partially retracted their tissue. From this data, the percentages for all the individuals in a treatment who (partially) retracted their tissue were calculated for mean measurement point after 6 weeks and at the end of the experiment after 12 weeks.

2.4.3 Respiration rates

Respiration is one of the most used response variables to measure physiological activity in changing environmental conditions (Hennige et al., 2014; Eder et al., 2018; Gori et al., 2016). Since higher turbidity values can be a stress factor, as corals require more energy for example cleaning their surface from sediment (Tseng et al., 2011), an *in-vitro* respiration experiment was conducted to determine if the different treatments show an effect on the oxygen consumption of juvenile corals. It was also investigated whether there is a difference between animals that are newly (short-term) exposed to sediment and those out of the long-term experiment.

2.4.3.1 Set-up respiration experiment

To study the long-term effect of increased sedimentation on respiration rates, ten (five facing horizontal, five facing vertical downwards) randomly selected juvenile corals per treatment were taken at the end of the three-month experiment (after 13 weeks, see chapter 2.2). In order to compare the long-term with the short-term effects, further 20 previously untreated juvenile individuals (same size and age as corals in chapter 2.2) were glued horizontally and vertically onto screws as described previously (see chapter 2.2.1) and left in the husbandry aquarium for a two-week acclimatization period prior to the performance of the experiments. The short-term exposed corals were only tested for the natural and the highest concentration to compare the two extremes. For each treatment, respiration rates of ten individuals were measured, as well as of two controls consisting of a screw, which was provided with glue and an opalite plate, and the sediment solution for the different treatments. Test corals were last fed approx. 24 h before the start of the respiration measurements.

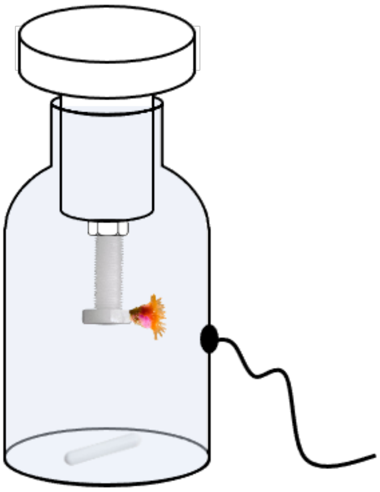

Figure 12: Example of an incubation chamber. Figure shows coral glued horizontally on a plastic screw, which is screwed in the lid of the incubation chamber. The chamber is filled with sediment suspension and a magnetic stir bar is placed inside. An oxygen sensor spot is glued on the outside of the chamber and connected to an optical fiber oxygen sensor.

To ensure that the sediment suspension was equal and homogeneous in the incubation chambers (made by a glass blower of Erich Eydam KG, Kiel, Germany, Fig. 12), they were filled with the sediment suspension from reservoir glasses (Fig. 13, A). Therefore, the reservoir glasses were filled with 650 ml of filtered artificial seawater and the corresponding sediment concentration for each treatment (natural, 100-fold and 1000-fold concentration; see chapter 2.2.2). A stirrer was set inside the reservoir glass and they were placed on a multi-magnetic-stirring plate at 350 rpm (Fig. 13 C). The incubation chambers were submerged in the reservoir glasses until they were fully filled (without air bubbles that could interfere the measurements) with the sediment suspension. Subsequently, coral-screws were cleaned with a toothbrush and placed in an aquarium tank (3 l; Fig. 13 B), which had the same sediment concentration as the reservoir glasses. The aquarium was also placed on the multi-magnetic-stirring-plate with two stirrers inside to keep the sediment in suspension. In the aquarium tank the coral-screw was screwed into the lid of the incubation chambers and possible air bubbles were gently removed with a brush. The previous filled incubation chambers were placed in the aquarium to the lid with the corals screw and closed under water to exclude any air within them. Salinity and pH were measured at the start of the experiment, and turbidity of the sediment suspension was measured after the incubations.

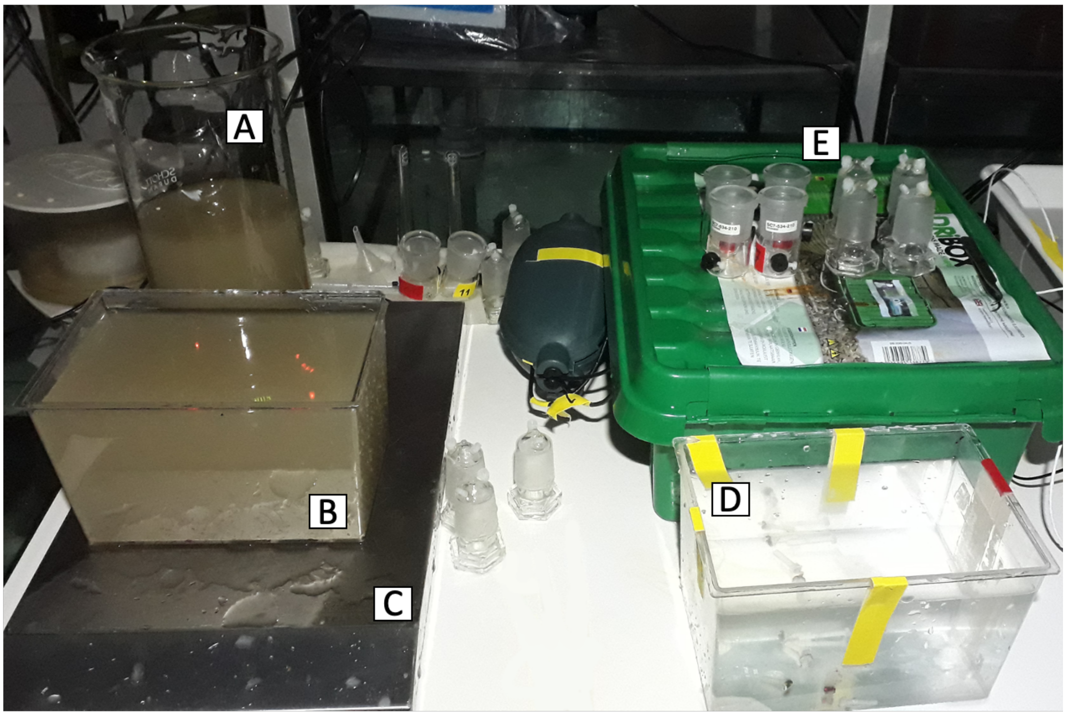

Figure 13: Preparation incubation chambers. A) reservoir glass filled with 650 ml sediment suspension according to the treatment (control, treatment 1 or treatment 2), B) aquarium filled with the sediment suspension in the same concentration as the reservoir glass and placed on multi-magnetic-stirring-plate (C). D) Aquarium with corals for the treatment, E) incubation chambers with lid.

Individuals were incubated for the experimental period of 24 hours (due to their small size and low respiration rate) in a water bath on top of a magnetic stir plate (MIXdrive 15, 2mag AG, München, Germany; Fig 14, C) to keep the temperature constant and the sediment in suspension. Furthermore, a pump (Fig 14, F) and a heating rod (Fig 14, E) were installed in the tank to keep a constant temperature (~ 11 °C) in the incubation chambers, as this has been done in previous trials. Each incubation chamber was equipped with an oxygen sensor spot, (OXSP5, PyroScience GmbH, Aachen, Germany) which was connected with contactless optical fiber oxygen sensors (2 m, SPFIB-BARE, PyroScience GmbH, Aachen, Germany) to a multi-channel fibre optic oxygen and temperature transmitter (FireSting®-O2 [4 Channels], PyroScience GmbH, Aachen, Germany). Further, temperature probes (Pt100 TSUB21, PyroScience GmbH, Aachen, Germany) where connected with each transmitter. The oxygen saturation was constantly (every 10 sec.) measured by light reflected from oxygen sensor spot and directly displayed with the software PyroScience Workbench (V1.2.0.1359; PyroScience GmbH, Aachen, Germany) on a computer. Previous to the measurements, the oxygen sensors were calibrated with O_2-free and 100% O_2 saturated artificial seawater. For the oxygen-free water, sodium dithionite was dissolved in artificial seawater, by stirring it for 24 h. For oxygen saturated water, artificial seawater was stirred, and compressed air was bubbled through a hose connected to an air stone (aquarium use) for 30 minutes before calibrating. Shortly before calibration, the air hose was removed from the water to allow micro-bubbles to escape. One calibration was performed for all three respiration measurements conducted in the same week (K. Beck, personal communication). At the end of the experiment, the water volume of each chamber was measured. Corals were gently removed of the screw and directly frozen at -80 °C to be able to determine the ash free dry mass later.

Dphi (phase shift, unit measured by the optoelectronics) values were calculated in µmol l^{-1} and mg l^{-1} using the Oxygen Calculation Tool (© 2019 by PyroScience GmbH) for Excel, considering the salinity, temperature and calibration settings. The calculated respiration values were grouped in three-hour sections, to check whether the respiration was linear over the time (R^2 above 0.95), to subsequently calculate the metabolic rates with the r package rMR (function MR.loops; Moulton, 2018). Thereafter, mean respiration rates (R) were calculated and adjusted to the volume of the incubation suspension (V_{Inc}, ml). The average oxygen consumption of the measured bacterial background respiration (R_{BG}, see above) was subtracted, the rates related to the ash-free dry mass (AfDM, mg (Eq. 11)) and calculated in respiration rates per day (R_d). From this, the average respiration rate was calculated as mean value for all chambers per treatment. Negative respiration rates, caused by the withdrawal of bacterial background respiration (see above) in animals with a very low respiration rate, were excluded.

$$R_d = \frac{R \times \frac{V_{Inc}}{1000} - R_{BG}}{AfDM} \times 24 \qquad \text{(Eq. 8)}$$

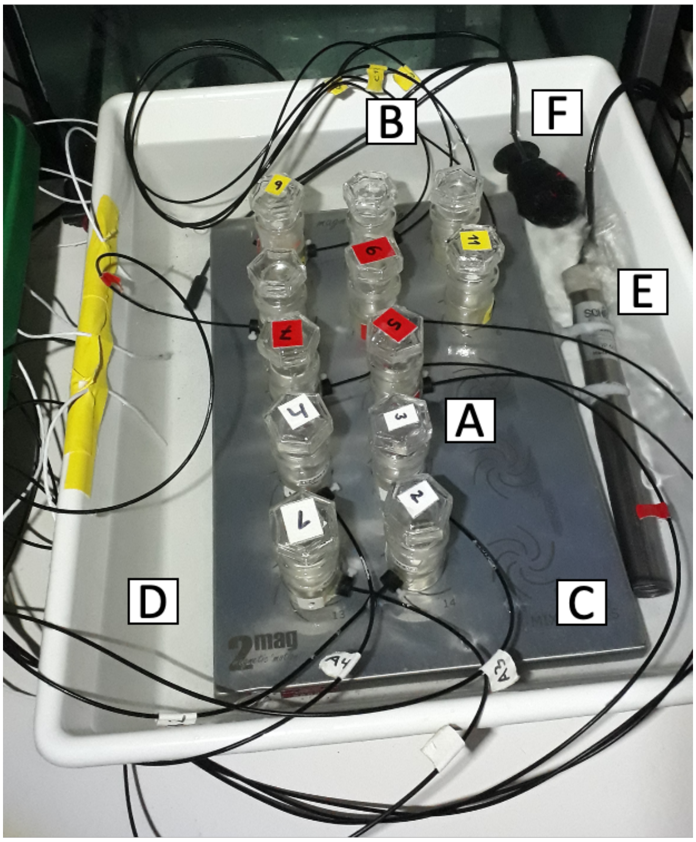

Figure 14: Experimental set-up for respiration measurements. Incubation measurement with incubation chambers (A) connected to contactless optical fibre oxygen sensors (B) on a multi-magnetic-stirring-plate (C) placed in a tray with water bath (D) that is equipped with a pump (E) and a heating rod (F).

2.4.3.2 Ash-free-Dry-Mass

To determine the Ash-free-Dry-Mass, aluminum bowls were combusted at 550 °C for 24 h and weighed on a high-resolution scale (readability ≤ 0.1 mg, error-free result lie with a statistical certainty of generally 95%, CPA225D-0CE, Sartorius Weighing Technology, Goettingen, Germany) to determine the mass of the bowl (M_{alu}). Then frozen animals from the respiration experiment were examined under a stereomicroscope (LEICA MZ 16, Leica Microsystems GmbH, Wetzlar, Germany) for possible glue residues, which were removed as required. Observed individuum's were placed in pre-combusted single aluminum bowls. The bowls with the corals were dried in a drying cabinet at 40 °C for 24 h (J. Laudien, personal communication) and were weighed afterwards (M_{D+alu}) and the dry mass (M_D) was calculated (Eq. 9).

$$(M_D = M_{D+alu} - M_{alu}) \tag{Eq. 9}$$

To remove all the organic material, the animals (in the bowl) were then incinerated in a muffle oven (P330, Nabertherm GmbH, Lilienthal, Germany) at 550 °C (Widbom, 1984) for 24 h and thereafter weight again (M_{A+alu}). Corals from all treatments were treated simultaneously to exclude possible variations due to time, temperature, or handling.

To obtain the ash-free dry mass ($AfDM$), the mass of the combusted coral (M_A, Eq. 10) was subtracted from the dry coral mass (M_D) (Eq. 11). Further, the percentage of tissue from the total coral mass was determined (Eq. 12).

$$(M_A = M_{A+alu} - M_{alu}) \tag{Eq. 10}$$

$$AfDM = (M_D - M_A) \tag{Eq. 11}$$

$$\frac{AfDM}{M_D} \times 100 \tag{Eq. 12}$$

2.5 Statistical Analysis

Data was managed and calculated in Microsoft Excel (Microsoft® Excel for Mac 365, 16.51, © 2021 Microsoft). Statistical analyses and graphs were created in R-Studio (RStudio 1.3.1093, © 2009-2020 RStudio, PBC). All Data were tested for normal distribution using the Shapiro-Wilk test and variance homogeneity with Levene-test. Statistically significant differences were determined via analysis of variance (ANOVA) and identified between groups using Tukey's honestly significant difference (HSD) (Tukey, 1949) for normal distributed data. Since a normal distribution could not be generated for non-normally distributed data by transformation (logarithmic, Box-Cox), the Kruskal-Wallis test (Kruskal and Wallis, 1952) and Dunn-Bonferroni test (Dunn, 1964) as post-hoc test was used. To conduct statistical comparisons between response variables in the different treatment and their orientation, a two-way ANOVA or for non-parametric Scheirer-Ray-Hare test (SRH-test) (Scheirer et al., 1976) were conducted. For the comparison between two groups, a two-sample t-test was conducted. All results will be expressed as mean ± SD.

3 Results

3.1 Granulometry

The grain size distribution for sediment from Comau Fjord and the Wadden Sea sediment used, is displayed in Figure 15. The analyses showed that the untreated sediment from Comau Fjord and both Wadden Sea sediments (collected October 2020 and February 2021) have the same grain size range from < 2 µm to approximately 200 µm with a bimodal distribution. Wadden Sea sediment collected later (February 2021) shows a slightly different grain size composition. After processing the samples with H_2O_2 and rinsing them with MQ, the grain size composition of the Wadden Sea sediment from October 2020 was slightly modified towards a larger proportion in the fine sand range (see dotted blue line in Figure 15).

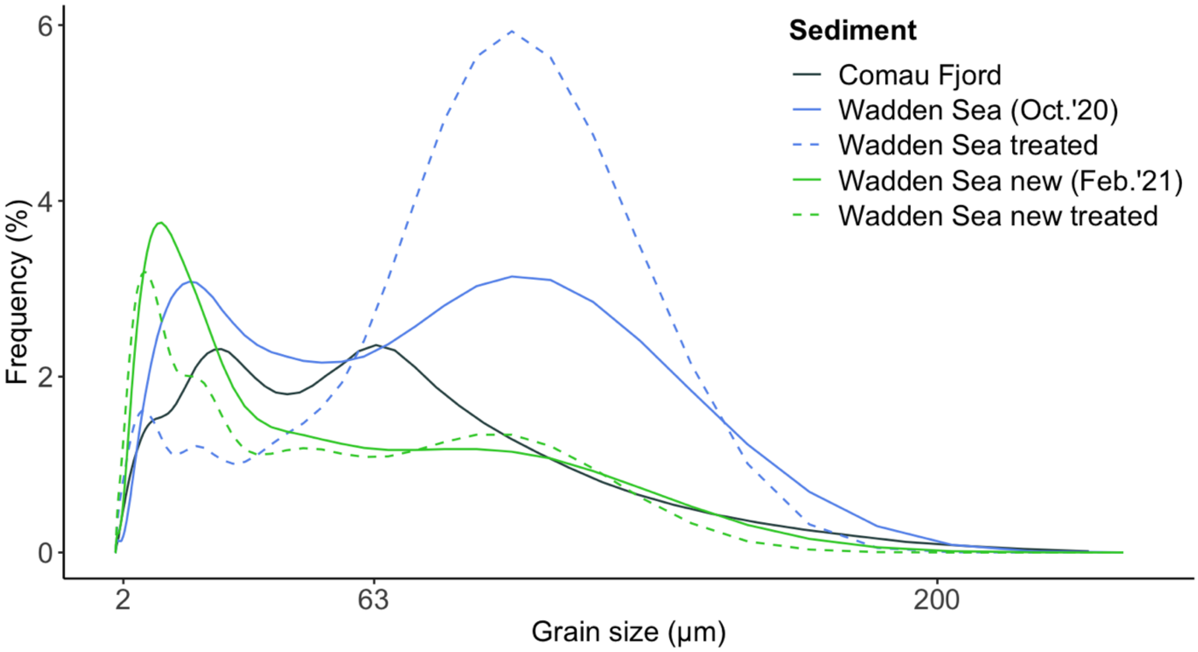

Figure 15: Grain size distribution displayed as "frequency" (%) for Comau Fjord (dark grey) and mixed Wadden Sea sediment from the first collection in October '20 (blue) and in February '21 (green), and after processing (freeze-dried, boiled with H_2O_2, washed three times; dashed line). The x-axis shows the grain size in µm. Clay (< 2 µm), silt (2 – 63 µm) and fine-sand (63 – 2000 µm).

The sediment collected from the beakers from the 100- and 1000-fold treatments showed a highly similar grain size distribution independent of the date when the origin sediment (see above) was sampled (Kruskal-Wallis test: p-value > 0.05, Fig. 16). Thereby, the sediment consists mainly of a high proportion of fine to middle silt (> 2 µm to 20 µm, frequency 77.38 ± 1.94 %) and clay (< 2 µm, frequency 15.11 ± 3 %), while sand-sized particles (> 60 µm) were scares (frequency < 1 %). The amount of material collected from the natural sediment concentration was not enough for the analyses.

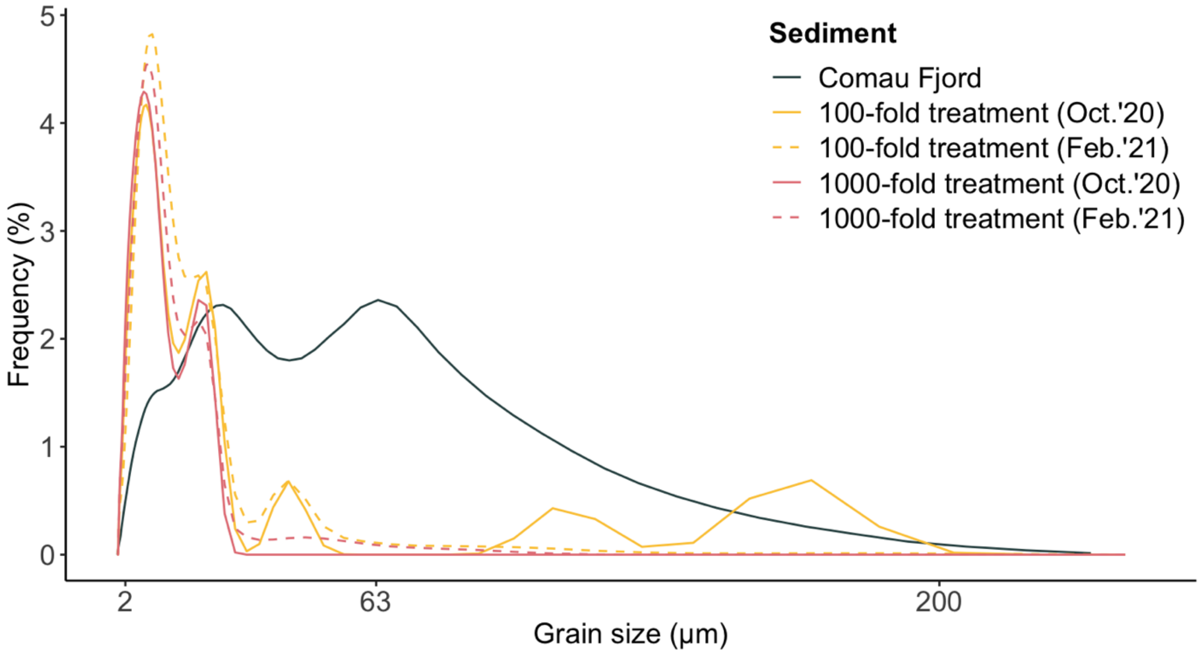

Figure 16: Grain size distribution displayed as "frequency" (%) for sediment collected from beakers compared to sediment from Comau Fjord (dark grey). The sediment is plotted from the 100-fold (In yellow) and the 1000-fold (red) natural sediment concentration. Solid lines show sediment from autumn '20, dashed sediment from February '21.

3.2 Water parameters

3.2.1 Nutrients

The Nitrate (Kruskal-Wallis: p-value > 0.05), Nitrite (Kruskal-Wallis: p-value > 0.05) and Ammonium (Kruskal-Wallis: p-value > 0.05) values did not show any significant difference between the treatments over the duration of the experiment. The phosphate values increased with the amount of sediment and showed significant differences between all three treatments (Kruskal-Wallis, post-hoc Dunn-Bonferroni: p-value < 0.001). The aside experiment, to see if increased phosphate values have an impact, showed phosphate values (0.88 ± 0.072 mg l^{-1}) similar high as in the 1000-fold concentration (0.83 ± 0.145 mg l^{-1}) (Tab. 2).

3.2.2 Physical water parameters and total alkalinity

Temperature

The temperature within the beakers was around ~11 °C with small deviations for all three treatments over the experimental time (Fig. 17, A). On average, the water temperature in the natural concentration was 10.89 ± 0.576 °C (lowest: 9.52 °C, highest: 12.16 °C), in the 100-fold 11.06 ± 0.733 °C (lowest: 9.32 °C, highest: 12.17 °C), and 11.3 ± 0.68 °C (lowest: 9.77 °C, highest: 11.96 °C) in the 1000-fold higher sediment concentration. The temperature within the treatments varied over time with the lowest values and strongest fluctuations in the first month. Also, the temperature of the controls, to see if increased phosphate levels had an effect, was done at ~11° C (10.98 ± 0.646 °C, lowest: 10.4 °C, highest: 12.4 °C).

Salinity

The Salinity in the beakers was approximately 32.5 for all three treatments (Fig. 17, B). The mean salinity in the natural concentration was 32.79 ± 0.48, in the 100-fold 32.78 ± 0.46, in the 1000-fold concentration 32.34 ± 0.39 and for the aside experiment with increased phosphate values 32.74 ± 0.46.

Oxygen and pH

There were no significant differences in pH between the three treatments neither to aside experiment with increased phosphate values (ANOVA, p-value > 0.05, Fig 17, C). The average pH value in the beaker was 8.12 ± 0.03 (natural: 8.11 ± 0.03, 100-fold: 8.12 ± 0.02, 1000-fold concentration: 8.12 ± 0.04, aside experiment with increased phosphate values: 8.12 ± 0.02).

The oxygen concentration between the treatments was not significant different (Kruskal-Wallis test: p-value > 0.05), averaged values were 8.91 ± 0.89 mg l^{-1} and 98.61 ± 8.34 % (Tab. 3). The increase in oxygen content around the 26th of March is due to a replacement of the oxygen sensor with a slightly different calibration (Fig. 17, D).

Total Alkalinity and aragonite saturation

The Total Alkalinity (TA) measured in the natural and 100-fold concentration as the artificial sea water (2999.71 ± 50.42 µmol kg^{-1}) did not show any significant differences (Tab 3). The TA in the 1000-fold sedimentation rate was significant lower (ANOVA, post-hoc Tuckey HSD: p < 0.001) than for the other treatments.

The aragonite saturation (Ω_{arag}) is slightly lower in the 1000-fold concentration but showed no significant differences from the ones of the other treatments (ANOVA, p-value > 0.05; Tab 3). The filtered artificial seawater (2.67 ± 0.378) showed significant lower Ω_{arag} values compared to the natural and 100-fold concentration (ANOVA, post-hoc Tuckey HSD: p-value < 0.01).

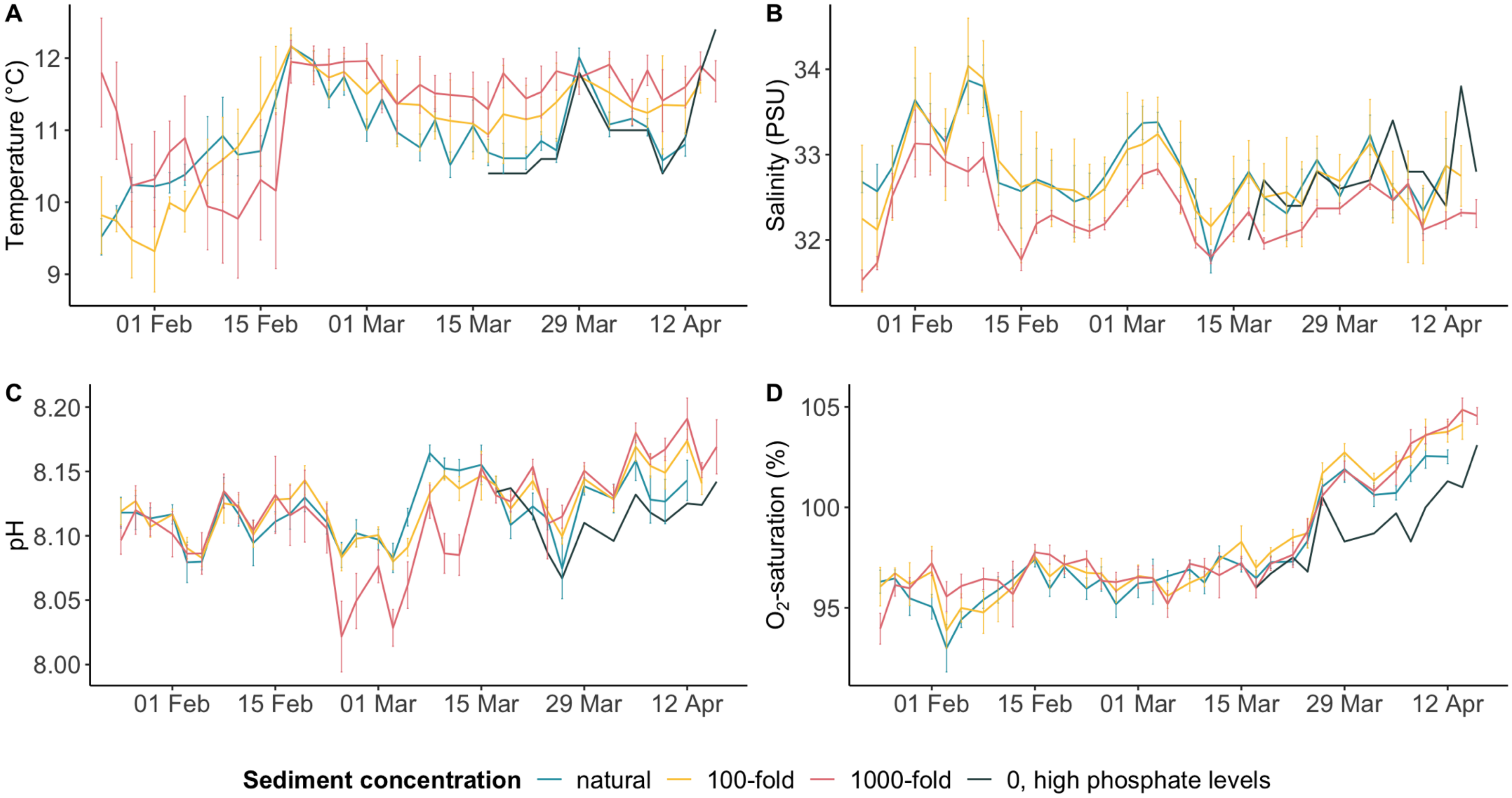

Figure 17: Water parameters for the beaker during the experimental time. Mean A) temperature, B) salinity, C) pH and D) oxygen-concentration for the natural concentration (0.0042 ml/l) in turquoise, 100-fold higher concentration (0.42 ml/l) in yellow, 1000-fold (4.2 ml/l) higher concentration in red as well as for the control with high phosphate values, but without sediment (0 ml/l) in dark grey. SD is displayed as error bar in the same colour as the treatment.

Table 2: Results of the weekly photometrically measured nutrient content (expressed as mean (± SD)). Beside the results from the treatments values for filtered artificial seawater, water in the husbandry aquarium and measured values from Comau Fjord are included.

Sediment concentration	**NH_4** (mg l^{-1})	**NO^{2-}** (mg l^{-1})	**NO^{3-}** (mg l^{-1})	**PO_4^{3-}** (mg l^{-1})
Natural (0.0042 m l^{-1})	0.16 ± 0.074	1.55 ± 0.005	1.42 ± 1.551	0.18 ± 0.06
100-fold (0.42 m l^{-1})	0.13 ± 0.048	2.51 ± 0.008	1.59 ± 2.511	0.33 ± 0.062
1000-fold (4.2 m l^{-1})	0.14 ± 0.048	2.05 ± 0.015	1.39 ± 2.049	0.83 ± 0.145
Aside experiment increased phosphate values	0.23 ± 0.059	0.25 ± 0.019	0.87 ± 0.251	0.88 ± 0.072
Filtered artificial seawater	0.01 ± 0.041	0.22 ± 0.004	0.59 ± 0.227	0.11 ± 0.196
Husbandry aquarium (Jan – Aug 2021)	0.01 ± 0.012	< 0.01	2.49 ± 1.136	0.19 ± 0.074
Comau-Fjord (Laudien et al., 2014; Wurz, 2014)	n.d.	n.d.	ca. 0.1 – 1.53	ca. 0.005-0.363

Table 3 Results of the statistical analysis of physical and chemical water parameters between the different treatments. Results are display as mean ± SD. Significant values p > 0.05 are highlighted in bold.

Sediment concentration	**Temp** (°C)	**Salinity**	**pH**	**Oxygen** (mg l^{-1})	**TA** (µmol kg^{-1})	$\boldsymbol{\Omega_{arag}}$
Natural (0.0042 m l^{-1})	10.89 ± 0.576	32.79 ± 0.48	8.115 ± 0.035	8.815 ± 0.227	3039.64 ± 76.66	3.35 ± 0.57
100-fold (0.42 m l^{-1})	11.06 ± 0.733	32.78 ± 0.46	8.124 ± 0.024	8.838 ± 0.235	3040.17 ± 77.69	3.46 ± 0.5
1000-fold (4.2 m l^{-1})	11.3 ± 0.68	32.34 ± 0.39	8.116 ± 0.039	9.056 ± 1.588	2819.81 ± 85.53	3.17 ± 0.43
Significance tests	Kruskal-Wallis	Kruskal-Wallis	ANOVA	Kruskal-Wallis	ANOVA	ANOVA
p-value	**0.01728**	**5.166 e^{-05}**	0.707	0.07257	**1.52 $e^{-0.7}$**	0.393

3.2.3 Turbidity

The turbidity values correlated positive with the added sediment concentration resulting in a determination coefficient of nearly 1 ($R^2 = 0.998$) (Fig. 18).

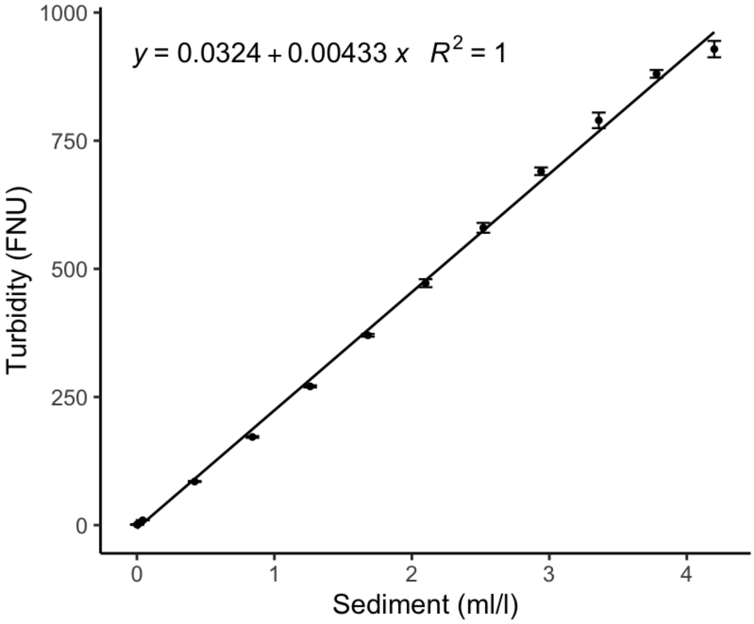

Figure 18: Turbidity calibration grades. Turbidity values (FNU, Formazine Nephelometric Units) for added sediment concentrations with determination coefficient.

To verify that the corals in the different sediment concentrations experienced different turbidity's, the latter were determined and were highly significant different between the treatments (Kruskal-Wallis: p-value < 0.001). Compared to the turbidity values of the control from artificial sea water, only the natural concentration does not show a significant difference (Kruskal-Wallis + Dunn-Bonferroni: p-value > 0.05; Fig. 19). Mean turbidity measured for artificial seawater is 1.3 ± 0.73 FNU (Formazine Nephelometric Units), for the natural concentration 1.5 ± 0.59 FNU, for the 100-fold 30.4 ± 26.25 FNU and for the 1000-fold concentration 425.1 ± 228.82 FNU. The turbidity varied over the time, highest values (natural concentration 1.7 ± 0.45 FNU; 100-fold 59.9 ± 19.68 FNU; 1000-fold 629.4 ± 206.31 FNU) were measured directly after the water exchange and lowest (natural concentration 1.1 ± 0.6 FNU; 100-fold 12.3 ± 3.41 FNU; 1000-fold 276.9 ± 113.45 FNU) three days thereafter, just before a new water change was conducted. This resulted in a decrease of suspended sediment of 12.31 % for the natural concentration, 79.43 % for the 100-fold, and 56 % for the 1000-fold concentration. The drop in turbidity values in the 100- and 1000-fold concentration between the 25th of February and the 12th of March was due to the different characteristics of the added sediment: in this case the sediment was frozen and thawed again. This led to the formation of clumps, which prevented a proper homogenizing of the sediment before the addition to the experimental chambers (Fig. 20).

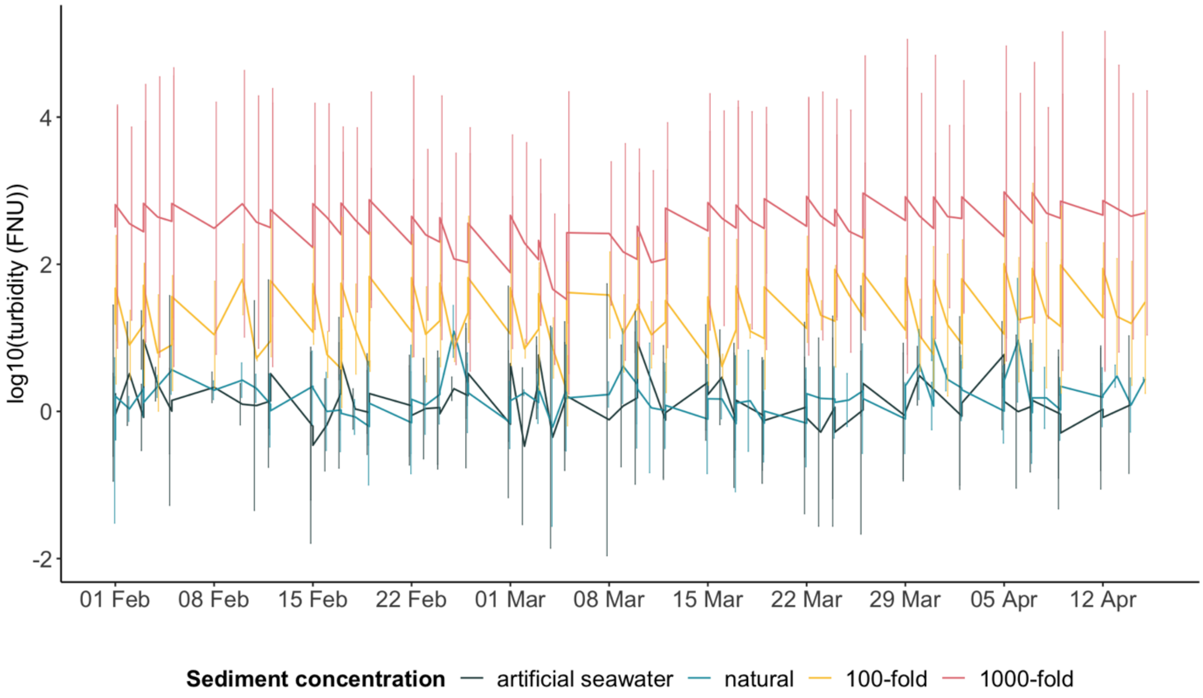

Figure 19: Logarithmically represented turbidity values according to artificial seawater (grey) and sediment concentration of the treatments (turquoise: natural concentration, yellow: 100-fold, red: 1000-fold higher concentration) over the entire study period. Error bar represent 1 standard deviation.

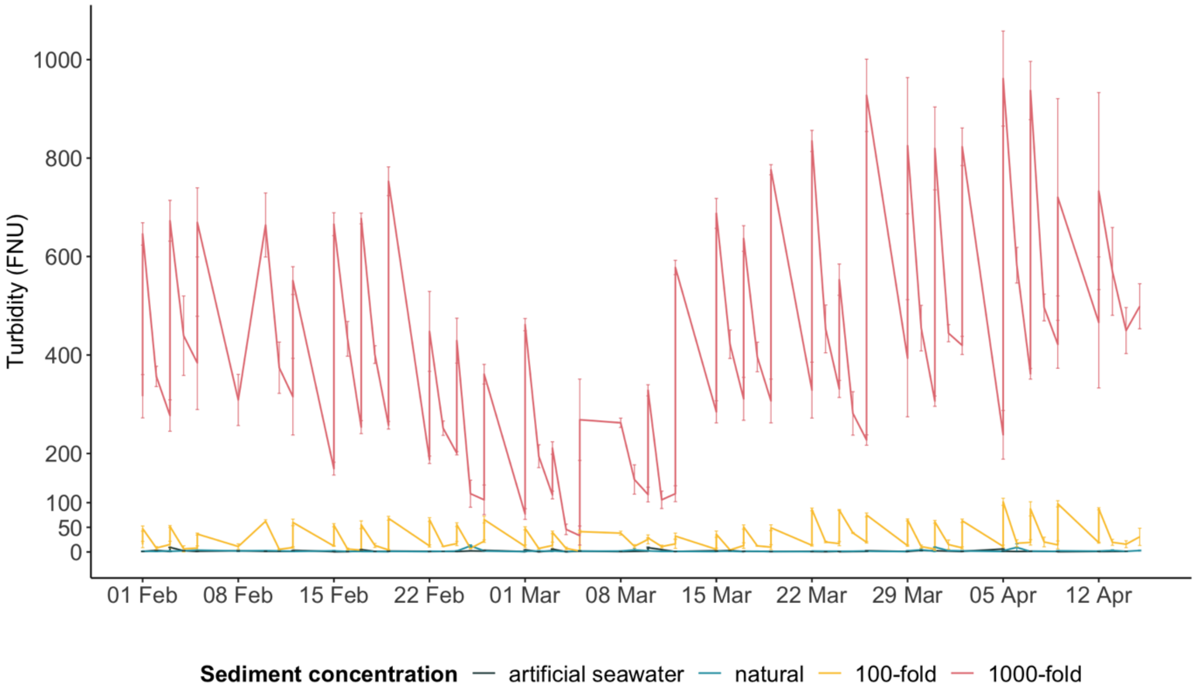

Figure 20: Turbidity in FNU over the experimental time for filtered artificial sea water as a control group (0 m l $^{-1}$, grey), the natural concentration (0.0042 m l $^{-1}$, turquoise), the 100-fold (0.42 m l $^{-1}$, yellow) and 1000-fold (4.2 m l $^{-1}$, red). Error bar represent 1 standard deviation.

3.3 Response variables

No coral mortality was observed during the whole duration of the experiment. However, in some cases a replicate was excluded from calculation of the growth rate, since the individuum detached from the screw and was reglued. The results of the response variables growth, behaviour and respiration are presented below.

3.3.1 Growth rate

3.3.1.2 Skeleton growth rate (mass variation)

The skeletal growth rate determined by weighting the juvenile specimens of *C. huinayensis* under the three sediment concentrations shows significant differences between treatments (SRH-test, $p < 0.001$). Corals exposed to the natural concentration ($n = 20$) show a mass increase of 0.14 ± 0.087 mg d^{-1} which corresponds to an annual mass increase of 51.67 ± 31.65 mg and a calcification rate of 1.4 ± 0.87 µmol $CaCO_3$ mg^{-1} d^{-1}. Individuals in the 100-fold sediment concentration ($n = 19$) showed a slightly lower mass increase of 0.09 ± 0.067 mg d^{-1} (36.4 ± 24.38 mg y^{-1}) and a calcification of 1 ± 0.67 µmol $CaCO_3$ mg^{-1} d^{-1}. A highly significant lower mass increase (Kruskal-Wallis test, post-hoc Donn-Bonferroni: p-value < 0.001) evince corals exposed to the highest sediment load ($n = 19$), with a growth rate of 0.003 ± 0.009 mg d^{-1} (1.17 ± 3.14 mg y^{-1}) and a calcification of 0.03 ± 0.09 µmol $CaCO_3$ mg^{-1} d^{-1}. Thereby horizontally oriented corals show a lower growth rate than vertically oriented corals (SRH-Test, $p < 0.05$).

Figure 21 shows the growth rate per day in percent separated into horizontally and vertically oriented corals out of the natural concentration (horizontal: 0.12 ± 0.06 % d^{-1}; vertical: 0.24 ± 0.13 % d^{-1}) the 100-fold (horizontal: 0.09 ± 0.06 % d^{-1}; vertical: 0.17 ± 0.1 % d^{-1}) and 1000-fold concentration (horizontal: 0.003 ± 0.006 % d^{-1}; vertical: 0.01 ± 0.2 % d^{-1}).

Corals in the aside experiment with increased phosphate values but without sediment did not show any significant difference in growth rate (0.21 ± 0.22 % d^{-1}) compared to the ones of the natural and 100-fold (Kruskal-Wallis test, post-hoc Dunn-Bonferroni: $p > 0.05$) sediment concentration, however, significant differences have been detected between them and the ones exposed to the 1000-fold concentration (Kruskal-Wallis test, post-hoc Dunn-Bonferroni: $p > 0.01$).

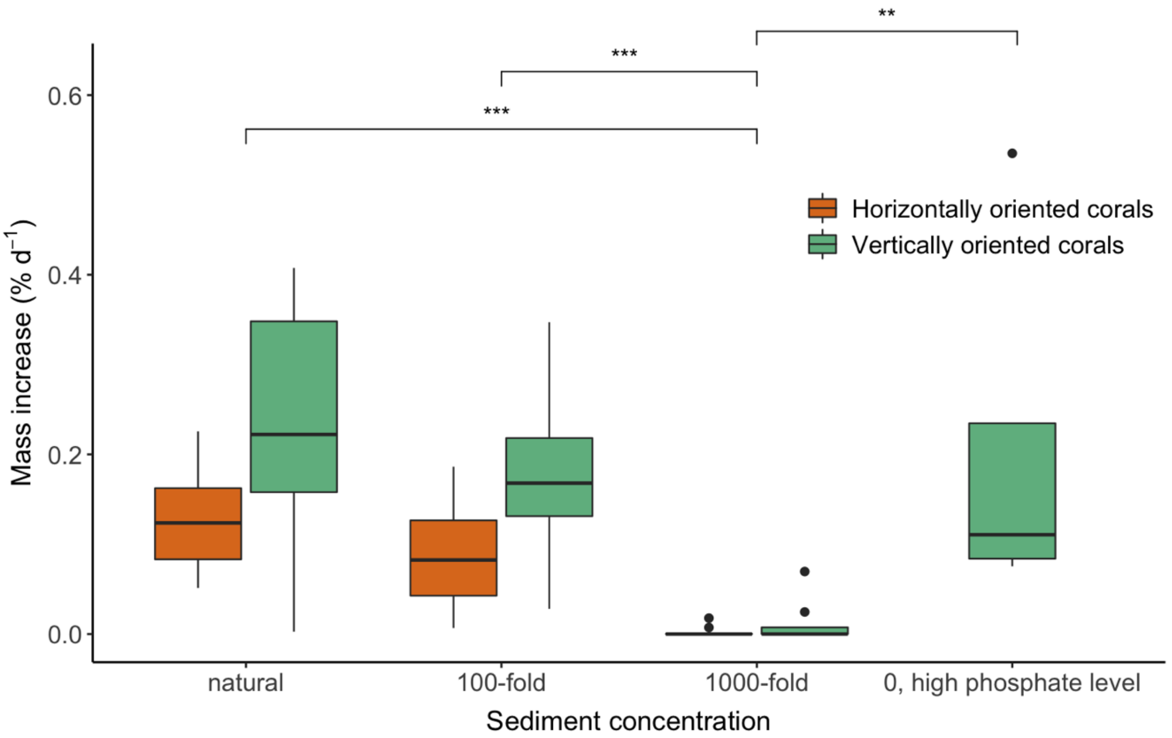

Figure 21: Mass increase for *C. huinayensis* expressed in % per day for the natural sedimentation rate (0.0042 ml/l), 100-fold (0.42 ml/l) and 1000-fold higher sediment concentration (4.2 ml/l), where orange boxplots display the horizontally and green the vertically oriented corals. The box of the boxplot represents the lower quartile with 25 % and the upper quartile with 75 % of the data. The median is drawn horizontally in the box with a thicker line. Vertical lines show the whiskers with minimum and maximum values. If a value exceeds 1.5-times the length of the box, it is considered as an outlier and shown as a dot. Furthermore, the significance levels between the treatments are shown with asterisk, with * < 0.05, ** < 0.01, *** < 0.

3.3.1.2 Calix diameter variation

The calix diameter increase (Fig. 22) shows a significance between the corals in the different treatments, with corals under the highest sedimentation rate showing a lower growth rate (Kruskal-Wallis, post-hoc Dunn-Bonferroni: $p < 0.001$) with an average of 0.017 ± 0.029 % d^{-1} (0.59 ± 1.028 µm d^{-1}, 0.22 ± 0.38 mm y^{-1}). Higher increase in calix diameter was displayed by corals exposed to the natural and 100-fold concentration with an average of 0.337 ± 0.124 % d^{-1} (13.64 ± 5.11 µm d^{-1}, 4.98 ± 1.87 mm y^{-1}) and 0.319± 0.154 % d^{-1} (12.86 ± 6.56 µm d^{-1}, 4.49 ± 2.39 mm y^{-1}), respectively. There were no significant differences in the increase of the calix diameter for the corals horizontally and vertically oriented (SRH-test, $p = 0.7$). Furthermore, a different increase between the first (week 0-6) compared to the second half (week 6-12) of the experiment was not detected. There was no correlation between the calix diameter and coral mass ($R^2 = 0.1$).

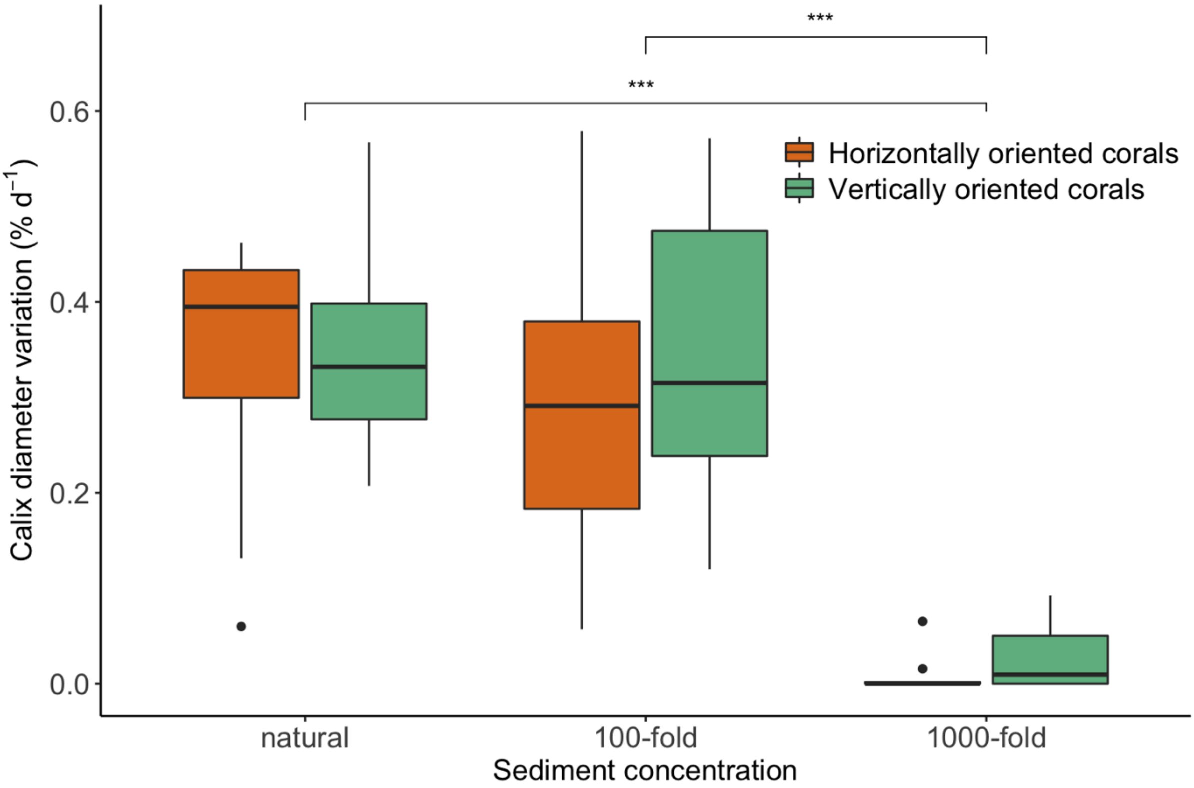

Figure 22: Calix diameter increase for *C. huinayensis* expressed as daily growth rate in percent for corals exposed to the natural (0.0042 ml l^{-1}), 100-fold (0.42 ml l^{-1}) and 1000-fold concentration (4.2 ml l^{-1}), where orange boxplots display the horizontally and green the vertically oriented corals. Significance levels are displayed with asterisk, where * < 0.05, ** < 0.01, *** < 0.

3.3.2 Polyp extension and tissue retraction

3.3.2.1 Polyp extension

The polyp extension of *C. huinayensis* measured as response to different sediment levels was significantly reduced (Kruskal-Wallis: $p < 0.001$) under the highest sediment concentration (1000-fold, n = 20), with an average extension of 36.3 ± 15.54 %, whereas corals under the natural concentration (n = 20) showed an average extension of 92.2 ± 7 % and the ones under the 100-fold concentration (n = 20) displayed 92.6 ± 11.85 % extension (Fig. 23). The position of the corals had a significant influence (SRH-test, $p < 0.05$) on the extension rate whereby horizontally orientated individuals displayed overall, and within the 1000-fold concentration a lower extension (Tukey HSD: p-value < 0.05). The potential influence of feeding in polyp behaviour was also documented: polyp expansion shows a very similar trend for corals under the control treatment, during and without feeding. While corals under the 100- and 1000-fold sediment concentration extended their tentacles significantly less (Tukey HSD: $p < 0.05$; Fig. 24, Tab. 4) on a day without feeding, which is even more significantly decreased for corals in the 1000-fold concentration being horizontally than vertically oriented. The extension rate of corals within the different treatments was relatively similar over time (Fig. 24).

The corals, which were exposed to the phosphate enriched water without sediment, had an average polyp extension of 91.7 ± 18.09 %, which was significantly higher as the one of corals experiencing the 1000-fold concentration (Dunn-Bonferroni: $p < 0.05$), significant differences to the other treatments were not detected.

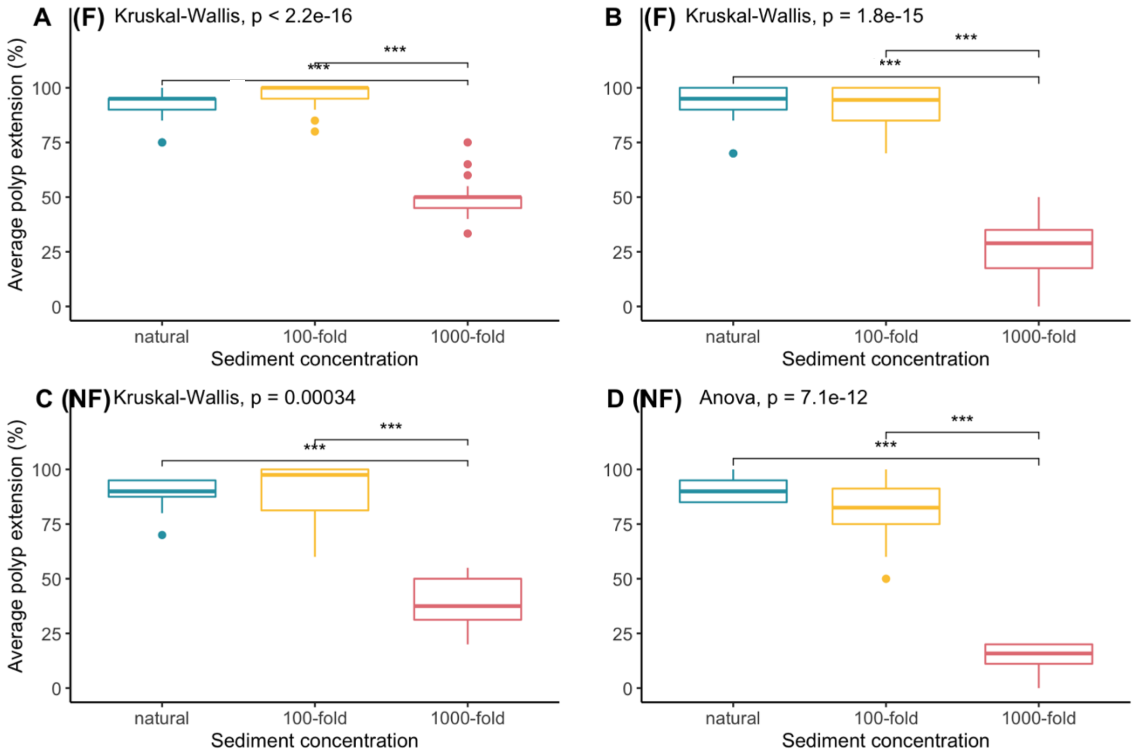

Figure 23: Averaged polyp extension displayed in boxplot for A) vertically oriented and B) horizontally oriented during feeding (F) and C) vertically oriented and D) horizontally oriented corals without feeding (NF), where turquoise displays animals exposed to the natural concentration (0.0042 ml l^{-1}), yellow to a 100-fold higher (0.42 ml l^{-1}) and in red to a 1000-fold higher concentration (4.2 ml l^{-1}). Level of significance ($p < 0.05$) between groups is shown as asterisk, where * < 0.05, ** < 0.01, *** < 0.001.

Table 4 Mean polyp extension in % with SD. Separated according to treatment, orientation (n = 10) and time of measurement with significant values $p > 0.05$ (highlighted in bold) between corals out of the same treatment but with different orientations.

Sediment concentration		**Natural** (0.0042 ml l^{-1})	**100-fold** (0.42 ml l^{-1})	**1000-fold** (4.2 ml l^{-1})
During feeding	p-value	1	0.11	**< 0.001**
	Horizontal	93.4 ± 7.97 %	92.1 ± 7.65 %	28.1 ± 11.81 %
	Vertical	92.3 ± 5.53 %	97.12 ± 5 %	49.2 ± 7.8 %
Without feeding	p-value	1	0.68	**< 0.001**
	Horizontal	90.6 ± 5.63 %	80 ± 17.11 %	14.2 ± 6.85 %
	Vertical	88.1 ± 8.84 %	88.75 ± 15.75 %	38.1 ± 13.35 %

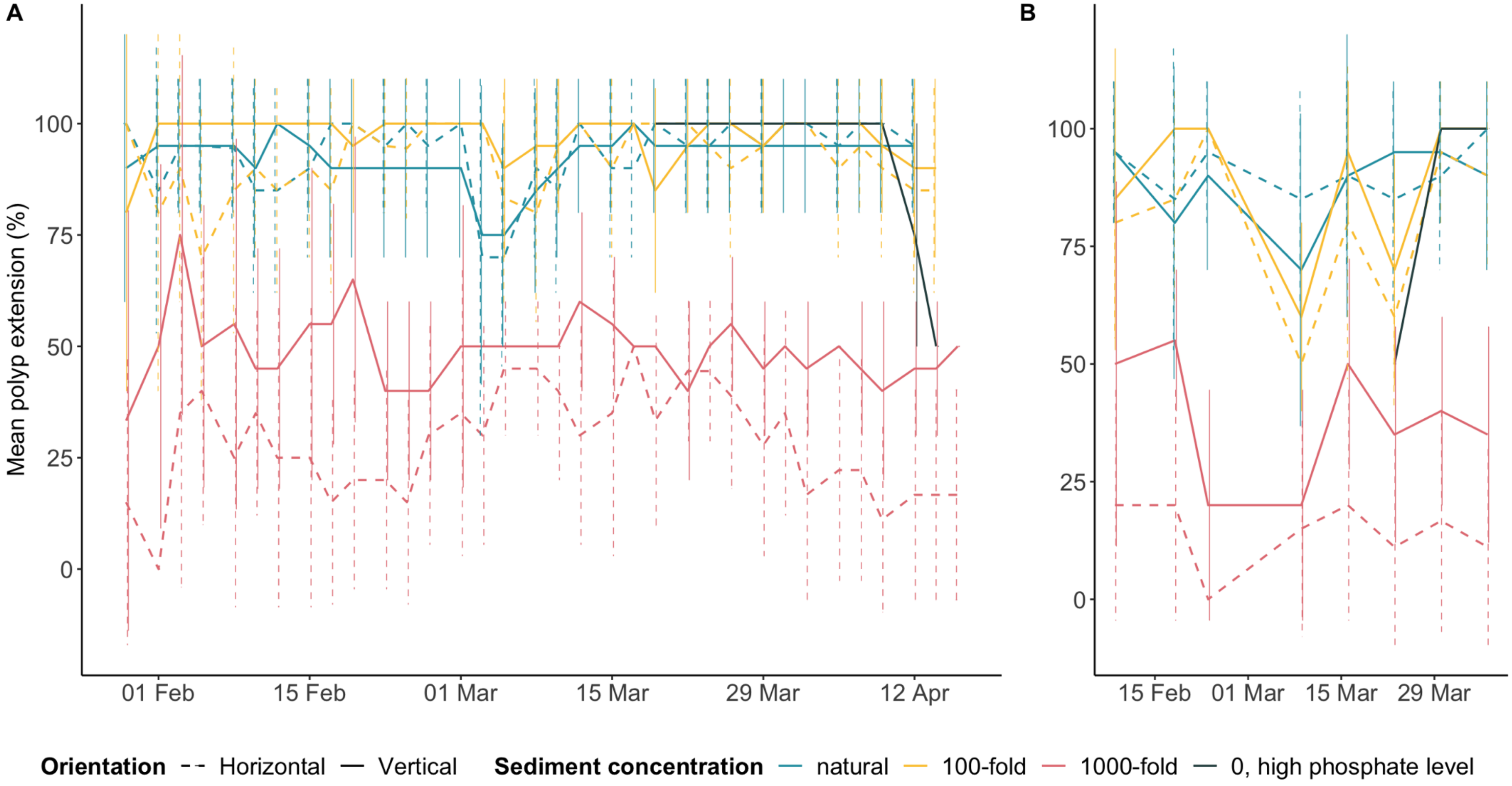

Figure 24: Mean polyp extension over the experimental period for *C. huinayensis* under natural sediment load (blue), 100-fold (yellow) and 1000-fold (red) as well as for the phosphate control (dark grey) and considering the polyp orientation (n = 10) with standard deviation in the same colour. Solid lines show the behaviour of corals facing vertical downwards and dashed lines horizontal oriented corals. A) observed polyp extension 2 h after food was supplied (observation: 3 × week) and B) without feeding (observation: 1 × week).

3.3.2.2 Tissue retraction

The retraction of tissue differed significantly between treatments (SRH: $p < 0.001$). Under natural sediment concentration, no tissue retraction was observed by any coral, instead some animals expanded their tissue over the glue (Fig. 25, picture D). Under the 100-fold higher sedimentation rate, 40 ± 51.6 % of the horizontally and 27 ± 44.5 % of the vertically oriented polyps partially retracted their tissue. A significantly higher number of corals (Kruskal-Wallis, post-hoc Dunn-Bonferroni: $p < 0.01$) exposed to a 1000-fold sediment load retracted their tissue from their skeleton (horizontally oriented: 90 ± 31.6 %, vertically oriented: 70 ± 45.8 %) (Fig. 25 B, C). Although not significant (SRH-Test: $p > 0.5$), a trend was seen that horizontally oriented corals retracted their tissue more often than downward oriented corals (Fig. 26).

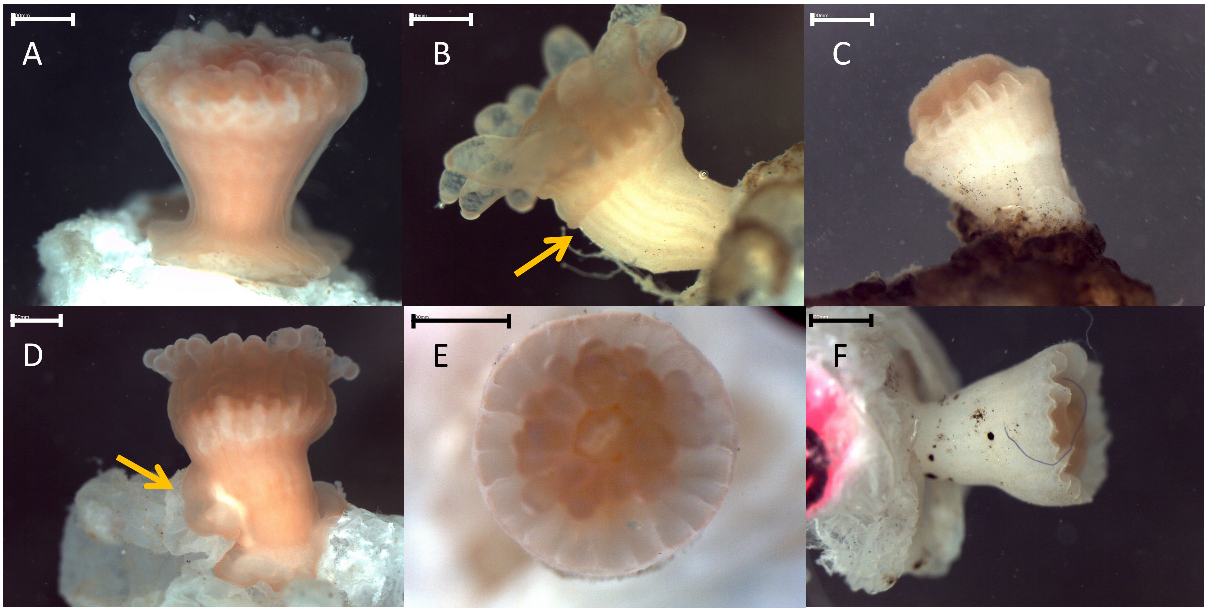

Figure 25: Pictures of tissue condition of *C. huinayensis* during the experiment. A) and D) showing corals after twelve weeks under the natural concentration. Pictures B, E, showing corals after six weeks, C, F after twelve weeks with partly retracted tissue in the 1000-fold concentration. Yellow arrow in picture B shows the part where the tissue retracts from the skeleton, in D tissue expands and growth over the glue. Scale in the pictures 1 mm.

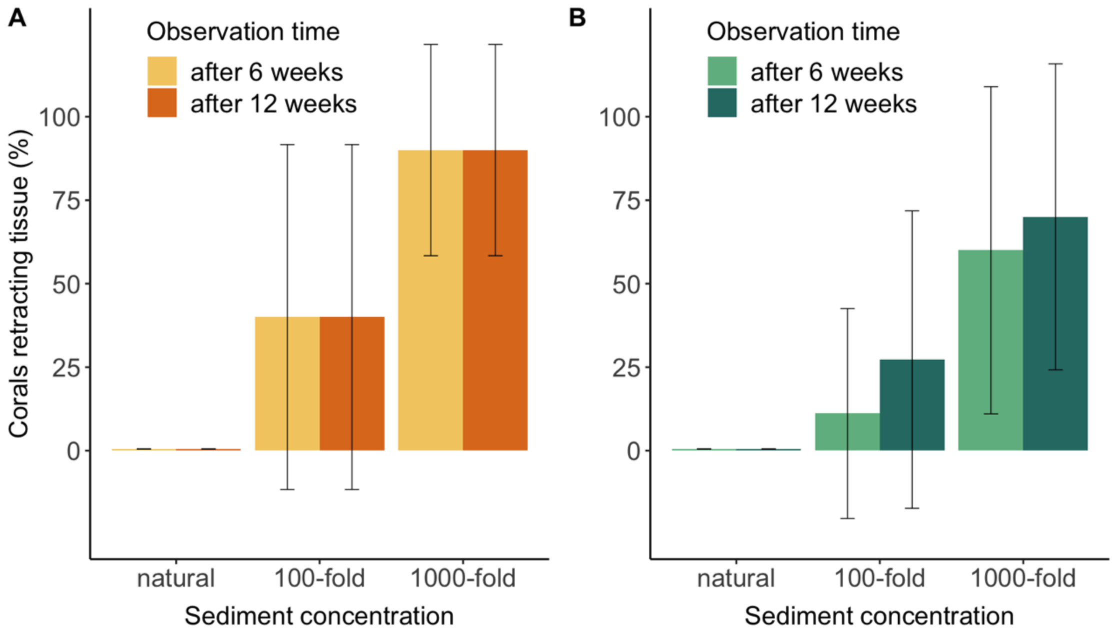

Figure 26: Partially tissue retraction in individuals of *C. huinayensis* as percentage, during the experiment after 6 (lighter colour) and 12 weeks (darker colour) divided into horizontal (A, blue) and vertical (B, red) oriented corals with SD expressed as error bars in grey.

3.3.3 Biomass and mass specific respiration

3.3.3.1 Ash-free dry mass (AFDM)

To obtain the mass specific respiration rate, the AFDM was determined for all coral individuals used in the respiration experiments. Thereby, the dry mass of the corals exposed to the 1000-fold concentration was lower, confirming that corals under heavy sedimentation load have a reduced growth rate in respect to corals from the other treatments (ANOVA, post-hoc Tuckey's HSD: p-value < 0.01). Further, the percentage of organic components (AFDM; natural concentration 13.3 ± 1.8 %, 100-fold concentration 19.8 ± 4.2 %, 1000-fold 29.6 ± 13.5 %) is higher for corals that were exposed to the 1000-fold concentration, but the mass of organic matter is similar between all three treatments with a p-value of 0.118 (Kruskal-Wallis test; natural concentration 2.6 ± 1.1 mg, 100-fold concentration 3.7 ± 1.2 mg, 1000-fold 2.7 ± 1 mg). The mass (exposed to natural concentration: 1.01 ± 0.396 mg, exposed to 1000-fold concentration: 1.05 ± 0.689 mg) and percentage (15.76 ± 5.33 % and 15.98 ± 8.43 %, respectively) of AFDM for newly glued corals used for short-term incubation was almost the same among each other.

3.3.3.2 Mass specific respiration rate

The respiration rate of the horizontal and vertical orientated corals showed no significant difference between each other (two-way ANOVA, p-value > 0.05). Therefore, all individuals were pooled.

After long-time exposure (three months) to different sediment concentrations, the mass specific respiration rate of *C. huinayensis* was significantly different between corals of the distinct treatments (ANOVA, p-value < 0.001; Fig. 27, A). The oxygen consumption for corals exposed to the highest sedimentation concentration was lowest (natural: 0.0113 ± 0.0038 mg O_2 mg AFDM d^1, 100-fold: 0.0075 ± 0.0024 mg O_2 mg AFDM d^1 and 1000-fold concentration: 0.0039 ± 0.0019 mg O_2 mg AFDM d^1).

Individuals, newly exposed (24 h) to sedimentation load showed no significant different mass specific respiration rates (Welch Two Sample T-Test, p-value > 0.05) with a mean of 0.0081 ± 0.0042 mg O_2 mg AFDM d^1 when exposed to the natural concentration (n = 8) and 0.0103 ± 0.0066 mg O_2 mg AFDM d^1 when exposed to the 1000-fold higher concentration (n = 10). However, 50 % of the corals in the 1000-fold treatment showed higher respiration rates than the other half (indicated in dots in Fig. 27, B).

Furthermore, corals under the natural sediment concentration in the short- and long-time experiment did not reveal a significance between their oxygen consumption (two-way ANOVA, p-value > 0.05).

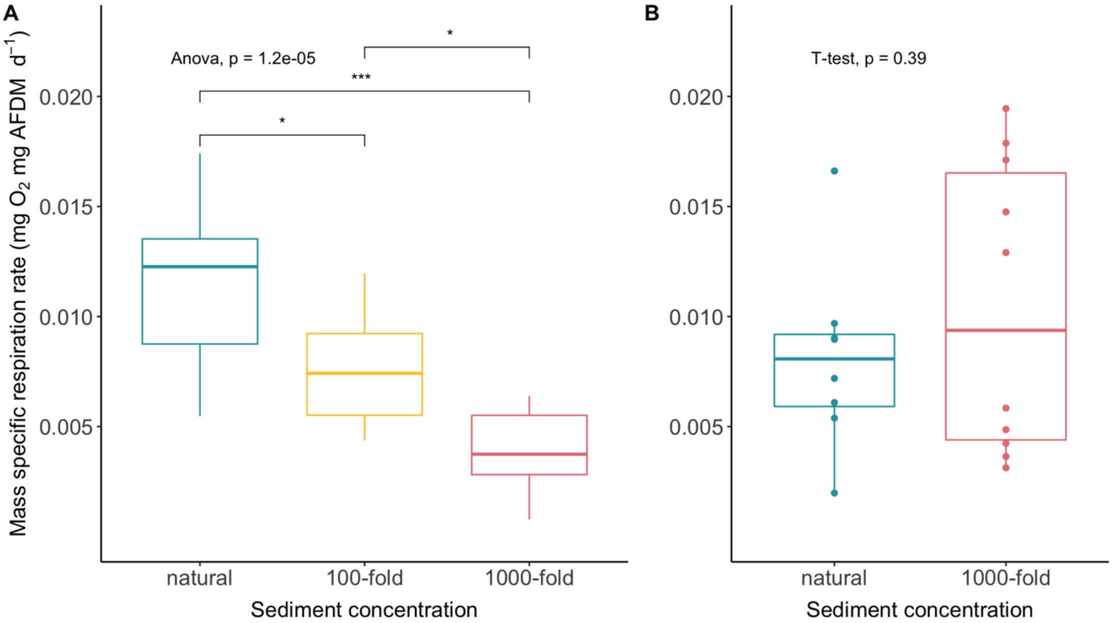

Figure 27: Mass specific respiration rates of long- (A) and short-time (B) exposed *C. huinayensis* to different sediment concentrations, natural (0.0042 ml/l, turquoise) 100-fold (0.42 ml/l, yellow) and 1000-fold concentration (4.2 ml/l, red). Dots in B show the individual data points of the calculated respiration rates of the corals in the respective concentration (same colour). With level of significance ($p < 0.05$) shown as asterisk, where * < 0.05, ** < 0.01, *** < 0.001.

4 Discussion

4.1 Methodical considerations and technical issues

The characteristics of this study as *ex-situ* experiment mean, that the experimental conditions have been generated trying to simulate a real scenario as much as possible, but with the advantage that all important factors (e.g., temperature, salinity, oxygen, nutrition) can be controlled. Especially nutrition has great effects on the overall fitness (i.e., Eder et al., 2018) and therefore on the outcome of the experiment. In this study all individuum's could be provided with the same amount of food to exclude variabilities which are likely to occur in nature. Another advantage is that animals can be studied, that otherwise live at great depts where it is difficult and expensive to study their biological processes in the natural environment (Orejas et al., 2019). Therefore, laboratory studies are a good way to demonstrate the effects of single or coupled stressors in a managed environment (i.e., Eder et al., 2018; Gori et al., 2016) and this experiment offers the possibility to reveal causalities but must simplify complex interactions by disregarding or stabilizing other parameters.

4.1.1 Sediment

The granulometry from Comau Fjord sediment and Wadden Sea sediment showed a broad similarity with a bimodal distribution and grain sizes from minimum sizes of < 2 µm to approx. 200 µm. Although the sediment from the Wadden Sea has a shift in frequency towards the smaller grain sizes particles. Further, sediment collected in February 2021 showed an even higher component of fine to middle silt compared to the earlier collected sediment from (October 2020). Reasons for the differences in the Wadden Sea sediments may be due to minor differences between the exact sampling spot, seasonal differences in the sampling period (autumn 2020 — winter, with partial ice cover: see Fig. 28) and possible variations in the sieving process carried out by different people in October and February.

Figure 28: Ice layer over the Wadden Wea sediment off Spieka-Neufeld on 16.02.2021. © J. Laudien

Sediment from Comau Fjord was collected at different angles of inclination via sediment traps attached to cement pipes in the subtidal zone for 4 weeks (20.01. – 16.02.14) (Gottschlich, 2014). The mean grain size distribution from that provides an average sediment load to which animals in Comau Fjord are exposed to. However, artificial sediment, which could be mixed exactly according to the composition in the fjord sample, would not have the same physical properties (size, form, weight) as natural sediment grains and therefore have an impact on a realistic outcome of the experiment. Further, sediment samples are always influenced through the origin, the seasonality, way of sampling and processing. As it was not possible to obtain sediment from Comau Fjord and because there will be different sources (blasting, various input through roads, salmon farms, etc.) with unpredictable influence, which increase the sediment load, sediment from the Wadden Sea is the best alternative to sediment from the fjord itself.

After processing the sediment with H_2O_2, the grain size frequency of the collected Wadden Sea sediment from February stayed similar, while the one collected earlier shifted towards a larger frequency in fine sand. Likely, larger parts of the fine fraction were discharged during washing.

Nevertheless, sediment, collected from the overspill of the treatments with 100- and 1000-fold concentration showed for both sampling times (October ‘20, February ‘21) a highly similar grain size distribution (no significant differences, Kurskal-Wallis-test: $p\text{-value} > 0.05$, see Fig. X), thus the same grain size distribution may also be assumed for the natural concentration. The highest grain size frequency was in clay < 63 µm, indication that larger sediment particles settled during the experiment, which is confirmed by the fluctuations in the turbidity values. Regarding to the calibration coefficient of the turbidity, the 100-/1000-fold concentration in mean was more a ~30/400 times the amount of the natural concentration, respectively. By the decreased turbidity values over time, a natural situation was simulated, as it occurs in Comau Fjord, in which fine sediment on the one hand remains longer in the water column and on the other hand also has a greater drift, hence a more widespread effect (Försterra, 2009). As in the fjord, corals in the experiment thus had a longer exposure to fine sediment particles. In addition, the reintroduction of sediment simulated events that would also occur under the influence of anthropogenic influences, such as the sequence of blasting events, interruptions of construction activities during the night/weekend, cyclical changes in the water body, and similar events.

4.1.2 Some considerations regarding the experimental set-up

To achieve comparable results, corals of the same size were selected. Since an exact age determination was not possible due to the constant reproduction in the husbandry aquarium, which in comparison to many warm water corals (Richmond and Wolanski, 2011), does not show a common reproductivity event. Another advantage is that the animals have different parents, which increases the genetic diversity and minimises the possible influence of the same resistances against sediment in the genes of the parents (Baums, 2008).

During the respiration measurements it was observed that the sediments in the 1000-fold concentration partially settled. The effect seemed stronger in some incubation chambers than in others. However, this could not be measured since after the experiment incubation chambers were moved to remove the corals, which stirred up the settled sediment again and thus falsified the measurements. To create a more even turbidity in the incubation chambers, an increase in the stirring speed would certainly have helped. Nevertheless, this was not done for two reasons: first, an increasement of the stir-speed would have had affected the temperature, which has influences on the outcome and comparability with the other measurements; second, the increased flow velocities could cause changing tentacles movement. This is reported for *L. pertusa*, which had a lower polyp expansion under higher velocities (Orejas et al., 2016). Therefore, this may cause additional stress. However, the fluctuations in turbidity could explain the greater fluctuations in the respiration rate of the corals from the short-term experiment under the highest concentration (see Chapter 3.3.3.2).

4.1.3 Considerations on the methods applied to measure the response variables

The calculation of the calyx diameter variation showed for some individuals a decrease. This occurred, with one exception in the 100-fold concentration, only in corals exposed to the highest sediment concentration (1000-fold). There are two possible sources of error. The first is that small differences in distance from coral to microscope can cause errors in size. To rule this out, the corals were always treated the same and placed in a homemade holder. However, some specimens had not grown straight and had to be rotated a little to photograph an even calix. If these were photographed a second or third time, it is possible that the coral was rotated a little more or a little less, which led to minimal changes in the measurement. The second is related to the coverage of the calix by tissue and occurred due to the generally low growth rate of animals in the 1000-fold concentration. At the beginning of the experiment, the skeleton of the corals was completely covered with tissue; this was also the case when the animals retracted their tentacles. However, this also means that the tissue probably caused a slight blurring or a scattering of light through the tissue layer of the calix. At the end of the experiment, the calix was partially exposed, so that it could be measured much more accurately. This probably led to a smaller calix circumference measured for the same individual as in the measurement before, and therefore to negative rates in the end.

The results of the growth rates revealed slightly different results when measured through calix diameter increase and through the buoyant weight method. While with the buoyant weight method showed lower growth rates for horizontally orientated corals, the measured calix diameter does not show differences between the orientation of the individuals. This points out that, when considering and comparing growth rates, the method must always be taken into account. However, depending on the study, the mentioned methods have advantages or disadvantages. In this case, both methods have the advantage of being non-destructive and thus can be carried out continuously. For example, the buoyant weight method is one of the most commonly used methods for measuring skeletal growth in corals (Orejas et al., 2019), but can only be used in aquarium experiments. In contrast, the calix diameter method offers the advantage of being able to be used in *in-situ* studies with simple equipment. However, growth by calix diameter alone is not a sufficient proxy as it can lead to under- or overestimation since corals may show different levels of growth in diameter or length (Fig. 29). This can also be particularly pronounced with different parameters. Therefore, in addition to the diameter of the calix, the length of the coral skeleton should also be measured. Nevertheless, a comparable result was shown by both methods in this experiment.

Figure 29: Two individuals of *C. huinayensis* in approximately same high but with different calix size. Image from Domansky (2020)

4.2 Effects of increasing sediment load on the physiological performance of *C. huinayensis*

After three months under sediment exposure no lethal effects were observed for juvenile *C. huinayensis*, suggesting that they are relatively resistant to long-term increased sediment loads and that their threshold level lies above the 1000-fold sedimentation load of 4.2 ml l^{-1}. This is not surprising considering their natural occurrence in a region with high run off (Försterra, 2009). The results also indicate that juvenile can cope with an increase of 100-fold the natural concentration, which is the amount that would be expected from a gravel road (Reid and Dunne, 1984), under sufficient nourishment. Despite that, large amounts of sediment show a high impact on the physiological performance and behaviour of juveniles. If these conditions sustained over a longer period than three-month, they may cause mortality in the juveniles (Erftemeijer et al., 2012).

4.2.1 Effect of increasing sediment load on the growth rate

After 12 weeks of exposure to different sediment concentration juveniles of *C. huinayensis* showed a similar increase in calix diameter in the natural and 100-fold sediment concentration (4.98 ± 1.87 mm y^{-1}; 4.49 ± 2.39 mm y^{-1}) as reported for recruits of *C. huinayensis* maintained under aquarium conditions

(4.2 ± 0.03 mm y^{-1}) (Heran, unpublished data). However, significantly decreased growth ~95 % (assessed through buoyant weight and calix diameter) under the 1000-fold sedimentation concentration compared to the natural concentration was detected. This confirms the first hypothesis that corals show reduced growth under heavy sediment loads and rejects the null-hypothesis.

An influence through the pH value (8 – 8.2) on the different growth rates, which lie in the upper range of the pH in the fjord (7.4 – 8.3) (Jantzen et al., 2013a) can be ruled out since there was no significant difference between the treatments. The same applies for the oxygen concentration, which was always above 90 % for all treatments and thus provides an adequate oxygen supply for calcification (Nelson and Altieri, 2019).

Temperature is an important factor that affects growth rate of scleractinian corals (Orejas et al., 2011; Gori et al., 2016). Although, the temperature and salinity between the 1000-fold towards the natural and 100-fold concentration showed significant differences, these were not relevant regarding the small deviations and the overall fluctuations. All treatments showed a temperature of ~11 °C (natural: 10.89 ± 0.576, 100-fold: 11.06 ± 0.733, 1000-fold concentration: 11.3 ± 0.68) and salinity of ~32.5 (natural: 32.79 ± 0.48, 100-fold: 32.78 ± 0.46, 100-fold concentration: 32.34 ± 0.39) and therefore, stayed in the natural temperature of 8 °C to 13.5 °C and salinity range of 28.5 to 34.1 (Cairns et al., 2005; Jantzen et al., 2013a; Laudien et al., 2014) as corals of *C. huinayensis* experiences in the fjord.

Reichardt (2017) showed average TA of 2233 µmol l^{-1} for Comau Fjord. The measured TA in the treatments lie above that value. However, there is a significant lower TA for the 1000-fold concentration compared to the artificial sweater and the other concentration. As phosphate is part of the ion concentration of TA (Kawahata et al., 2019), the lower values in the 1000-fold concentration are probably due to the increased phosphate content in the beakers of the 1000-fold concentration. Nevertheless, the Ω_{arag} does not differ significantly between the treatments, while there is a small decrease in the highest sediment concentration. In Comau Fjord, Ω_{arag} lies between 0.76-1.6 (Jantzen et al., 2013a), thus is lower than in the experiment with a mean Ω_{arag} above 3. Indeed, all treatments where oversaturated ($\Omega_{arag} > 1$) which offers a good basis for calcification (Jiang et al., 2015; Hoegh-Guldberg et al., 2017) and excludes impacts on growth through missing calcium carbonate.

The PO_4 content increased with sediment load, suggestion the accumulation of phosphate in the water due to the addition of sediment. Since high phosphate values may negatively affect calcification of corals (Dunn et al., 2012), the impact was checked through a side experiment. A negative effect through the increased PO_4 content in the 1000-fold concentration can be excluded as corals, exposed to the same amount of PO_4 without sediment, did not show a significant different growth rate as corals in the natural and 100-fold concentration but towards corals in the 1000-fold concentration.

While there is a significant reduced growth rate detected for juvenile *C. huinayensis* exposed to the highest sediment load, no significant differences in the growth rate between corals exposed to the natural and 100-fold treatment could be measured. However, the long-term respiration experiment showed that juveniles under the 100-fold sediment concentration had a lower metabolic rate then corals under the natural sediment load. They also partly retracted their tissue. These results indicate that the corals in the 100-fold concentration were affected by increased sediment load. However, they could keep their growth rate. A reason for that could be the sufficient feeding. High food supply helps animals to compensate for stress. For example, Eder et al. (2018) showed that the effect of elevated temperature on juvenile hydroids (*Hydractinit echinata*) was mitigated by an increased food supply, under which the animals maintained their former growth rate. For the CWC *D. dianthus* maintained in different pH milieus, Martínez et al. (2020) found a positive effect on the net calcification rate and the overall performance with a higher feeding frequency. The fact, that corals in the 100-fold treatment showed a similar high polyp behaviour and therefore maybe the same sufficient food intake as corals under the natural sediment concentration, supports this hypothesis.

A decreased growth rate in corals exposed to different stressors , such as microplastic (Chapron et al., 2018) or ocean acidification (Gori et al., 2016) have already been reported. In this cases corals could not catch sufficient nutrition (Chapron et al., 2018) or used their energy for essentials to survive (Gori et al., 2016).

The sedimentation load in the 1000-fold treatment was higher than in most other studies (see Tab. 1). However, the turbidity values dropped sharply in the 100- (~70%) and 1000-fold concentration (~40) between the water changes, simulating natural variability as they will be occurring for the different influences on the fjord (e.g. landslides, multiple blast events, construction work, varying rainfall intensity). Larsson and Purser (2011) found that the addition of natural sediment and drill cuttings (65 and 195 mg cm^{-2}, grain size < 1 mm) settling on test corals (*L. pertusa*) had no effect on their growth rate, but some polyps became covered in drill cuttings and consequently smothered (Tab. 5). In contrast, Larsson et al. (2013) showed significant decreased growth rates, when exposing the same species to drill cuttings and natural sediment kept in suspension of 25 mg l^{-1} (Tab. 5). Moller et al. (2017) studied the effect of sediment on juvenile warm-water corals and documented the highest influence on the growth rate in the first four weeks after settling. In the present study, no effect on the calix growth of the CWC between the first half of the experiment (week 1-6) and the second half (week 7-12) was detected. This suggests that the effect is constant on juveniles after settlement and acclimatization.

The calculation of the AFDM revealed, that corals from the long-term experiment showed a higher percentage of organic components (e.g tissue) under the 1000-fold concentration, in which the corals also had a lower growth compared to the other treatments. This could be due to the fact that the tissue in all tested animals hardly grew at all over time and only the skeletal mass increased, or that under high sediment load stressed animals relate more energy into tissue growth than in skeletal growth. The division between tissue and skeletal growth is an important trade in Scleractinia under resource limitation or physiological stress (Anthony et al., 2002). A higher energy allocation into tissue growth is also suggested for other CWC's as *D. dianthus* and *L. pertusa*. Orejas et al. (2011) suggested the greater polyp size as a cause. Whereby, Anthony et al. (2011) showed that under sedimentation stress two warm-water Scleractinia (*G. retiformis* and *P. cylindrica*) invested more energy in skeletal mass than in tissue growth. These are considerations that cannot be substantiated by the measured methods alone, as it is not known how much weight the tissue represented at the beginning of the experiment.

4.2.2 Behaviour of *C. huinayensis* under increased sediment load

Under the highest sediment concentration (1000-fold), the polyp extension significantly decreased. Therefore, the second hypotheses, that corals reduce their activity under strong sedimentation can be confirmed and the null hypotheses rejected.

A decreased polyp extension was also shown by Larrson et al. (2013), when the CWC *L. pertusa* was exposed to the highest concentration of suspended sediment smaller than 63 µm (25 mg l^{-1}), which was further related to a lower growth rate. Withdrawn tentacles and a mucus release by *L. pertusa* was also reported by Allers et al. (2013) when corals were covered with anoxic sediments (see Tab. 5). Furthermore, a contracted polyp for a prolonged period, was also documented by Liefmann (2018) for the cold-water soft coral *Duva florida*, when exposed to 8 mg l^{-1} rough edged mine tailings. For the warm water gorgonia *Subergorgia suberosa*, Tseng et al. (2011) reported a lower polyp extension when exposed to sediment loads of 50, 150, 250 mg l^{-1}.

The retraction of the sensitive tentacles may provide protection of their tissue against the suspended sediment grains. Further, this could protect the corals feeding mechanism, as finer particle may be harder to reject and could clog the feeding mechanism. However, the lower extension rate impairs prey capture und thus nutrition of the corals, which can be confirmed by significantly lower growth rate of corals exposed to the highest sediment load (see Fig 21 and 22). When *L. pertusa* was exposed to micro- and macroplastic, the coral decreased their polyp activity (measured as moving polyps) in the first 7 days. Thereafter, corals increased their activity slowly, but still had a lower activity when exposed to microplastic compared to the control group without plastic particles. While corals exposed to macroplastic increased their activity significant. The authors discussed that the increased polyp movement could compensate the lower prey capture (Chapron et al., 2018). However, as under microplastic (<5 mm) the activity was still decreased. Together with the results of this study and the knowledge that corals show a similar ability to reject particles of the same size (Larsson and

Purser, 2011) this may indicate, that smaller particles are harder to reject and therefore the retraction of tentacles is a “protection” mechanism of the corals. This can further be supported by the result, that on days were corals were not fed, the extension of the polyps in the 100- and 100-fold concentration, was significantly lower.

The corals' repulsive behaviour towards sediments includes increased cilia and tentacle activity, body expansion and mucus secretion (Thompson and Bright, 1977; Rogers, 1990). However, active cleaning behaviour through increased tentacle movements could not be observed in this experiment and due to the small size of the corals, it was also not evident whether the individuals expanded their body differently among treatments. However, there were observations of mucus production, which is a well-known “clearing behaviour” to get rid of sediment and has been reported from various authors for warm- (Rogers, 1990; Wild et al., 2004; Jones et al., 2019) and CWC (Larsson and Purser, 2011; Allers et al., 2013). The sediment gets captured in the mucus and the mucus is than repelled by the corals. Thereby mucus can form “sediment aggregates” (Wild et al., 2004). During the experiment, small apparent lumps of sediment on the ground and rarely small filaments hanging from the coral could be observed in all treatments, which are probably sediment-mucus aggregations. Beside these observations, a coral specimen from the experiments (100-fold concentration) was observed under the stereomicroscope and a mucus sheet was detected (Fig. 30), indicating that *C. huinayensis* produce mucus under stress situation. This is the first-time mucus production on *C. huinayensis* could be observed.

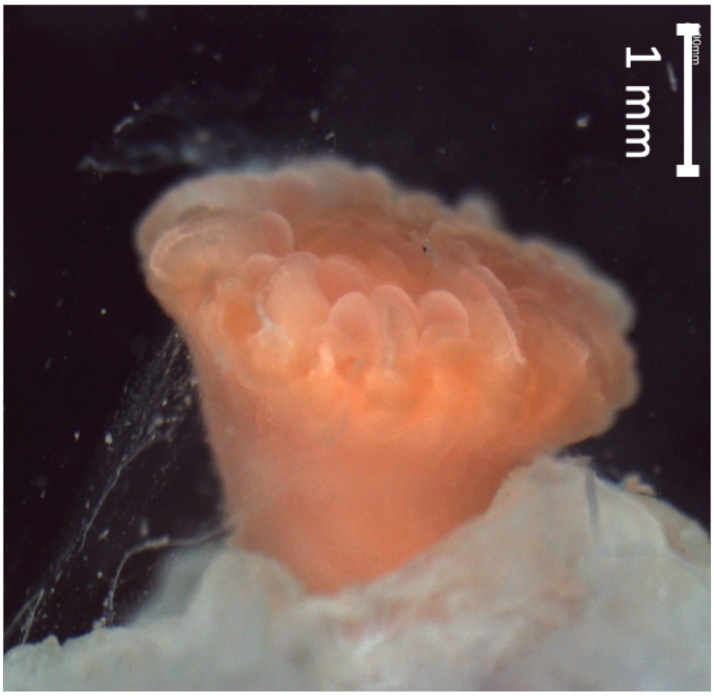

Figure 30: Mucus filaments on juvenile *C. huinayensis* glued on a screw and six weeks exposed to a sediment concentration of 0.42 ml l^{-1} (T1)

As detailed in the results section (chapter 3.3.2.2), retraction of tissue from the skeleton of the corals towards the calix has been observed as a consequence of the increase in sediment concentration. This confirms the third hypothesis that corals (partly) retract their tissue under high sedimentation and rejects the null-hypothesis.

Warm-water corals can cyclically expand and retract their tissue (Brown et al., 2002). An example is, that corals fall dry due to the tide and retract their tissue as a "protective mechanism" against increased solar radiation (Brown et al., 2002, 1994). However, in this case there is no periodically effect and the retraction of tissue shows therefore a stress response towards increased sediment load. Furthermore, sediment can injure the tissue and lead to loss. In both cases, the loss of tissue has negative effects on corals, as the bare skeleton is no longer protected from the colonization of microborers and putrefactive organisms (Försterra and Häussermann, 2008; Larsson and Purser, 2011). On the exposed skeleton of some individuals that retracted their coenosarc during the experiment, an accumulation of fine sediment grains was observed. This is supported by the observation that sediment accumulated mainly on the side facing the current, while the other side had hardly any sediment grains (Fig. 31). Larson and Purser (2011) found a similar situation in the CWC *L. pertusa*, where drill cuttings attached to the tissue-free skeleton and accumulated but resulting in the inability of self-cleaning and smothering of the polyps. The authors also suggest that tissue loss is further accelerated with the accumulation of sediment and coenosarc covering the skeleton is essential in preventing accumulation of sediment. Combined with the observation that the proportion of animals retracting their tissue increased over time, the retraction of tissue may be a sign that the corals no longer have enough energy to successfully repel the sediment. Therefore, they either retract their tissue to prevent damage or suffocation or they lose tissue as effect of increased sedimentation. The extent to which the retraction of the tissue harms the young animals or helps them to survive longer stress situations with possibly lower energy expenditure should be investigated more closely. Furthermore, it would be important to see the recovery capability of *C. huinayensis*, suffered from tissue loss and if there is a point were recovery can no longer take place. In *L. pertusa* high tissue recovery potential was found under aquarium conditions for coral fragments, which break off during sampling (Maier, 2008). While after repeated exposure to sediment, *L. pertusa* decreased their efficient to grow new coral tissue (26 %) over the free skeleton, which was exposed through consequences of sedimentation (Larsson and Purser, 2011). If sedimentation is stopped, juveniles are likely to recover and re-grow their tissue (Jones et al., 2019), but this depends on the condition of the polyp (Larsson and Purser, 2011) and whether other stressors are affecting the animals (Rogers, 1990).

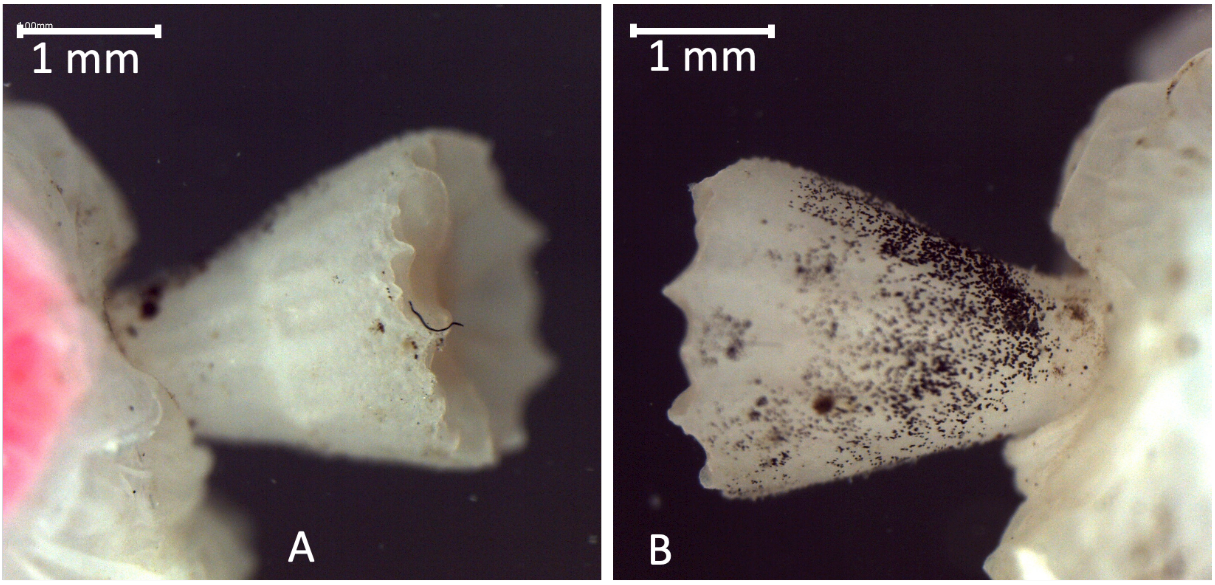

Figure 31: Sediment accumulation on horizontally oriented individuum of *C. huinayensis* with retracted coenosarc exposed to the 1000-fold concentration of sediment at the end of the experiment from A) current averted and B) towards the current faced side.

Under high sediment concentration, some corals in the 1000-fold concentration showed extruded mesenterial filaments (Fig. 32). For warm-water corals an extrusion of their mesenterial filaments as defence mechanism or as competition behaves for space is reported (Logan, 1984; Nugues et al., 2004). Furthermore, this is also described for external digestion (Wijgerde et al., 2013). But the extrusion of mesenterial filaments can also be a sign of stress (Bak and Elgershuizen, 1976). The CWC *D. dianthus* showed under acidified conditions (314 d), together with the decrease in skeletal growth the evagination of its mesenteries (Movilla et al., 2014). Since a defending mechanism against competitors can be excluded, the extrusion of the mesenterial filaments may further indicate a stress situation. Nevertheless, in Fig 31. A, mesenterial filaments seeming to come out of the body wall, which is rather uncommon (Laudien et al., 2021). A recent study by Laudien et al. (2021) showed a polyp dropout, by even putative non-stressed adults of *C. huinayensis*, which was preceded by tissue retraction and by the extrusion of mesenterial filaments through perforations in body wall, that led to the detachment of the entire polyp. Nonetheless, a detachment of the polyp in stressful situations is known from Scleractinia corals (i.e. Kramarsky-Winter et al., 1997; Fordyce et al., 2017). By a polyp bail out for example, the coral detaches from its calcareous skeleton as an escape strategy, drifts to a place with better environmental conditions and settle again (Kramarsky-Winter et al., 1997; Kvitt et al., 2015). However, a polyp detachment through sedimentation stress was not observed in the juveniles exposed to sediment load for twelve weeks.

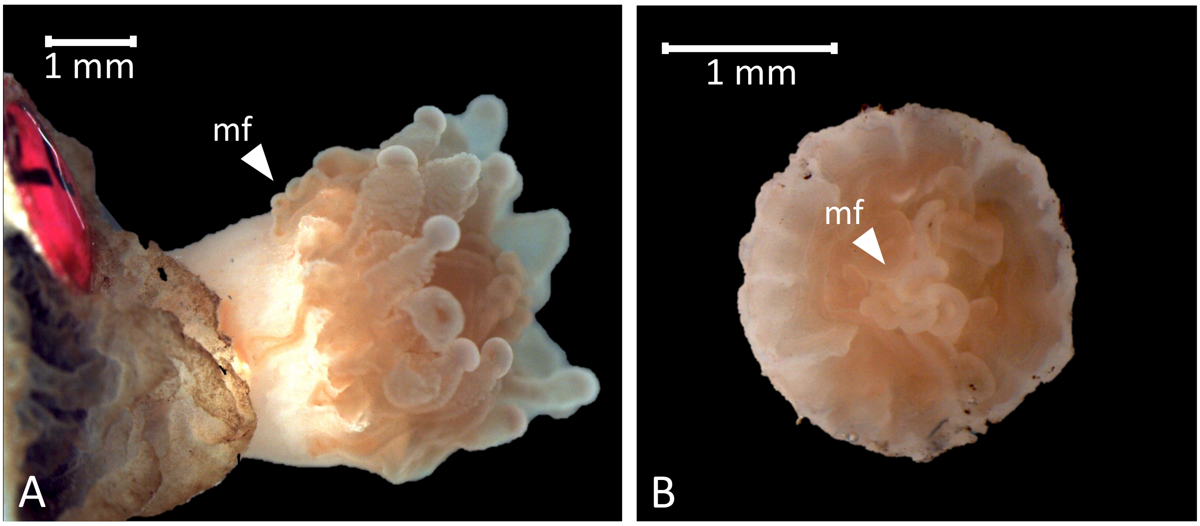

Figure 32: Two individuum's of *C. huinayensis* maintained under high sediment concentration extruding the mesenterial filaments (mf) probably as a signal of stress reaction.

The analysed response variables: growth rate, polyp extension and tissue retraction, reveal different results for vertical and horizontal oriented corals. Individuals placed in a horizontal position were more affected with significant differences between the two orientations for growth rate (buoyant weight method) and polyp extension responses. Sedimentation is a vertically oriented process (Clark et al., 2017). The higher influence of sediment on horizontally oriented corals can therefore be explained by gravity since sediment is less likely to remain on vertically downward oriented animals. This is also shown for *L. pertusa* branches, where more sediment settled on horizontal than on vertical oriented branches (Larsson and Purser, 2011).

4.2.3 Oxygen consumption of *C. huinayensis* under increasing sediment concentration

The respiration measurements revealed different oxygen consumption rates for corals during short-term (24 h) and long-term (13 weeks) exposure to increasing sediment loads. For the short-term exposed corals, no significant effects on the respiration rates were detected between the treatments. On the contrary, long-time exposed juveniles showed a significant decrease in their respiration rate with increasing sediment concentrations. This does not support the fourth hypothesis that corals increase their respiration as a stress response to sediment, which is therefore rejected. But the null-hypotheses cannot be confirmed either, since corals decreased their respiration with increasing sedimentation.

Feeding can increase the respiration rate of corals and thus has influences that make actual differences in the respiration through "stressors" invisible (Larsson et al., 2013; van Oevelen et al., 2016; Eder et al., 2018). However, no differences in respiration rates were observed in juvenile

C. huinayensis immediately after feeding and 3 days later (K. Beck, personal communication), therefore an effect of food intake on the respiration rates of the animals can be excluded.

Nevertheless, 50 % of newly exposed corals showed a higher respiration rate in the 1000-fold compared to the natural concentration, showing a trend towards an increased respiration as a response towards increased sediment. In comparison to that, the respiration rates of corals exposed to the 1000-fold concentration in the long-time experiment, where significantly reduced. This indicates that corals may increase their respiration in the beginning but under constant sediment stress they slow all their functions down, displayed in the decreased metabolic rate, but also in reduced growth and spend all their energy in survival.

Through metabolic respiration corals produce ATP, which is required for energy consuming processes, such as calcification, tissue growth or strategies to actively remove sediment such as mucus production (Rogers, 1990; Hennige et al., 2014; Moeller et al., 2017). The decreased respiration rate of *C. huinayensis* in the long-term experiment could thus speak for a reduced metabolism, resulting in a lower growth rate. In the warm-water coral *Pocillopora acuta* high sediment and nutrient load led to decreased metabolic-rate, calcification and decreasing coral cover (Becker and Silbiger, 2020). Hennige et al. (2014) showed a decreased respiration for *L. pertusa* under increased carbon dioxide (CO_2), but no change in calcification which indicates an energetic imbalance that is probably favoured by the use of lipid reserves. Gori et al. (2016) showed a decreased respiration rate and calcification for *D. dianthus* when exposed to multiple stressors of elevated temperature and carbon dioxide partial pressure (pCO_2). This is explained by the shift from a mixed use of proteins and carbohydrates or lipids to a much less efficient protein-dominated catabolism for energy production (Gori et al., 2016). Deep sea corals (Caryophyllidae, *Dendrophyllia* sp., *Eguchipsammia fistula*) from the red sea may adapted to oxygen-limited, highly oligotroph and 20 °C warm waters with low respiration and calcification rates, they keep their tissue at the tips of their skeleton alive to minimize the metabolic needs (Roder et al., 2013).

In marine invertebrates, stress tolerance and thus their acclimatization potential is closely linked to their metabolism (Sokolova et al., 2012). The results indicate that under constant high sediment load, recruits of *C. huinayensis* may become exhausted, probably being able to keep the vital functions for a limited time, not being able to invest energy in calcification and in tissue regeneration or protective mechanisms against sediment load (as mucus production). As a response, the corals reduce their metabolic rate, slowing down all their functions to just survive. Therefore, the reduced metabolism may show an adaption to prevailing non favourable environmental conditions.

4.2.4 Interaction of various factors of sediment load on *C. huinayensis*

The effects of sediment on coral performance vary among studies, which is also related to the different concentration, application of sediment (e.g., sedimented, held in suspension), different properties of the particles and the exposure time of the sediment load (see Table 5).

Through the different anthropogenic impacts on the fjord, the increase in sediment will also occur with different particle characteristics. Fine grains such as silt have a greater impact than the larger sand grains (Tseng et al., 2011), as they remain in the water column longer and have a greater impact on the turbidity of the water. There, for example, they reduce the light available to symbiotic zooxanthellae of warm water corals (Erftemeijer et al., 2012). Larger particles bind more nutrients and pollutants and harbour more microorganisms that can make the surface stickier and more difficult for corals to repel (Larsson et al., 2013; Jones et al., 2015; Liefmann et al., 2018). Oceanic material shows a lower impact on benthic animals, while the affect is greater for terrestrial material and for artificially mixed material such as that used for drill cuttings (Tseng et al., 2011; Larsson et al., 2013). Drill cuttings could possibly be released, due to the upcoming construction work. Rogers (1990) reported already concentrations of 0.1 ml l^{-1} of drill fluids as critically affecting tropical corals. The lower effect of benthic marine material is not surprising, as it is a natural component of the animals' habitat. As long as the material does not settle on the animals and suffocate them, or a high permanent load is generated, CWCs probably can cope with natural variations (this study, Larsson et al., 2013). While terrestrial material may have a more heterogenies particle size and form, with also sharper edges (since water flow may not have rounded the edges of the grain). However, similar abilities to free themselves from a particular type of sediment and grain size has been reported for corals (Thompson and Bright, 1977; Larsson and Purser, 2011).

Fine grain fractions (< 105 µm), as used in this study, are typically occurring in the runoff water after heavy rain falls (Tseng et al., 2011), which characterize the fjord region (Försterra, 2009). Furthermore, although the used sediment is marine material from the Wadden Sea, it is highly influenced from terrestrial sources (Quante et al., 2016). The serious impacts that mostly took place at the highest sediment load, however, could be greater through different material input or terrestrial material (e.g., through road construction, landslide) alone. In this study only the effect of suspended sediment was observed, by attaching the corals to screws that were hanging in the water column. This corresponds with the natural occurrence in the fjord. The small solitary coral may therefore not successfully settle on horizontally ground, since sedimentation is possible to high and buries the recruits, which consequently smoother and die. Therefore, a settlement is more successful on the steep walls and overhangs as sediment can harder accumulate. When Rogers et al. 1984 studied the recruitment patterns off warm-water corals, he found higher recruitment on the vertical surfaces and suspected, that this is because of the higher sedimentation rate in the area. Highly increased turbidity values may also reduce the successfully settlement and lead to lower recruitment since sediment can for example clog the feeding and swimming structures. Furthermore, there is a certain risk that the clogged larvae sinks to the ground (Järnegren et al., 2020). As natural survival rates are already low for recruits, this reduces the success (Rogers, 1990; Trapon et al., 2013; Moeller et al., 2017). This is supported by Moeller et al. (2017) who showed mortality for newly settled recruits of *Leptastrea purpurea* under sediment rates of 16 mg cm^{-2} d^{-1}, while adults of these species did not show a significant higher mortality under sedimentation rates of 333.3 mg cm^{-2} d^{-1}.

Therefore, even if juveniles of *C. huinayensis* show relatively good resilient under increased natural sedimentation, the question is how different life stages (larvae and newly settled recruits) and other species of the community may cope with the higher sediment load. The associated reef building *D. dianthus* may be more sensitive to sedimentation, since they dominate over *C. huinayensis* on well ventilated sites and mainly grow under overhangs (Cairns et al., 2005). Nevertheless, organisms living in benthic communities are exposed to similar conditions. Therefore, tolerance to abiotic stressors may overlap. The loss of a single species can disrupt a functioning ecosystem in an uncertain way. However, if several species are affected or habitat forming species, there is a loss in ecosystems and therefore also their "services" (Thrush and Dayton, 2002; Försterra et al., 2017). This is underlined by the coral mass mortality of *D. dianthus* in Comau Fjord in 2012 on which a decline of Cape redfish abundance followed (Försterra et al., 2017, 2014).

All in all, large amounts of sediment, such as those presumably found in landslides or construction work, have a strong impact, which increases with the influence of other stressors occurring in the fjord. For instance, the increased nutrient input through aquaculture, which supports harmful algae blooms in this area and can lead to hypoxic conditions (Försterra et al., 2014). Furthermore, ocean acidification and global warming are threats and especially communities bound to a certain habitat area (e.g., sessile filter feeders) must adapt faster (Hofmann and Todgham, 2010). As Comau Fjord already presents a pH level which is predicted for the oceans by the end of the century (Jantzen et al., 2013a), rising sediment loads are a big risk.

Table 5 Overview of studies on responses to increased sedimentation on Scleractinia CWCs and juvenile warm-water corals

Source	Species	Sediment	Exposure time and application	Experimental outcome
This study	Juvenile *Caryophyllia huinayensis* (Cairns 2005) CWC	Natural benthic sediment, collected in the Wadden Sea, freeze dried and boiled with H_2O_2 0.0042/0.42/4.2 ml l^{-1} Grain size < 200 µm	1. 12 weeks, 2. 24 h As solution, kept in suspension through stir bar on magnetic-stir-plate	- 1. Under highest concentration decreased growth rate, polyp extension, tissue retraction. - 2. Long-term exposure decreasing metabolic rate with increasing sediment load. Short-term exposure trend to increased respiration with increasing sediment load - Evidence of mucus production, accumulation of sediment on coral skeleton and extruding mesenterial filaments
Moeller et al. (2017)	Newly settled juvenile and adults *Leptastrea purpurea*, newly settled juvenile *Acropora hyacinthus* Warm-water coral	Natural benthic sediment, sampled near shore in Guam Driet for 3 d at 60 °C A. hyacinthus juveniles: 0/8.3/16.6 mg cm^{-2} d^{-1} *L. purpurea* juveniles: 0/16.6/33.3 mg cm^{-2} d^{-1} Adults: 0 / 33.3 / 333.3 mg cm^{-2} d^{-1} Grain size 2 – 630 µm	3-5 Weeks Kept in suspension	- Growth and survival of newly settled juveniles negatively affected by sediment load, not seen for juveniles older than a month - No significant difference in mortality for adults under all concentrations
Allers et al. (2013)	*Lophelia pertusa* CWC	Natural benthic sediment, collected from same spot as individuals for the experiment Drill cuttings, Mixture of drill cuttings and natural sediment 66/198/462 mg cm^{-2} Grain size < 1 mm	Poured evenly into the "standing" water as a homogeneous suspension and allowed to settle for 12 hours before restarting the flow Complete burial 24, 48 and 72 h	- Decrease of oxygen concentration on coral surface by coverage with all three sediment types - Natural sediment higher effect in inducing anoxia than drill cuttings - Exposure to anoxic sediment mucus release and withdrawn tentacles, duration of exposure > 24 h lead to death of polyps

Larsson et al. (2013)	*Lophelia pertusa* CWC	Natural benthic sediment, sampled close to *L. pertusa* reef Water-based drill cuttings 0/5/25 mg l-1 Grain size (< 63 µm)	12 weeks As solution, circulation pumps kept sediment in suspension	- Lower growth rates (50 %) under high exposure - Trend drill cuttings have a higher impact on growth than natural benthic sediment - Polyp extension less under high sedimentation - No effect on respiration, proportions of tissue and fatty acids. No significant effect of additional mucus release on coral energy expenditure
Larsson and Purser (2011)	*Lophelia pertusa* CWC	Natural benthic sediment (sampled close to L. pertusa reef), wetsieved Grain size < 1 mm Water-based drill cuttings Grain size < 1 mm and < 63 mm Sediment rejection: 66/196 mg dry weight (DW) cm^{-2} Repeated exposure: 33 mg DW cm^{-2} Drilling Event/Burial study: 65/195 mg DW cm^{-2}	Sediment rejection: 12 h Repeated exposure: 45 days Mimicked drilling-event: 3 weeks As solution evenly distributed on the aquaria surface with a syringe, sediment was allowed to settle for 6-12 h without generating water flow	- Tissue-covered surfaces are efficiently cleaned - Equal ability to reject different sediment types with same grain size - Starved and fed corals same ability to reject sediment - Sediment accumulated on tissue free skeleton, with repeated exposure, the sediment accumulated to the extent that it also spread to the adjacent regions of the skeleton covered with coenosarc, leading in some cases to smothering of the tissue and death of the polyps. - “Drilling event”: Number of coral fragments with smothered tissue and polyp mortality increased with sediment load, but skeletal growth was not significantly affected.

Brooke et al. (2009)	*Lophelia pertusa* CWC	Natural benthic sediments, sampled close to the coral collection site Autoclaved 0/50/150/250/350 mg l^{-1} Grain size: < 5 mm	1. 14 days, introduced as concentrated slurries into aquarium bottom, creating suspended concentrations 2. 7 days, complete burial under sediment > 1 cm 3. 10h, sediment gently deposited on calyx surface with glass pipette until poured over the side	- 1. Polyp survival decreased with increasing concentration - 2. Critical survival-mortality between 2 – 4 days - 3. Sediment was removed by the calyx after 9 h

5 Conclusion and Outlook

This is the first study to assess the impact of sedimentation on juvenile CWC's. Juveniles of the CWC *C. huinayensis* exposed to high sedimentation rates displayed tissue retraction, reduced respiration rates, reduced polyp extension, as well as lowered growth rates. However, lesser increases in the sediment load (up to 100-fold the natural concentration) seem to have minor effect on coral recruits, at least in the 12-weeks' time frame of the present experiment. Presumably, they can survive short-term increases in sediment loads, such as those caused by a landslide, and recover thereafter, if they are not exposed to a high sediment concentration for a longer period. However, if the sediment inputs are chronically, or if the naturally high values rise, fatal effects on the young animals are expected (96 % decreased growth under the 1000-fold concentration (4.2 ml l^{-1})).

Through anthropogenic activities such as road constructions and aquaculture farms, sedimentation rates in Comau Fjord are likely to increase in the future. A synergy between sedimentation and other stressors, cumulative effects might occur with a significant impact (Fisher et al., 2019). Therefore, impacts on the ecosystems, present in the area, need to be assessed and diminished. Furthermore, aquaculture in these sensitive areas should be strongly controlled, minimized, and banned from marine protected areas (Häussermann et al., 2021).

This study proves that a highly increased natural sediment has negative effects on the physiology performance of juvenile CWC, but further studies are needed to assess the consequences of anthropogenically increased sediment concentrations in an increasingly changing marine environment. More research on the effect of sedimentation on larvae of *C. huinayensis* and on other juvenile CWC species is required. Also, the effect of different sediment particles (terrestrial, oceanic, drill cuttings) on the same species, as the habitat forming *D. dianthus* and *C. huinayensis,* could improve the knowledge and create better comparability within and among species. Multiple-stressor experiments may provide greater insight into the impact and future development of the CWC banks, as ocean warming and the associated ocean acidification will increase in the future.

The severe reduction or even disappearance of a habitat forming species can have a strong impact on complex ecological systems (Thrush and Dayton, 2002;Försterra et al., 2017; Häussermann et al., 2021). Considering the results of this study and taking into account that CWC ecosystems are considered vulnerable marine ecosystems protected in national and international waters (Freiwald et al., 2004; ICRI, 2004), management plans need to consider the deleterious effects of increased sedimentation on vulnerable CWC's.

Reference

Allers, E., Abed, R.M.M., Wehrmann, L.M., Wang, T., Larsson, A.I., Purser, A., de Beer, D., 2013. Resistance of *Lophelia pertusa* to coverage by sediment and petroleum drill cuttings. Marine Pollution Bulletin 74, 132–140. https://doi.org/10.1016/j.marpolbul.2013.07.016

Anthony, K.R.N., Connolly, S.R., Willis, B.L., 2002. Comparative Analysis of Energy Allocation to Tissue and Skeletal Growth in Corals. Limnology and Oceanography 47, 1417–1429.

Ashford, O.S., Kenny, A.J., Barrio Froján, C.R.S., Downie, A.-L., Horton, T., Rogers, A.D., 2019. On the Influence of Vulnerable Marine Ecosystem Habitats on Peracarid Crustacean Assemblages in the Northwest Atlantic Fisheries Organisation Regulatory Area. Frontiers in Marine Science 6, 401. https://doi.org/10.3389/fmars.2019.00401

Bak, R.P.M., Elgershuizen, 1976. Patterns of Oil-Sediment rejection in corals. Marine Biology 37, 105–113.

Baums, I.B., 2008. A restoration genetics guide for coral reef conservation. Molecular Ecology17, 2796–2811. https://doi.org/10.1111/j.1365-294X.2008.03787.x

Becker, D.M., Silbiger, N.J., 2020. Nutrient and sediment loading affect multiple facets of functionality in a tropical branching coral. Journal of Experimental Biology 15.

Beschta, R.L., 1978. Long-term patterns of sediment production following road construction and logging in the Oregon Coast Range. Water Resources Research 14, 1011–1016. https://doi.org/10.1029/WR014i006p01011

Bianchi, T.S., Arndt, S., Austin, W.E.N., Benn, D.I., Bertrand, S., Cui, X., Faust, J.C., Koziorowska-Makuch, K., Moy, C.M., Savage, C., Smeaton, C., Smith, R.W., Syvitski, J., 2020. Fjords as Aquatic Critical Zones (ACZs). Earth-Science Reviews 203, 103145. https://doi.org/10.1016/j.earscirev.2020.103145

Brown, B.E., Downs, C.A., Dunne, R.P., Gibb, S.W., 2002. Preliminary evidence for tissue retraction as a factor in photoprotection of corals incapable of xanthophyll cycling. Journal of Experimental Marine Biology and Ecology 277, 129–144. https://doi.org/10.1016/S0022-0981(02)00305-2

Brown, B.E., Le Tissier, M.D.A., Dunne, R.P., 1994. Tissue retraction in the scleractinian coral *Coeloseris mayeri*, its effect upon coral pigmentation, and preliminary implications for heat balance. Mar. Marine Ecology Progress Series 209–218.

Buschmann, A.H., Riquelme, V.A., Hernández-González, M.C., Varela, D., Jiménez, J.E., Henríquez, L.A., Vergara, P.A., Guíñez, R., Filún, L., 2006. A review of the impacts of salmonid farming on marine coastal ecosystems in the southeast Pacific. ICES Journal of Marine Science 63, 1338–1345. https://doi.org/10.1016/j.icesjms.2006.04.021

Bustamante, M.S., 2009. The Southern Chilean Fjord Region: Oceanographic Aspects, in: Häussermann, V., Försterra, G. (Eds.), Machado, B. (Tran.), Marine Benthic Fauna of Chilean Patagonia. Nature in Focus, Santiago, pp. 53–60.

Cairns, S.D., Häussermann, V., Försterra, G., 2005. A review of the Scleractinia (Cnidaria: Anthozoa) of Chile, with the description of two new species. Zootaxa 1018, 15. https://doi.org/10.11646/zootaxa.1018.1.2

Chapron, L., Peru, E., Engler, A., Ghiglione, J.F., Meistertzheim, A.L., Pruski, A.M., Purser, A., Vétion, G., Galand, P.E., Lartaud, F., 2018. Macro- and microplastics affect cold-water corals growth, feeding and behaviour. Scientific Reports 8, 15299. https://doi.org/10.1038/s41598-018-33683-6

Clark, G.F., Stark, J.S., Palmer, A.S., Riddle, M.J., Johnston, E.L., 2017. The Roles of Sea-Ice, Light and Sedimentation in Structuring Shallow Antarctic Benthic Communities. PLoS ONE 12, e0168391. https://doi.org/10.1371/journal.pone.0168391

Davies, S.P., 1989. Short-term growth measurements of corals using an accurate buoyant weighing technique. Marine Biology 101, 389–395. https://doi.org/10.1007/BF00428135

Duckworth, A., Giofre, N., Jones, R., 2017. Coral morphology and sedimentation. Marine Pollution Bulletin 125, 289–300. https://doi.org/10.1016/j.marpolbul.2017.08.036

Dunn, J.G., Sammarco, P.W., LaFleur, G., 2012. Effects of phosphate on growth and skeletal density in the scleractinian coral *Acropora muricata*: A controlled experimental approach. Journal of Experimental Marine Biology and Ecology 411, 34–44. https://doi.org/10.1016/j.jembe.2011.10.013

Dunn, O.J., 1964. Multiple Comparisons Using Rank Sums. Technometrics 6, 241–252. https://doi.org/10.1080/00401706.1964.10490181

Eder, Y., Tschink, D., Gerlach, G., Strahl, J., 2018. Physiology of juvenile hydroids - High food availability mitigates stress responses of *Hydractinia echinata* to increasing seawater temperatures. Journal of Experimental Marine Biology and Ecology 508, 64–72. https://doi.org/10.1016/j.jembe.2018.07.009

Environmental Sciences Division, O.R.N.L., 2012. MS Excel Program Developed for CO2 System Calculations. https://doi.org/10.3334/CDIAC/OTG.CO2SYS_XLS_CDIAC105A

Erftemeijer, P.L.A., Riegl, B., Hoeksema, B.W., Todd, P.A., 2012. Environmental impacts of dredging and other sediment disturbances on corals: A review. Marine Pollution Bulletin 64, 1737–1765. https://doi.org/10.1016/j.marpolbul.2012.05.008

FAO (Ed.), 2021. GLOBEFISH Highlights - A quarterly update on world seafood markets, 1st issue. ed. Food and Agriculture Organization of the United Nations, Rome. https://doi.org/10.4060/cb4129en

Fillinger, L., Richter, C., 2013. Vertical and horizontal distribution of *Desmophyllum dianthus* in Comau Fjord, Chile: a cold-water coral thriving at low pH. PeerJ 1, e194. https://doi.org/10.7717/peerj.194

Fisher, R., Bessell-Browne, P., Jones, R., 2019. Synergistic and antagonistic impacts of suspended sediments and thermal stress on corals. Nature Communications 10, 2346. https://doi.org/10.1038/s41467-019-10288-9

Fordyce, A.J., Camp, E.F., Ainsworth, T.D., 2017. Polyp bailout in *Pocillopora damicornis* following thermal stress. F1000Research 6, 687. https://doi.org/10.12688/f1000research.11522.2

Försterra, G., 2009. Ecological and Biogeographical Aspects of the Chilean Fjord Region, in: Häussermann, V., Försterra, G. (Eds.), Marine Benthic Fauna of Chilean Patagonia. Nature in Focus, Santiago, pp. 61–79.

Försterra, G., Häussermann, V., 2010. Marine benthic fauna of Chilean Patagonia: illustrated identification guide, Nature in Focus. Chile.

Försterra, G., Häussermann, V., 2008. Unusual symbiotic relationships between microendolithic phototrophic organisms and azooxanthellate cold-water corals from Chilean fjords. Marine Ecology Progress Series 370, 121–125. https://doi.org/10.3354/meps07630

Försterra, G., Häussermann, V., Laudien, J., 2017. Animal Forests in the Chilean Fjords: Discoveries, Perspectives, and Threats in Shallow and Deep Waters, in: Rossi, S., Bramanti, L., Gori, A., Orejas, C. (Eds.), Marine Animal Forests: The Ecology of Benthic Biodiversity Hotspots. Springer International Publishing, Cham. https://doi.org/10.1007/978-3-319-21012-4

Försterra, G., Häussermann, V., Laudien, J., Jantzen, C., Sellanes, J., Muñoz, P., 2014. Mass die-off of the cold-water coral *Desmophyllum dianthus* in the Chilean Patagonian fjord region. Bulletin of Marine Science 90, 895–899. https://doi.org/10.5343/bms.2013.1064

Freiwald, A., Fosså, J.H., Grehan, A., Roberts, J.M., 2004. Cold-water Coral Reefs. UNEP-WCMC, Cambridge UK.

Freiwald, A., Roberts, J.M. (Eds.), 2005. Cold-water corals and ecosystems, Erlangen Earth conference series. Presented at the International Symposium on Deep-Sea Corals, Springer, Berlin.

Gazeau, F., Urbini, L., Cox, T., Alliouane, S., Gattuso, J., 2015. Comparison of the alkalinity and calcium anomaly techniques to estimate rates of net calcification. Marine Ecology Progress Series 527, 1–12. https://doi.org/10.3354/meps11287

Gori, A., Ferrier-Pagès, C., Hennige, S.J., Murray, F., Rottier, C., Wicks, L.C., Roberts, J.M., 2016. Physiological response of the cold-water coral *Desmophyllum dianthus* to thermal stress and ocean acidification. PeerJ 4, e1606. https://doi.org/10.7717/peerj.1606

Gottschlich, S., 2014. Einfluss des Substrat-Neigungswinkels auf die Hartsubstratlebensgemeinschaft im Comau Fjord, Chile. Bachelor Thesis 64.

Gran, G., 1952. Determination of the Equivalence Point in Potentiometric Titrations. Part 11 77, 11.

Grant, J., Hatcher, A., Scott, D.B., Pocklington, P., Schafer, C.T., Winters, G.V., 1995. A Multidisciplinary Approach to Evaluating Impacts of Shellfish Aquaculture on Benthic Communities. Estuaries 18, 124. https://doi.org/10.2307/1352288

Hargrave, B., 2010. Empirical relationships describing benthic impacts of salmon aquaculture. Aquaculture Environment Interactions 1, 33–46. https://doi.org/10.3354/aei00005

Häussermann, V., Försterra, G., 2007. Large assemblages of cold-water corals in Chile: a summary of recent findings and potential impacts. Bulletin of Marine Science 81, 195–207.

Häussermann, V., Försterra, G., Laudien, J., 2021. Macrobenthos De Fondos Duros De La Patagonia Chilena: Énfasis En La Conservación De Bosques Sublitorales De Invertebrados Y Algas, in: Castilla, J.C., Armesto, J.J., Martínez-Harms, M.J. (Eds.), Conservación En La Patagonia Chilena. Santiago, Chile.

Häussermann, V., Försterra, G., Melzer, R.R., Meyer, R., 2013. Gradual changes of benthic biodiversity in Comau Fjord, Chilean Patagonia – lateral observations over a decade of taxonomic research. Spixiana 36, 161–171.

Häussermann, V., Försterra, G., Plotnek, E., 2012. Sightings of marine mammals and birds in the Comau Fjord, Northern Patagonia, between 2003 and mid 2012. Spixiana 35, 247–262.

Hennige, S.J., Wicks, L.C., Kamenos, N.A., Bakker, D.C.E., Findlay, H.S., Dumousseaud, C., Roberts, J.M., 2014. Short-term metabolic and growth responses of the cold-water coral *Lophelia pertusa* to ocean acidification. Deep Sea Research Part II: Topical Studies in Oceanography 99, 27–35. https://doi.org/10.1016/j.dsr2.2013.07.005

Henry, L.-A., Roberts, J.M., 2016. Global Biodiversity in Cold-Water Coral Reef Ecosystems, in: Rossi, S., Bramanti, L., Gori, A., Orejas Saco del Valle, C. (Eds.), Marine Animal Forests. Springer International Publishing, Cham, pp. 1–21. https://doi.org/10.1007/978-3-319-17001-5_6-1

Hervé, F., Quiroz, D., Duhart, P., 2009. Principal Geological Aspects of the Chilean Fjord Region, in: Häussermann, V., Försterra, G. (Eds.), Machado, B. (Tran.), Marine Benthic Fauna of Chilean Patagonia. Nature in Focus, Santiago, pp. 30–42.

Hoegh-Guldberg, O., Poloczanska, E.S., Skirving, W., Dove, S., 2017. Coral Reef Ecosystems under Climate Change and Ocean Acidification. Frontiers in Marine Science 4, 158. https://doi.org/10.3389/fmars.2017.00158

Hofmann, G.E., Todgham, A.E., 2010. Living in the Now: Physiological Mechanisms to Tolerate a Rapidly Changing Environment. Annual Review of Physiology. 72, 127–145. https://doi.org/10.1146/annurev-physiol-021909-135900

Hromic, T., 2009. Estructura Comunitaria del Taxa Foraminiferida (Protozoa), Según Profundiad, en el Fiordo Comau, Chiloé, Chile. Anales Instituto Patagonia (Chile) 37. https://doi.org/10.4067/S0718-686X2009000100004

ICRI, 2004. Decision on Cold-Water Coral Reefs. International Coral Reef Initiative, Okinawa, Japan.

Jantzen, C., Häussermann, V., Försterra, G., Laudien, J., Ardelan, M., Maier, S., Richter, C., 2013a. Occurrence of a cold-water coral along natural pH gradients (Patagonia, Chile). Marine Biology 160, 2597–2607. https://doi.org/10.1007/s00227-013-2254-0

Jantzen, C., Laudien, J., Sokol, S., Försterra, G., Häussermann, V., Kupprat, F., Richter, C., 2013b. In situ short-term growth rates of a cold-water coral. Marine and Freshwater Research 64, 631. https://doi.org/10.1071/MF12200

Järnegren, J., Brooke, S., Jensen, H., 2020. Effects and recovery of larvae of the cold-water coral *Lophelia pertusa* (*Desmophyllum pertusum*) exposed to suspended bentonite, barite and drill cuttings. Marine Environmental Research 158, 104996. https://doi.org/10.1016/j.marenvres.2020.104996

Jiang, L.-Q., Feely, R.A., Carter, B.R., Greeley, D.J., Gledhill, D.K., Arzayus, K.M., 2015. Climatological distribution of aragonite saturation state in the global oceans: Aragonite saturation climatology. Global Biogeochemical Cycles 29, 1656–1673. https://doi.org/10.1002/2015GB005198

Jones, R., Fisher, R., Bessell-Browne, P., 2019. Sediment deposition and coral smothering. PLoS ONE 14, e0216248. https://doi.org/10.1371/journal.pone.0216248

Jones, R., Ricardo, G.F., Negri, A.P., 2015. Effects of sediments on the reproductive cycle of corals. Marine Pollution Bulletin 100, 13–33. https://doi.org/10.1016/j.marpolbul.2015.08.021

Kawahata, H., Fujita, K., Iguchi, A., Inoue, M., Iwasaki, S., Kuroyanagi, A., Maeda, A., Manaka, T., Moriya, K., Takagi, H., Toyofuku, T., Yoshimura, T., Suzuki, A., 2019. Perspective on the response of marine calcifiers to global warming and ocean acidification—Behavior of corals and foraminifera in a high CO2 world "hot house." Progress in Earth and Planetary Science 6, 5. https://doi.org/10.1186/s40645-018-0239-9

Kilian, R., Baeza, O., Steinke, T., Arevalo, M., Rios, C., Schneider, C., 2007. Late Pleistocene to Holocene marine transgression and thermohaline control on sediment transport in the western Magellanes fjord system of Chile (53°S). Quaternary International 161, 90–107. https://doi.org/10.1016/j.quaint.2006.10.043

Kramarsky-Winter, E., Fine, M., Loya, Y., 1997. Coral polyp expulsion. Nature 387, 137–137. https://doi.org/10.1038/387137a0

Kruskal, W.H., Wallis, W.A., 1952. Use of Ranks in One-Criterion Variance Analysis. Journal of the American Statistical Association 47, 583–621. https://doi.org/10.1080/01621459.1952.10483441

Kutti, T., Ervik, A., Hansen, P.K., 2007. Effects of organic effluents from a salmon farm on a fjord system. I. Vertical export and dispersal processes. Aquaculture 262, 367–381. https://doi.org/10.1016/j.aquaculture.2006.10.010

Kvitt, H., Kramarsky-Winter, E., Maor-Landaw, K., Zandbank, K., Kushmaro, A., Rosenfeld, H., Fine, M., Tchernov, D., 2015. Breakdown of coral colonial form under reduced pH conditions is initiated in polyps and mediated through apoptosis. Proceedings of the National Academy of Sciences 112, 2082–2086. https://doi.org/10.1073/pnas.1419621112

Larsson, A., Lundälv, T., van Oevelen, D., 2013. Skeletal growth, respiration rate and fatty acid composition in the cold-water coral *Lophelia pertusa* under varying food conditions. Marine Ecology Progress Series 483, 169–184. https://doi.org/10.3354/meps10284

Larsson, A.I., Purser, A., 2011. Sedimentation on the cold-water coral *Lophelia pertusa*: Cleaning efficiency from natural sediments and drill cuttings. Marine Pollution Bulletin 62, 1159–1168. https://doi.org/10.1016/j.marpolbul.2011.03.041

Larsson, A.I., van Oevelen, D., Purser, A., Thomsen, L., 2013. Tolerance to long-term exposure of suspended benthic sediments and drill cuttings in the cold-water coral *Lophelia pertusa*. Marine Pollution Bulletin 70, 176–188. https://doi.org/10.1016/j.marpolbul.2013.02.033

Laudien, J., Häussermann, V., Försterra, G., Goehlich, H., 2014. Physical oceanographic profiles of seven CTD casts from Gulf of Ancud into Comau Fjord in 2014. https://doi.org/10.1594/PANGAEA.832187

Laudien, J., Heran, T., Häussermann, V., Försterra, G., Schmidt-Grieb, G.M., Richter, C., 2021. Polyp dropout in a solitary cold-water coral. Coral Reefs. https://doi.org/10.1007/s00338-021-02148-0

Lepland, A., Mortensen, P.B., 2008. Barite and barium in sediments and coral skeletons around the hydrocarbon exploration drilling site in the Træna Deep, Norwegian Sea. Environmental Geology 56, 119–129. https://doi.org/10.1007/s00254-007-1145-4

Liefmann, S., Järnegren, J., Johnsen, G., Murray, F., 2018. Eco-physiological responses of cold-water soft corals to anthropogenic sedimentation and particle shape. Journal of Experimental Marine Biology and Ecology 504, 61–71. https://doi.org/10.1016/j.jembe.2018.02.009

Logan, A., 1984. Interspecific aggression in hermatypic corals from Bermuda. Coral Reefs 3, 131–138. https://doi.org/10.1007/BF00301957

Loya, Y., 1976. Effects of Water Turbidity and Sedimentation on the Community Structure of Puerto Rican Corals. Bulletin of Marine Science 26, 17.

Lu, X.X., Zhang, S., Xu, J., 2010. Climate change and sediment flux from the Roof of the World. Earth Surface Processes and Landforms https://doi.org/10.1002/esp.1924

Maier, C., 2008. High recovery potential of the cold-water coral *Lophelia pertusa*. Coral Reefs 27, 821–821. https://doi.org/10.1007/s00338-008-0398-z

Martínez-Dios, A., Pelejero, C., López-Sanz, À., Sherrell, R.M., Ko, S., Häussermann, V., Försterra, G., Calvo, E., 2020. Effects of low pH and feeding on calcification rates of the cold-water coral *Desmophyllum dianthus*. PeerJ 8, e8236. https://doi.org/10.7717/peerj.8236

Maynou, F., Cartes, J.E., 2012. Effects of trawling on fish and invertebrates from deep-sea coral facies of Isidella elongata in the western Mediterranean. Journal of the Marine Biological Association of the United Kingdom 92, 1501–1507. https://doi.org/10.1017/S0025315411001603

Mayr, C., Rebolledo, L., Schulte, K., Schuster, A., Zolitschka, B., Försterra, G., Häussermann, V., 2014. Responses of nitrogen and carbon deposition rates in Comau Fjord (42°S, southern Chile) to natural and anthropogenic impacts during the last century. Continental Shelf Research 78, 29–38. https://doi.org/10.1016/j.csr.2014.02.004

Miller, D.C., Muir, C.L., Hauser, O.A., 2002. Detrimental effects of sedimentation on marine benthos: what can be learned from natural processes and rates? Ecological Engineering 19, 211–232. https://doi.org/10.1016/S0925-8574(02)00081-2

Min, J.-E., Ryu, J.-H., Lee, S., Son, S., 2012. Monitoring of suspended sediment variation using Landsat and MODIS in the Saemangeum coastal area of Korea. Marine Pollution Bulletin 64, 382–390. https://doi.org/10.1016/j.marpolbul.2011.10.025

Moeller, M., Nietzer, S., Schils, T., Schupp, P.J., 2017. Low sediment loads affect survival of coral recruits: the first weeks are crucial. Coral Reefs 36, 39–49. https://doi.org/10.1007/s00338-016-1513-1

Moulton, T.L., 2018. Package ʻrMR, Importing Data from Loligo Systems Software, CalculatingMetabolic Rates and Critical Tensions.

Movilla, J., Orejas, C., Calvo, E., Gori, A., López-Sanz, À., Grinyó, J., Domínguez-Carrió, C., Pelejero, C., 2014. Differential response of two Mediterranean cold-water coral species to ocean acidification. Coral Reefs 33, 675–686. https://doi.org/10.1007/s00338-014-1159-9

Naumann, M.S., Orejas, C., Ferrier-Pagès, C., 2013. High thermal tolerance of two Mediterranean cold-water coral species maintained in aquaria. Coral Reefs 32, 749–754. https://doi.org/10.1007/s00338-013-1011-7

Nelson, H.R., Altieri, A.H., 2019. Oxygen: the universal currency on coral reefs. Coral Reefs 38, 177–198. https://doi.org/10.1007/s00338-019-01765-0

Nugues, M., Delvoye, L., Bak, R., 2004. Coral defence against macroalgae: differential effects of mesenterial filaments on the green alga *Halimeda opuntia*. Mar. Ecol. Prog. Ser. 278, 103–114. https://doi.org/10.3354/meps278103

Orejas, C., Ferrier-Pagès, C., Reynaud, S., Gori, A., Beraud, E., Tsounis, G., Allemand, D., Gili, J., 2011. Long-term growth rates of four Mediterranean cold-water coral species maintained in aquaria. Marine Ecology Progress Series 429, 57–65. https://doi.org/10.3354/meps09104

Orejas, C., Gori, A., Rad-Menéndez, C., Last, K.S., Davies, A.J., Beveridge, C.M., Sadd, D., Kiriakoulakis, K., Witte, U., Roberts, J.M., 2016. The effect of flow speed and food size on the capture efficiency and feeding behaviour of the cold-water coral *Lophelia pertusa*. Journal of Experimental Marine Biology and Ecology 481, 34–40. https://doi.org/10.1016/j.jembe.2016.04.002

Orejas, C., Taviani, M., Ambroso, S., Andreou, V., Bilan, M., Bo, M., Brooke, S., Buhl-Mortensen, P., Cordes, E., Dominguez-Carrió, C., Ferrier-Pagès, C., Godinho, A., Gori, A., Grinyó, J., Gutiérrez-Zárate, C., Hennige, S., Jiménez, C., Larsson, A.I., Lartaud, F., Lunden, J., Maier, C., Maier, S.R., Movilla, J., Murray, F., Peru, E., Purser, A., Rakka, M., Reynaud, S., Roberts, J.M., Siles, P., Strömberg, S.M., Thomsen, L., van Oevelen, D., Veiga, A., Carreiro-Silva, M., 2019. 38 Cold-Water Coral in Aquaria: Advances and Challenges. A Focus on the Mediterranean, in: Orejas, C., Jiménez, C. (Eds.), Mediterranean Cold-Water Corals: Past, Present and Future, Coral Reefs of the World. Springer International Publishing, Cham, pp. 435–471. https://doi.org/10.1007/978-3-319-91608-8_38

Pantoja, S., Luis Iriarte, J., Daneri, G., 2011. Oceanography of the Chilean Patagonia. Continental Shelf Research 31, 149–153. https://doi.org/10.1016/j.csr.2010.10.013

Quante, M., Colijn, F., Bakker, J.P., Härdtle, W., Heinrich, H., Lefebvre, C., Nöhren, I., Olesen, J.E., Pohlmann, T., Sterr, H., Sündermann, J., Tölle, M.H., 2016. Introduction to the Assessment—Characteristics of the Region, in: Quante, M., Colijn, F. (Eds.), North Sea Region Climate Change Assessment, Regional Climate Studies. Springer International Publishing, Cham, pp. 1–52. https://doi.org/10.1007/978-3-319-39745-0_1

Reichardt, A.M., 2017. What Happens After – Succession of an Epibenthic Hard-Bottom Community after Coral Mass Mortality in Chilean Patagonia (Master thesis). Universität Bremen, Bremen.

Reid, L.M., Dunne, T., 1984. Sediment production from forest road surfaces. Water Resources Research 20, 1753–1761. https://doi.org/10.1029/WR020i011p01753

Richmond, R.H., Wolanski, E., 2011. Coral Reserach: Past Efforts and Future Horizons, in: Dubinsky, Z., Stambler, N. (Eds.), Coral Reefs: An Ecosystem in Transition. Springer Netherlands, Dordrecht, pp. 3–10. https://doi.org/10.1007/978-94-007-0114-4

Roberts, J.M., 2006. Reefs of the Deep: The Biology and Geology of Cold-Water Coral Ecosystems. Science 312, 543–547. https://doi.org/10.1126/science.1119861

Roder, C., Berumen, M.L., Bouwmeester, J., Papathanassiou, E., Al-Suwailem, A., Voolstra, C.R., 2013. First biological measurements of deep-sea corals from the Red Sea. Scientific Reports 3, 2802. https://doi.org/10.1038/srep02802

Rogers, C., 1990. Responses of coral reefs and reef organisms to sedimentation. Marine Ecology Progress Series 62, 185–202. https://doi.org/10.3354/meps062185

Rogers, C.S., Fitz, H.C., Gilnack, M., Beets, J., Hardin, J., 1984. Scleractinian coral recruitment patterns at Salt River submarine canyon, St. Croix, U.S. Virgin Islands. Coral Reefs 3, 69–76. https://doi.org/10.1007/BF00263756

Sanchez, N., Gonzalez, H.E., Iriarte, J.L., 2011. Trophic interactions of pelagic crustaceans in Comau Fjord (Chile): their role in the food web structure. Journal of Plankton Research 33, 1212–1229. https://doi.org/10.1093/plankt/fbr022

Scheirer, C.J., Ray, W.S., Hare, N., 1976. The Analysis of Ranked Data Derived from Completely Randomized Factorial Designs. Biometrics 32, 429–434. https://doi.org/10.2307/2529511

Sellanes, J., Quiroga, E., Neira, C., 2008. Megafauna community structure and trophic relationships at the recently discovered Concepción Methane Seep Area, Chile, ∼36°S. ICES Journal of Marine Science 65, 1102–1111. https://doi.org/10.1093/icesjms/fsn099

Smith, L.D., Devlin, M., Haynes, D., Gilmour, J.P., 2005. A demographic approach to monitoring the health of coral reefs. Marine Pollution Bulletin 51, 399–407. https://doi.org/10.1016/j.marpolbul.2004.11.021

Sokolova, I.M., Frederich, M., Bagwe, R., Lannig, G., Sukhotin, A.A., 2012. Energy homeostasis as an integrative tool for assessing limits of environmental stress tolerance in aquatic invertebrates. Marine Environmental Research 79, 1–15. https://doi.org/10.1016/j.marenvres.2012.04.003

Soto, M.V., 2009. Geography of the Chilean Fjord Region, in: Häussermann, V., Försterra, G. (Eds.), Machado, B. (Tran.), Marine Benthic Fauna of Chilean Patagonia. Nature in Focus, Santiago, pp. 43–52.

Sweetman, A.K., Thurber, A.R., Smith, C.R., Levin, L.A., Mora, C., Wei, C.-L., Gooday, A.J., Jones, D.O.B., Rex, M., Yasuhara, M., Ingels, J., Ruhl, H.A., Frieder, C.A., Danovaro, R., Würzberg, L., Baco, A., Grupe, B.M., Pasulka, A., Meyer, K.S., Dunlop, K.M., Henry, L.-A., Roberts, J.M., 2017. Major impacts of climate change on deep-sea benthic ecosystems. Elementa: Science of the Anthropocene 5, 4. https://doi.org/10.1525/elementa.203

Thompson, J.H., Bright, T.J., 1977. Effects of Drill Mud on Sediment Clearing Rates of Certain Hermatrophic Corals. International Oil Spill Conference Proceedings 1977, 495–498. https://doi.org/10.7901/2169-3358-1977-1-495

Thrush, S.F., Dayton, P.K., 2002. Disturbance to Marine Benthic Habitats by Trawling and Dredging: Implications for Marine Biodiversity. Annual Review of Ecology and Systematics 33, 449–473.

Trapon, M., Pratchett, M., Adjeroud, M., Hoey, A., Baird, A., 2013. Post-settlement growth and mortality rates of juvenile scleractinian corals in Moorea, French Polynesia versus Trunk Reef, Australia. Marine Ecology Progress Series 488, 157–170. https://doi.org/10.3354/meps10389

Tseng, L.-C., Dahms, H.-U., Hsu, N.-J., Hwang, J.-S., 2011. Effects of sedimentation on the gorgonian Subergorgia suberosa (Pallas, 1766). Marine Biology 158, 1301–1310. https://doi.org/10.1007/s00227-011-1649-z

Tukey, J.W., 1949. Comparing Individual Means in the Analysis of Variance. Biometrics 5, 99–114. https://doi.org/10.2307/3001913 van Oevelen, D., Mueller, C.E., Lundälv, T., Middelburg, J.J., 2016. Food selectivity and processing by the cold-water coral L*ophelia pertusa*. Biogeosciences 13, 5789–5798. https://doi.org/10.5194/bg-13-5789-2016

Vásquez, F.A., 2017. Geodinamica de laderas en el fiordo Comau, región de los lagos, Chile (Master thesis). Universidad de Chile, Santiago.

Wagner, H., Purser, A., Thomsen, L., Jesus, C.C., Lundälv, T., 2011. Particulate organic matter fluxes and hydrodynamics at the Tisler cold-water coral reef. Journal of Marine Systems 85, 19–29. https://doi.org/10.1016/j.jmarsys.2010.11.003

Walling, D.E., 2006. Human impact on land–ocean sediment transfer by the world's rivers. Geomorphology 79, 192–216. https://doi.org/10.1016/j.geomorph.2006.06.019

White, H.K., Hsing, P.-Y., Cho, W., Shank, T.M., Cordes, E.E., Quattrini, A.M., Nelson, R.K., Camilli, R., Demopoulos, A.W.J., German, C.R., Brooks, J.M., Roberts, H.H., Shedd, W., Reddy, C.M., Fisher, C.R., 2012. Impact of the Deepwater Horizon oil spill on a deep-water coral community in the Gulf of Mexico. Proceedings of the National Academy of Sciences 109, 20303–20308. https://doi.org/10.1073/pnas.1118029109

Widbom, B., 1984. Determination of average individual dry weights and ash-free dry weights in different sieve fractions of marine meiofauna. Marine Biology 84, 101–108. https://doi.org/10.1007/BF00394532

Wijgerde, T., Schots, P., Van Onselen, E., Janse, M., Karruppannan, E., Verreth, J.A.J., Osinga, R., 2013. Epizoic acoelomorph flatworms impair zooplankton feeding by the scleractinian coral *Galaxea fascicularis*. Biology Open 2, 10–17. https://doi.org/10.1242/bio.20122741

Wild, C., Huettel, M., Klueter, A., Kremb, S.G., Rasheed, M.Y.M., Jørgensen, B.B., 2004. Coral mucus functions as an energy carrier and particle trap in the reef ecosystem. Nature 428, 66–70. https://doi.org/10.1038/nature02344

Wittenberg, M., Hunte, W., 1992. Effects of eutrophication and sedimentation on juvenile corals. Marine Biology 131-138 (8).

Wurz, E., 2014. Autökologie der Kaltwassersteinkoralle *Caryophyllia huinayensis* aus der patagonischen Fjordregion (Master thesis). Universität Rostock, Bremerhaven.

Appendix

Supplementary material 1

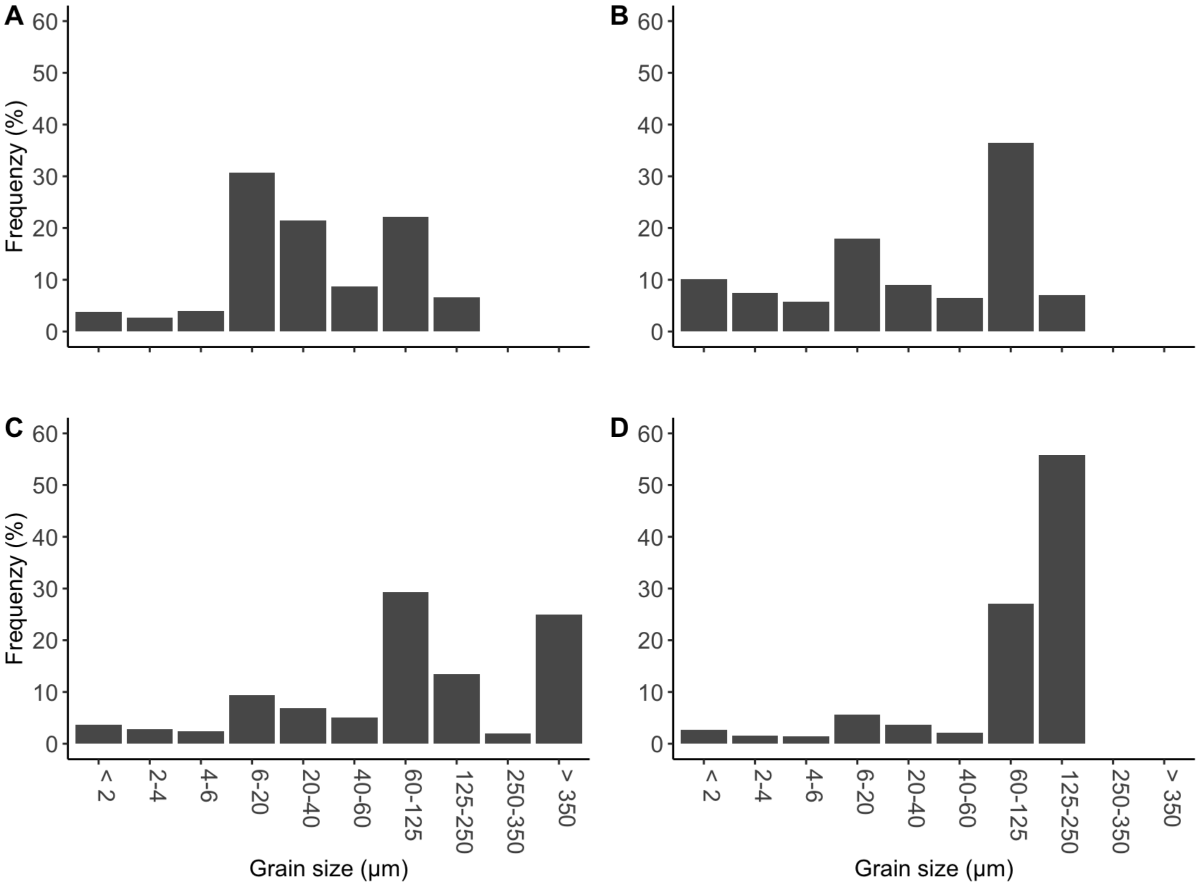

Supplementary material 1: rain size distribution of treated Wadden Sea sediment. A) untreated, B) freeze-dried, boiled with H_2O_2 and washed (used for the experiment), C) muffled at 500 °C, D) treated with H_2O_2 only

Supplementary material 2

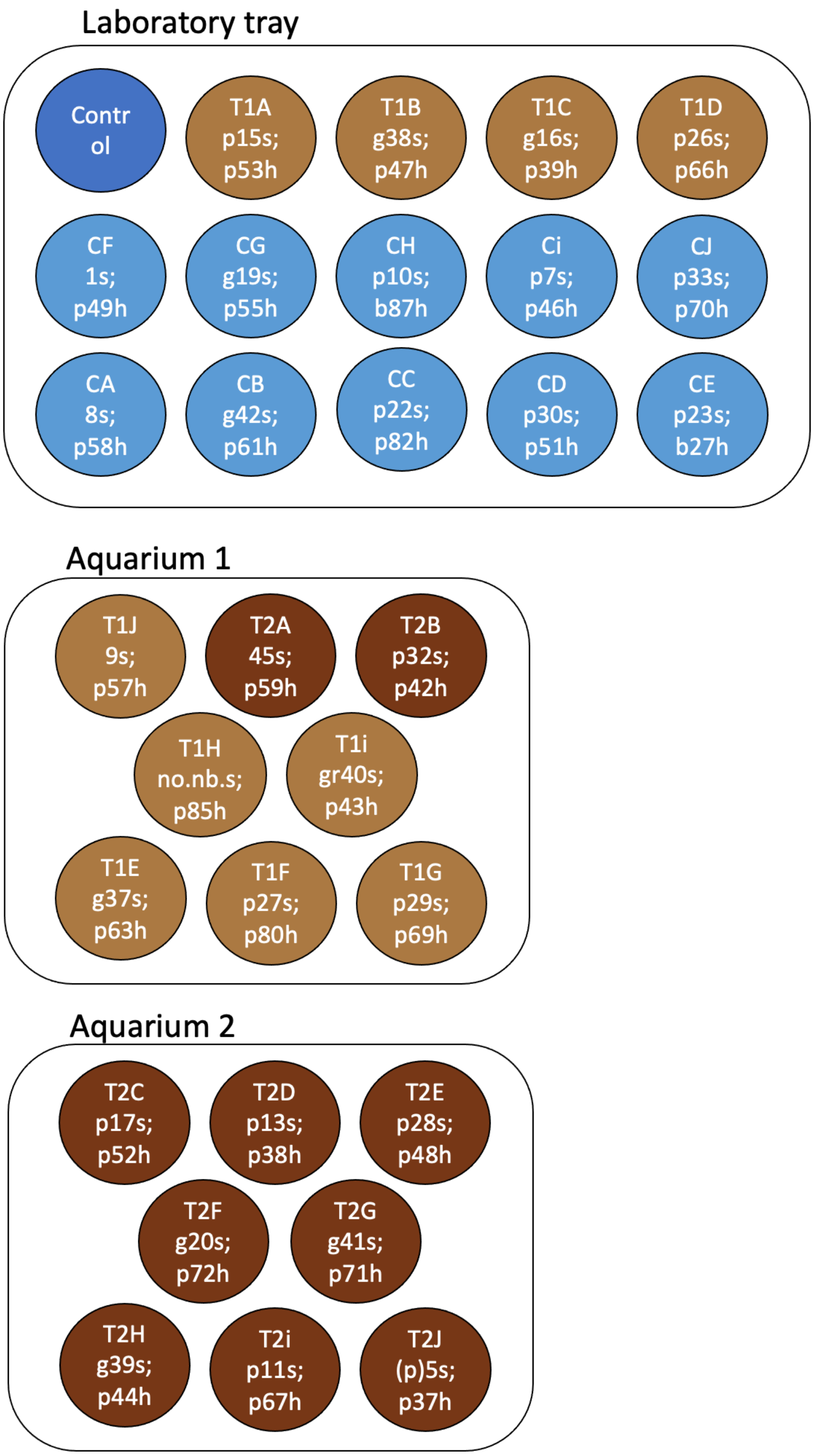

Supplementary material 2: Sketch of experimental set-up showing distribution of beakers on the collection tanks (laboratory tray, aquarium) and polyp-placement of individuum’s in the control group of the natural concentration (C) and in treatments with increased sedimentation rates: 100-fold (T1), 1000-fold (T2)

Supplementary material 3

Supplementary material 3: Nutrient values measured with aquarium test kit over the experimental period

	Natural concentration				**100-fold concentration**				**1000-fold concentration**			
	NO^{2-} (mg l^{-1})	**NO^{3-}** (mg l^{-1})	**NH_4** (mg l^{-1})	**PO_4^{3-}** (mg l^{-1})	**NO^{2-}** (mg l^{-1})	**NO^{3-}** (mg l^{-1})	**NH_4** (mg l^{-1})	**PO_4^{3-}** (mg l^{-1})	**NO^{2-}** (mg l^{-1})	**NO^{3-}** (mg l^{-1})	**NH_4** (mg l^{-1})	**PO_4^{3-}** (mg l^{-1})
25.01.21	0.025 - 0.05	< 0.5	0.1	< 0.02	0.025 - 0-05	< 0.5	< 0.05	0.05 - 0.1	< 0.01	< 0.5	< 0.05 - 0.1	0.04
26.01.21	0.01 - 0.025	< 0.5	< 0.05	< 0.02	0.025	< 0.5	< 0.05	0.05	0.025	< 0.5	< 0.05	0.2-0.4
27.01.21	0.025	< 0.5	< 0.05	< 0.02	0.025	< 0.5	< 0.05	0.05 - 0.2	0.025	< 0.5	< 0.05	0.4
29.01.21	0.025	< 0.5	< 0.05	0.02 - 0.05	0.025	< 0.5	< 0.05	0.05	0.025	< 0.5	< 0.05	0.4
03.02.21	0.01 - 0.025	/	< 0.05	< 0.02	0.025	/	< 0.05	0.05	0.025 - 0.05	NA	< 0.05	0.2 - 0.8
05.02.21	0.025 - 0.05	/	< 0.05	< 0.02	0.025 - 0.05	/	0.05 - 1	0.05	0.025	NA	< 0.05	0.2-0.4
10.02.21	< 0.01	/	< 0.05	0.02 - 0.05	0.025 - 0.05	/	< 0.05	/	0.025	/	< 0.05	/
24.02.21	0.025 - 0.05	< 0.5	0.05 -0.1	< 0.02	0.025 - 0.05	< 0.5	0.1	0.05	< 0.01	< 0.5	0.2	0.8 - 1.8
26.02.21	0.01 - 0.025	< 0.5	0.05 -0.1	0.02 - 0.05	0.025 - 0.05	0.5 - 1	0.1	0.05 - 1.8	0.025 - 0.05	< 0.5	0.1	0.4
03.03.21	< 0.01	< 0.5	0.1	< 0.02	0.025 - 0.05	0.5 - 1	0.1	0.05 - 0.2	0.025 - 0.05	< 0.5	0.1	0.4 - 1.2
05.03.21	< 0.01	< 0.5	< 0.05	0.2 - 0.6	0.025 - 0.05	< 0.5	0.1	0.1 - 0.4	0.025 - 0.05	< 0.5	0.2	0.2 - 0.4
10.03.21	0.025	< 0.5	< 0.05	< 0.02	0.025	< 0.5	< 0.05	0.1 - 0.2	0.025	< 0.5	0.1	< 0.02 - 0.05
12.03.21	0.025 - 0.05	< 0.5	0.1	0.03 - 0.1	0.025 - 0.05	< 0.5	0.1	0.1 - 0.25	0.025	< 0.5	0.1 - 0.2	0.5
17.03.21	< 0.01	< 0.5	0.05 - 0.1	0.03	0.025 - 0.05	< 0.5	0.1	0.1 - 0.25	0.05 - 1	< 0.5	0.1 - 0.2	0.5 - 1

19.03.21	0.05	< 0.5	0.1	0.03	0.025 - 0.05	< 0.5	0.1	0.1 - 0.25	0.025 - 0.05	< 0.5	0.1	0.5 - 1
24.03.21	0.05	< 0.5	< 0.05	0.03	0.025 - 0.05	< 0.5	< 0.05	0.25 - 0.5	0.025 - 0.05	< 0.5	0.1	1
26.03.21	0.025	< 0.5	< 0.05	0.03	0.05	< 0.5	< 0.05	0.25	0.025 - 0.05	< 0.5	0.1	1
02.04.21	0.025	< 0.5	0.1	0.1	0.025	< 0.5	0.1	0.25 - 0.5	0.025 - 0.05	< 0.5	0.1	0.5 - 1
05.04.21	0.025 - 0.05	< 0.5	0.1	0.1	0.025	< 0.5	0.1	0.25	0.025 - 0.05	< 0.5	0.1	1
07.04.21	0.025 - 0.05	< 0.5	0.1	0.1	0.025 - 0.05	< 0.5	0.1	0.1 - 0.25	0.05	< 0.5	0.1	0.4 - 0.6
09.04.21	0.025 - 0.05	< 0.5	0.1 - 0.2	< 0.02	0.025 - 0.05	< 0.5	0.1	0.1 - 0.25	0.025 - 0.05	< 0.5	0.1	0.6
14.04.21	/	/	/	/	0.025	< 0.5	0.05 - 1	0.05	0.05	0.5 - 1	0.1	0.7
16.04.21	/	/	/	/	/	/	/	/	0.05	< 0.5	0.1	0.4 - 0.6

Eidesstattliche Erklärung

Hiermit versichere ich an Eides statt, dass ich diese Arbeit selbstständig verfasst und keine anderen als die angegebenen Quellen und Hilfsmittel benutzt habe. Außerdem versichere ich, dass ich die allgemeinen Prinzipien wissenschaftlicher Arbeit und Veröffentlichung, wie sie in den Leitlinien guter wissenschaftlicher Praxis der Carl von Ossietzky Universität Oldenburg festgelegt sind, befolgt habe.

____

Melanie Fähse Oldenburg, 12.10.2021